

This document will be where Steven Brey and co-authors outline responses to reviewers of manuscript ACP-2017-245. To make this process easier, we have pasted the text of the reviews into this document and provide responses to reviewer comments immediately after their text.

After the reviewer comments and discussion, we have placed the entire manuscript and show track changes so that it will be easy to see what changes were made to the manuscript as a result of the reviewer comments/discussion. This starts on page 16.

Reviewer Comments are in black text. Our responses to the reviewer have been inserted in blue text. Red text is text that has been added to the manuscript as well as presented here to the reviewer.

Thanks to the two reviewers for their thoughtful comments on the manuscript. We were able to address all the comments. In particular, we took the time to explore the choice of land cover classification. As suggested by the reviewer, this did not change our results meaningfully. However, we have added a substantial number of figures to the Supplemental Materials so anyone interested in using the datasets we present can easily explore this.

Reviewer 1 Comments: Received and published: 13 July 2017

Dear Authors,

Thank you for a well-written concise manuscript describing your very interesting experiment. Leveraging the thousands of hours of analyst labor manifest in the NOAA hazard mapping system for science purposes is a very worthy goal. The basic climatological analysis of smoke influences over the US could not readily be performed without these HMS data.

I consider your study worthy of publication, but your results are only semi-quantitative and in some cases potentially subject to large errors, because of weaknesses in the input datasets. You will need to at least include a discussion of these potential errors and hopefully some analysis to approximate their magnitude in your final paper.

Land cover is the most egregious example: while the US landscape has not been radically reshaped over the past 25 years, this is not an excuse to use a truncated version of a dataset based on 25-year-old AVHRR data. The Hansen et al. 2000 paper with basic validation results for this dataset is a good place to start, it says “Comparisons of the final product with regional digital

land cover maps derived from high-resolution remotely sensed data reveal general agreement, except for apparently poor depictions of temperate pastures within areas of agriculture” (<http://www.tandfonline.com/doi/abs/10.1080/014311600210209>).

I do not think that your results would see large qualitative changes if you used a more modern dataset such as the North American Land Change Monitoring System (<https://landcover.usgs.gov/nalcms.php>) but I would expect much better answers from that dataset in areas such as the discrimination of cropland and forested land in the Southeast US (the best dataset for that purpose would be the Cropland Data Layer [<https://nassgeodata.gmu.edu/CropScape/>]). I am not recommending that you redo your entire analysis with a different land cover dataset (though it might not be that difficult to do so). However, you should include this in your discussion of uncertainties.

Our original choice in the use of the 1992 National Center for Earth Resources Observation and Science land cover dataset was driven by the availability of the dataset in an easy to use gridded format that was consistent over all North America. The dataset is available in a non proprietary format. However, we agree with the reviewer that using a different, updated land cover dataset is an important test of the uncertainty associated with this choice. Therefore, following the reviewer’s recommendation, we have taken the time to assign HYSPLIT points land cover using a dataset from the suggested *North American Land Cover Change Monitoring System*. The specific dataset we choose to use within this system was the *2010 Land Cover of North America at 250 meters* data published in 2013 by the Commission for Environmental Cooperation in Montréal, Québec, Canada (<http://www.cec.org/tools-and-resources/map-files/land-cover-2010>). These data are based on the Moderate Resolution Imaging Spectroradiometer (MODIS/TERRA) seven land spectral bands top of atmosphere reflectance. These data were created primarily to assess North American land cover changes between 2005 and 2010. Approximately 1% of land area land cover classifications changed during this time period.

Overall we find that the differences between the two datasets are driven by an inconsistent list of land cover classifications between the 1992 and 2010 data. Comparing the two different land cover classifications is challenging and requires subjectivity due to the fact that the land cover classification categories are not the same between the 1992 and 2010 data. For example, when assessing whether the two datasets agree on land cover for a given location there needs to be a decision as to whether “temperate or subpolar needleleaf forest” and “evergreen needleleaf forest” count as a match. As indicated by the reviewer, making this decision is not particularly pertinent to the presentation of land cover dependent results presented in the paper. Thus we did not re-do the figures in the main body of the text using the alternative land cover dataset. Instead we added figures to the Supplemental Information (S9.1 Fig. S8 - S24) materials that show how the HYSPLIT point land cover designations differ between the two datasets. We have sprinkled this throughout the text where HYSPLIT land cover is discussed.

Additions:

- Section 2.3
 - “We point readers to Hansen et al., 2000 for a discussion of the weaknesses of the 1992 land cover dataset. We have also completed a comparison to a 2010 land cover dataset, and this comparison is available in the Supplemental Information Sect 9.”
- Section 4, paragraph 1
 - “When we assess the land cover classification of HYSPLIT points using a 2010 land cover dataset, the most common alternative assignment for the most abundant cropland assignment type (“cropland/grassland mosaic”) is “temperate subpolar grassland”. Regional differences for alternative assignments exist. For example, in the U.S. Midwest and Great Plains, the most common alternative land cover assignment for cropland is “temperate subpolar grassland” while in the Southeast U.S. the most common alternatives are “temperate subpolar needleleaf forests” and “wetland”. These 2010 data show that the most common alternative land cover assignment for forested lands in North America is “subpolar shrubland”.

Citation for 2010 land cover data used in the supplemental material:

2005 North American Land Cover at 250 m spatial resolution. Produced by Natural Resources Canada/Canadian Center for Remote Sensing (NRCan/CCRS), United States Geological Survey (USGS); Insituto Nacional de Estadística y Geografía (INEGI), Comisión Nacional para el Conocimiento y Uso de la Biodiversidad (CONABIO) and Comisión Nacional Forestal (CONAFOR).

You are also using the HMS analyst-generated fire detection data, and for those data there is a published validation: Schroeder et al. IJRS 2008 (<http://www.tandfonline.com/doi/abs/10.1080/01431160802235845>) . This paper indicates good quality of the fire data, and does not point to significant source of error except to note that like all fire detection systems, small fires are much harder to detect and will be systematically underrepresented in the output products. A recent paper by Hu et al. JGR 2016 (<http://onlinelibrary.wiley.com/doi/10.1002/2015JD024448/abstract>) describes how these errors manifest as both drastic underdetection of individual fires and as imbalances in fire detection rates by ecosystem. The agreement in the coarse seasonality of North American burning between HMS and GFED data, while encouraging, does not rule out significant biases at the scale of your regional analysis.

Thank you for pointing out these papers. However, the Hu et al. (2016) paper analyzes the so-called ‘hybrid HMS’, referring to the fact that the HMS uses multiple satellites (there is only one HMS). The Hu et al. (2016) paper analyzes the automatic detections of the HMS, not the HYSPLIT points presented in this manuscript, thus the detection rate results presented are not applicable to our study. Mark Ruminiski is a co-author on our work, and on the Hu et al. (2016) JGR paper. We have included citations to both these papers and we have added an additional sentence reminding readers that any satellite-based detection system (whether automatic or human vetted) is likely to struggle with the detection of small fires and be limited to low cloud optical depth conditions.

We have added the following to the manuscript:

“Schroeder et al. (2008) assess the automatic detections; there are small false alarm rates (~2%) the conterminous U.S. As in all satellite-based fire detection systems, small fires are more difficult to detect and are under-reported (e.g. Hu et al., 2016).”

You cite the Rolph et al. (2007) paper about the NOAA Smoke Forecasting system, but you need to include the information on uncertainties from that paper in your discussion. That paper found very weak agreement between HMS smoke plumes and smoke transport model results, and while that paper was formulated as a validation of the transport model using HMS plumes, it remains that there is no published validation of the HMS smoke plume extent data, and it is likely to have both large uncertainties as well as some systematic biases due to discrimination of smoke being easier over some areas and seasons relative to others. The Rolph paper is a good place to start to formulate a discussion of how potential errors in the HMS smoke extent data could affect your results.

We had already included this discussion in the methods (Section 2.1 and 2.2), but now we note also that there is no comprehensive validation of the HMS plumes. We are interested in pursuing a validation of this dataset, but it is certainly beyond the scope of this paper. Potentially useful datasets include AERONET (as mentioned later by both reviewers), and also CALIPSO/CATS. However, validation will need to be thoughtfully designed to test the known specific weaknesses. For example, the largest uncertainty is likely to be at the edges of the plumes. We agree with the reviewer that it is ideal to remind readers of these caveats in the discussion and conclusions. So, we have used that approach here.

The following text is now included in the updated Section 2.2:

“Rolph et al. (2009) used the HMS smoke plumes to validate NOAA’s operational smoke forecasting system. There is no published validation of the HMS smoke plume extent data. It could have systematic biases because discrimination of smoke is easier over some areas, seasons,

and under certain synoptic weather conditions. For our aggregate smoke plume analysis, the largest uncertainty is at the edges of the plumes. The temporal information is also a source of uncertainty. During the day, the extent can be assessed hourly. However, this is not possible overnight. Smoke is sometimes transported to areas with anthropogenic haze pollution. In some cases the smoke will mix with and become indistinguishable from the anthropogenic haze pollution. The greater the distance travelled by a smoke plume, the more challenging it is to distinguish between smoke and anthropogenic haze. This challenge is particularly pronounced for aged smoke impacting the Southeastern U.S.”

The following has been added to section S10 (*Additional HMS smoke plume operational analysis details* section of the supplemental material)

“Presently, there is no comprehensive validation of HMS smoke plume analysis. One of the reasons in that there is no spatially and temporally comprehensive ground truth to compare to. Other satellite data would need to be used and these would have their own uncertainties. In the manuscript we state that the largest uncertainty for the smoke plume analysis is likely to be the edges of the smoke plume. In aggregate this is true, but may not be the largest uncertainty for every individual smoke plume.”

We have updated the Discussion and conclusions with the following sentences:

- Section 6, paragraph 1
 - “The location of smoke hours is restricted to locations where smoke plumes have been analyzed while the height is estimated from HYSPLIT forward trajectories.”
- Section 6, paragraph 1
 - “This dataset confirms that there is a substantial amount of smoke-producing fire activity in the Southeast, particularly along the lower Mississippi River Valley. This is likely an underestimate of the contribution of small fires to smoke abundance in this region given that small fires within this region can be substantially under-detected (Hu et al., 2016). In addition, it can be challenging to differentiate anthropogenic haze from smoke in this region.”

This last area is one where I will recommend additional analysis. Your current manuscript includes this analysis (page 2): “10% of these plume days are days where ground level PM2.5 is one standard deviation above average summertime concentrations.” That 10% was for Minnesota stations; you cite a figure of 30% for Washington and Oregon stations. This is a good basis for a test of the skill of your method; however, because you are using ground monitors, the additional uncertainty of the vertical profile means that no conclusion can be drawn from these results. I recommend repeating this analysis using AERONET stations in the Western and Eastern US, to determine whether the presence of HMS-diagnosed smoke corresponds with significantly

elevated aerosol optical depth relative to the seasonal mean values. This analysis would build confidence in the unvalidated HMS smoke plume extent that is the core of your study.

This is a miscommunication. We are not attempting to validate the HMS with the ground sites, and Figure 1 is presented before we even discuss the plumes themselves. Our intention was for this section to demonstrate that plumes do not necessarily result in elevated $PM_{2.5}$ values. This is an important piece of information to properly interpret the rest of the paper. An HMS smoke plume analyzed overhead does not ensure ground level air quality impacts. Figure 1 presents a summer climatology of the percent of time an overhead smoke plume has resulted in elevated ground level $PM_{2.5}$. When we point out that 10% of so-called plume days in Minnesota are observed to have elevated surface $PM_{2.5}$ concentrations we are not validating the HMS, we are pointing out that most plume days in Minnesota do not result elevated ground level $PM_{2.5}$. We have added the following sentences to this section to make this clear to all readers.

“Fig. 1 is not intended to validate the HMS smoke product. This figure is meant to set the stage for interpreting the analysis presented in later sections, *i.e.* a smoke plume overhead does not necessarily ensure elevated ground-level $PM_{2.5}$ concentrations.”

The following sentence has been added to the conclusion section:

“The location of smoke hours is restricted to locations where HMS analysts have drawn smoke plumes while the height is estimated from HYSPLIT forward trajectories emanating from HYSPLIT points.”

Good luck with completion of this study, and I look forward to its publication, but I hope to see an expanded discussion of the uncertainties in your analysis that will assist readers in drawing conclusions from these unique comprehensive datasets.

We thank you for your thoughtful review! We also want to provide the reviewers, editor, and readers with the following online interactive data viewing tools, which show raw HMS data. This data visualization increases the transparency of this work by showing the reader exactly how this data looks on a daily timescale.

- <http://sjbrey.atmos.colostate.edu/HMSExplorer/>
- <http://sjbrey.atmos.colostate.edu/smokeWheel/> (interactive version of Figure 13)

Reviewer 2 Comments: Received and published: 8 September 2017

Reviewer Comments are in black text. Our responses the reviewer have been inserted in blue text. Red text is text that has been added to the manuscript as well as presented here to the reviewer.

This manuscript primarily details an attribution analysis of the relative contribution of biomass burning smoke originating from the North America region to smoke observed over predefined areas within the continental US. The authors employ NESDIS HMS data and forward trajectory modelling using HYSPLIT to achieve their analysis and results. A smoke transport climatology is presented, which outlines the key smoke producing regions and their influence over themselves and other neighbouring receptor regions.

The narrative is generally well written and logically organised, with clear figures and diagrams – particularly the visual analytics style graphic at the end which provides a nice overview of the smoke pathways. The analysis of the smoke climatology follows a reason approach and the results are presented clearly.

Thank you for your feedback of our final figure! There is an interactive version of Figure 13 available at the following url: <http://sjbrey.atmos.colostate.edu/smokeWheel/>

In my opinion the main deficiencies are in the input datasets used for the analysis as outlined in the comments below, and a lack of discussion on the potential margin of error in the results. Overall, I think the results are of interest to the community, and would recommend publication after the following comments have been addressed.

Thank you. In response to Reviewer 1, we have added discussion on uncertainty resulting from:

- HMS HYSPLIT points (section 2.1)
- HMS smoke plumes (section 2.2)
- Section 5 & 6 (discussion and conclusion)

Please see specific responses and additions below.

1. The HMS is used operationally for smoke forecasting but clarification is needed why this is considered a more suitable choice of dataset for this paper over other established ones like GFED for example, which is compared in the paper and widely used in many studies. Since the HMS product is considerably subjective as it is based on analysts manually adding points for various situations as outlined in section 2.1, the consistency of the product needs to be put into question as a suitable dataset for such analysis. There are also limitations on available years of suitable

HMS data. The subjectivity and inconsistency of this operational dataset also limits its usefulness for future analysis.

The HMS human generated fire detections (HYSPLIT points) and smoke plumes are particularly valuable from an operational air quality perspective. Fire emission inventories, such as GFED, are useful to initialize model simulations. However, those model simulations are subject to additional uncertainties. For example, injection height is very difficult to simulate properly. In addition, GFED does not have a smoke plume product created in-tandem with the fire locations the way the HMS system does. Because this work is concerned with where smoke plumes originate and travel, this component of the work would not be possible using GFED or another “traditional” emission inventory. Case-study validation of the ability of chemical transport models (*e.g.* GEOS-Chem, WRF-Chem, *etc.*) shows that these models have difficulty 1) accurately representing smoke plume spatial extent, 2) cannot be run at 1 degree grid spacing at the daily or hourly timescale for the length of time needed for this analysis (*i.e.* covering 8 years) due to computational limitations. GFED also does not provide sub-daily information on fire occurrence the way HYSPLIT points do (hourly), this could have consequence for the timing of emissions and transport pathways. Though there are other emission inventories that have a higher time resolution (*e.g.* FINN), similar modelling challenges still result when this inventory is implemented into chemical transport models.

Gridded emission inventories do not provide the same spatial or temporal information as the HMS HYSPLIT points. GFED4s arguably represents the state of the science when it comes to emission inventories. This product is gridded to a $0.25 \times 0.25^\circ$ (~27 x 27 km) grid, which is much more coarse than the ~2-3 km accuracy of individual HYSPLIT points.

This paper offers orthogonal methods to answer smoke transport questions that are usually answered using gridded emission inventories and chemical transport models. Understanding the impact of smoke on the U.S. airshed is a very important problem that should be investigated using multiple methods. Because HMS HYSPLIT points are the analysed fires used to initialize US National Weather Service Air Quality Forecasts they represent a unique subset of fires, those that have been determined to potentially be of importance to air quality.

When developing or presenting a new dataset, due diligence requires comparing it to existing datasets. That is our goal in presenting a comparison with GFED4s. We also use this comparison to understand where approaching the problem of smoke transport with different underlying datasets/techniques may lead to different results.

2. The smoke plume analysis done operationally by the HMS analysts also have a large element of subjectivity and it would be useful to cross check this with another dataset (as was done with

the comparison between the HYSPLIT points and GFED). One possibility would be AOD for example, from satellite observations as well as AERONET stations.

In response to Reviewer 1, we had already updated our discussion of uncertainty in the methods (Section 2.1 and 2.2). We specifically note that there is no comprehensive validation of the HMS plumes. We are interested in pursuing a validation of this dataset, but it is certainly beyond the scope of this paper. Potentially useful datasets include AERONET (as mentioned later by both reviewers), and also CALIPSO/CATS. Validation will need to be thoughtfully designed to test the known specific weaknesses, rather than simply comparing AOD across the entire time period or geographic extent of this analysis. The largest uncertainty is likely to be at the edges of the plumes. This is likely what would be best to validate. However, we remind readers that the HMS smoke product is actually used to validate plume models (*e.g.* Rolph et al., 2009) as was mentioned by Reviewer 1.

The strengths and limitations of the smoke plume analysis are accurately described in section 2.2 and that the strengths justify the work and results presented in this paper. We have also added more discussion of the limitations of this work to both the discussion and conclusions sections.

3. Units of time (i.e. hours of smoke) are used for the analysis though it would have been better to use derived smoke emissions instead which would take into account land cover characteristics, fuel loading etc. Just using duration alone seems to be a self-imposed limitation when comparing with the amount of smoke observed. Some explanation to better justify this approach would help.

The goal of this work is to identify the common transport pathways associated with fires that initiate air quality forecasts. Our goal is not to predict the amount of smoke impacting a given surface site, and in fact, this work may be useful outside the air quality community because we have generically described smoke transport in the column. Smoke has radiative impacts in addition to composition impacts. Moving toward an emission approach would actually increase the uncertainty associated with this analysis. This would essentially scale our results by a set of emission factors, combustion efficiency estimates, fuel load estimates, *etc.*, and would not change the overall findings of the paper. In addition, using hours helps us better understand how quickly smoke plumes are moving and dispersing. It also helps us view smoke age efficiently, which is another goal of this paper.

4. The land cover map using data from 1992-93 is considerably old and it is difficult to see why a more updated map wasn't used since there are various newer maps available out there. Unless it could be shown that there weren't significant changes in the land cover over the 15 years or more to the analysis years of 2007-14 (quite unlikely), the results involving land cover classification are hampered by using the old map dataset.

Refer to the response of reviewer number 1 and our analysis showing just how different these are and if land cover matters. We have added several figures to the supplemental material (S9, S8 - S24) showing differences in land-cover characteristics assigned to HYSPLIT points using a 2010 dataset.

Specific comments:

1. P1, line 16 & P11, line 30: . . . ‘HYSPLIT’ . . .

Thank you for catching these typos. Both instances of ‘HYSPLIT’ have been changed to HYSPLIT.

2. P2, line 26 -35: There have been attribution studies conducted in other parts of the world using Lagrangian models with chemistry. Emissions information are available from global inventories including GFED, GFAS, FINN for example, so I would disagree that a modelling approach is unsuitable, because it would clearly be more comprehensive and could include full plume dispersion (compared to trajectories), deposition, attribution of secondary smoke particulates etc.

We agree that smoke attribution can be accomplished using chemical transport models, and this would allow for additional calculations. However, the strength of Figure 1 is that it is observationally grounded. We also note that our trajectories are only used when validated by observed smoke plumes and that CTMs struggle to accurately simulate smoke dispersion. We have changed this paragraph to read:

“The aggregate view provided by Fig. 1 is unique because it is observationally grounded. There are a number of challenges associated with using a chemical transport model (CTM) to produce an analogous representation of Figure 1. Rastigejev et al. (2010) show that CTMs have difficulty representing plume dispersion, but the plan view result of this process is captured in the HMS smoke plume analysis. There are other factors contributing to the modelling challenge (*e.g.* Lassman et al.(2017) and references within). For example, there have been a number of advances made in estimating the emissions inputs by improving burned area products (*e.g.* Randerson et al. (2012)) and combining these with emission factors for a wider range of trace species (*e.g.* Akagi et al. (2011) and Wiedinmyer et al. (2011)). However, incorporating the full suite of emitted species into models and simulating the rapid chemical evolution of smoke remains a challenge (Alvarado et al., 2015), as is proper treatment of injection height (Paugam et al., 2016) and the timing of emissions (Saide et al., 2015). Models are also subject to uncertainty associated with meteorological inputs (Garcia-Menendez et al., 2013). Finally, running and analyzing a chemical transport model at the fine grid resolution appropriate to simulate all the individual smoke plumes of interest from North American fires over the scale of a decade is currently too computationally expensive to be practical. Thus other lenses are needed to examine how the

smoke from North American fires is transported and dispersed in the atmosphere over seasonal and interannual timescales.”

Added to section 5.4:

“Due to the difficulty in detecting small fires, it is possible that the smoke hour budget in these regions underestimates local contributions of smoke in these regions.”

Added to section 6 where the age of transported smoke plumes is discussed:

“Due to the challenge of distinguishing aged smoke plumes from anthropogenic haze in the Southeast, the abundance of aged smoke hours is likely underestimated in this region.”

3. P3, line 3: What is meant to “trigger” a smoke forecast?

Trigger is used here to have the same meaning as “Initiate”. The sentence has been changed to “of fires that **initiate** National Weather Service (NWS) smoke forecasts”.

4. P3, line 26-29: Please clarify how the accuracy statistics stated here were determined.

The following text has been added to section 2.1 (describing HYSPLIT points)

“GOES visible band and polar orbiting satellites used by the HMS have 1 km resolution at nadir. The 2-3 km accuracy of the location of HYSPLIT points is an estimate based on the additional uncertainties introduced by navigation errors and loss of resolution for observations made away from nadir.”

“Visible satellite imagery was available every 30 minutes during the study period, HMS analysts estimate that this makes the start time of smoke emissions accurate to within 1-2 hours.”

Mark Ruminski (co-author and HMS team leader) exact comments on this matter:

“The reviewer is asking about the estimated accuracy in location of HYSPLIT points, in the start time assigned to them and the duration. For the location, this is based on the fact that we use visible imagery to identify smoke plumes. VIS imagery, whether polar or GOES, is at 1km resolution at nadir. By estimating 2-3 km accuracy I tried to account for navigation errors, loss of resolution as you move from nadir (i.e. VIS resolution for GOES-E in the western US is not 1km but more like 2-3 km). etc. For wildfires we also apply HYSPLIT points during the overnight period (no VIS imagery). For this we utilize the 4 micron channel on the polar satellites where the resolution at nadir again is 1 km but decreases as you move toward the limb.

For the start time, we normally go with the time when we first see smoke from the fire. For a very small percentage of the fires that start overnight (and we can't see smoke) we can add

HYSPLIT points when we see the hotspot. For the study period, we had imagery available every half hour. So we should be able to determine smoke that is visible within that time frame. Finally, for the duration, as is noted in the text, it is more uncertain since many of the ag/prescribe burns continue to produce smoke after usable visible imagery, so we cannot see when the smoke emissions cease. But our assumption is that if they are indeed ag or prescribed, they are not likely to continue burning through the night, so we normally assign a duration that will end an hour or two after sunset. For wildfires, we don't know when they will end. That depends on many other factors. We assume that they will continue to burn until we no longer see smoke one day. On top of all this there is analyst subjectivity. The estimates I provided are based on the above and are my best estimate.”

5. P3, line 30-31: Repeated phrase - “HYSPLIT points in proportion . . . smoke observed”.

P3, line 30-31 has been rewritten such that there is no repeated phrase. The new wording is shown below.

“Single fires that produce notable amounts of smoke are associated with a cluster of co-located, or nearly co-located, HYSPLIT points assigned roughly in proportion to the amount of smoke observed. The intended operational consequence of designating HYSPLIT points this way is to allow the NWS smoke forecast model to generate more smoke for large fires and less smoke for smaller fires.”

6. P4, line 5: On the relationship between HYSPLIT points and smoke quantity – is this purely based on duration assigned by the analyst or is land cover taken into account? Do all HYSPLIT points emit the same amount of smoke? This also raises the question again of why hours of smoke are being used instead of derived emissions.

The number of HYSPLIT Points analyzed, multiplied by their respective duration (Smoke Production Duration Hours or SPDH) is proportional to visual smoke produced for the land cover in which it is burning. This operational visual smoke analysis underpins our analysis, and this paper represents a different approach to CTM-based studies. However, this does not mean SPDH are proportional to emissions and we show this in Fig. 3c. Our primary objective is to estimate what fires are responsible for observed smoke plumes, attempting to derive emissions would add an additional layer of uncertainty to this analysis (uncertainties in emission factors, plant functional type, fuel moisture, combustion efficiency, weather conditions, fuel loading, *etc.*). SPDH reasonably distinguishes between fires that produce a small puff of smoke from fires that produce smoke plumes capable of covering entire states. We use HYSPLIT points because they are produced in tandem with the smoke plumes. You could not similarly use another emissions dataset to do this analysis. To answer the reviewer’s question very directly, the relationship between smoke quantity (as defined by particulate matter concentration [$\mu\text{g m}^{-3}$] or

kg of emissions for example) and HYSPLIT points is variable and does not account for land cover.

The following sentence was added to section 2.1, the section that describes HYSPLIT points.

“The number of HYSPLIT points analyzed, multiplied by their respective duration (SPDH) is proportional to visual smoke produced for the land cover in which it is burning, and the analyst determines this relationship. The relationship between smoke quantity (as defined by particulate matter concentration [$\mu\text{g m}^{-3}$] or kg of emissions for example) and HYSPLIT points is variable and does not account for land cover.”

The following sentences was added to the end of section 5.2, the section that defines smoke hours.

“A further weaknesses of smoke hours is that they have no way of accounting for secondary organic aerosol particle formation, which previous studies have shown can be significant (e.g. Sakamoto et al., 2015 & 2016; Janhall et al., 2010). However, these processes remain poorly understood and represented in chemical transport models, so an appreciation for the fact that these processes exist, but not attempting to account for them is sufficient for understanding the results presented in this work.”

New citations (due to SOA discussion):

Sakamoto, K. M., J. D. Allan, H. Coe, J. W. Taylor, T. J. Duck, and J. R. Pierce. “Aged Boreal Biomass-Burning Aerosol Size Distributions from BORTAS 2011.” *Atmos. Chem. Phys.* 15, no. 4 (February 16, 2015): 1633–46. doi:10.5194/acp-15-1633-2015.

Sakamoto, K. M., J. R. Laing, R. G. Stevens, D. A. Jaffe, and J. R. Pierce. “The Evolution of Biomass-Burning Aerosol Size Distributions due to Coagulation: Dependence on Fire and Meteorological Details and Parameterization.” *Atmos. Chem. Phys.* 16, no. 12 (June 24, 2016): 7709–24. doi:10.5194/acp-16-7709-2016.

Janhäll, S., M. O. Andreae, and U. Pöschl. “Biomass Burning Aerosol Emissions from Vegetation Fires: Particle Number and Mass Emission Factors and Size Distributions.” *Atmos. Chem. Phys.* 10, no. 3 (February 9, 2010): 1427–39. doi:10.5194/acp-10-1427-2010.

7. P7, line 6: Is the difference in magnitude actually due to comparison between ‘SPDH’ hours and actual C emissions rather than “varying emission factors for different ecosystems”?

We agree that there are more factors that could contribute to this difference, though we expect that varying emission factors for different ecosystems can partially explain the observed differences. We have removed the reference to emission factors in this sentence, and we have added the following sentences instead:

“The GFED4s estimate of grams of carbon emitted is a function of the estimated burn area, estimated fire combustion efficiency, soil moisture, the estimated land cover type, fuel loading, and emission factors (Giglio et al., 2013; Randerson et al., 2012; van der Werf et al., 2017). The observed difference between SPDH and GFED4s total grams of carbon emitted could be due to any of these factors.”

8. P9, line 30-31: Just a comment that a modelling approach would better allow altitude specific analysis to be conducted e.g. at surface level where air quality is of concern to the population.

To keep our analysis as useful as possible to others, we have chosen to avoid this. For most of the paper we did not set a limit on trajectory height, but we did link smoke plumes to elevated surface PM_{2.5} in Fig. 1.

The shortcomings of chemical transport models ability to estimate ground level PM_{2.5} resulting from smoke has been demonstrated repeatedly (e.g. Lassman et al., 2017; Reid et al., 2015; Alvarado et al., 2015; Paugam et al., 2016; Baker et al., 2016; Garcia-Menendez et al., 2013; Saide et al., 2015). Please see comments on a modelling approach listed above.

9. P11, line 2: It would be good to provide some explanation on why the trajectories run using the EDAS data are nearly identical and if this is something expected given the higher resolution of the meteorological input.

When we used the phrase ‘nearly identical’ we mean in terms of the impact of the interpretations of the results presented in the paper. Quantitatively the numbers are different, as shown in tables S1 and S2 and Fig. S4 - S6 in the Supplementary Information. The similarities of the results between the two different meteorology datasets show that our methods are not sensitive to the chosen meteorology, possibly since the results are dependent on long range transport, a spatial scale much greater than even the 1 degree GDAS data.

P11, line2: The sentence that used the phrase “nearly identical” has been changed to read:

“When the analysis presented in Fig. 11 is generated with trajectories run using EDAS meteorology data, the interpretation of the results is nearly identical and they are available in Sect S7 of the Supplemental Information.”

All changes to the manuscript resulting from reviewer comments discussed above are shown in the pages that follow. We show the “track changes” so that it is easy to see what was changed due to reviewer comments/discussion.

Connecting smoke plumes to sources using Hazard Mapping System (HMS) smoke and fire location data over North America

Steven J. Brey¹, Mark Ruminski², Samuel A. Atwood¹, Emily V. Fischer¹

¹Atmospheric Science, Colorado State University, Fort Collins, 80523, U.S.

²NOAA/NESDIS Satellite Analysis Branch, College Park, 20740, U.S.

Correspondence to: Steven J. Brey (sjbrey@rams.colostate.edu)

Abstract. Fires represent an air quality challenge because they are large, dynamic and transient sources of particulate matter and ozone precursors. Transported smoke can deteriorate air quality over large regions. Fire severity and frequency are likely to increase in the future, exacerbating an existing problem. Using the National Environmental Satellite, Data and Information Service (NESDIS) Hazard Mapping System (HMS) smoke data for North America for the period 2007 to 2014, we examine a subset of fires that are confirmed to have produced sufficient smoke to warrant the initiation of a U.S. National Weather Service smoke forecast. We find that gridded HMS analyzed fires are well correlated ($r = 0.84$) with emissions from the Global Fire Emissions Inventory Database 4s (GFED4s). We define a new metric, smoke hours, by linking observed smoke plumes to active fires using ensembles of forward trajectories. This work shows that the Southwest, Northwest, and Northwest Territories initiate the most air quality forecasts, and produce more smoke than any other North American region by measure of the number of HYSPLIT points analyzed, the duration of those HYSPLIT points, and the total number of smoke hours produced. The average number of days with smoke plumes overhead is largest over the north-central U.S. Only Alaska, the Northwest, the Southwest, and Southeast U.S. regions produce the majority of smoke plumes observed over their own borders. This work moves a new dataset from a daily operational setting to a research context, and it demonstrates how changes to the frequency or intensity of fires in the western U.S. could impact other regions.

Deleted: trigger

1 Introduction

North American fires represent a major source of atmospheric pollutants (Wiedinmyer et al., 2006), and they contribute to elevated ground level ozone (O_3) and fine particulate matter ($PM_{2.5}$) in the U.S. (Baker et al., 2016; Brey and Fischer, 2016; Jaffe et al., 2008; Park et al., 2007; Saide et al., 2015). Exposure to wildfire smoke has been shown to have negative impacts on respiratory and cardiovascular health (Dennekamp and Carey, 2010; Haikerwal et al., 2015; Rappold et al., 2011). The relative importance of the contribution of smoke, particularly wildfire smoke, as both an O_3 precursor and as a direct source of $PM_{2.5}$ will grow as anthropogenic emissions decline (Russell et al., 2012; Val Martin et al., 2015). In addition to air quality considerations, smoke is also thought to make a major contribution to absorbing aerosols observed throughout the

troposphere over North America (Forrister et al., 2015; Liu et al., 2015; Liu, 2014; Washenfelder et al., 2015). Thus understanding the sources and prevalence of smoke is relevant for air quality, visibility, and radiative forcing calculations.

Millions of hectares of forest burn in North America each year (Randerson et al., 2012), the area burned by wildfires in the western U.S. has increased (Westerling, 2016; Westerling et al., 2006), and models predict this trend will continue in a warmer climate (Hurteau et al., 2014; Keywood et al., 2013; Randerson et al., 2012; Scholze et al., 2006; Yue et al., 2013). Agricultural fires are also a significant source of smoke in North America. Over 1.2 million hectares of cropland are burned in the contiguous U.S. each year (McCarty et al., 2009). Though often smaller in size and shorter in duration, these fires have been shown to increase the abundance of gas and aerosol species that can deteriorate air quality (Akagi et al., 2011; Dennis et al., 2002; Jimenez et al., 2006). There are a growing number of case studies documenting instances of smoke traveling thousands of kilometers to affect atmospheric composition far downwind from the fire locations (Baker et al., 2016; Creamean et al., 2016; Miller et al., 2011; Pfister et al., 2008; Stein et al., 2009; Val Martin et al., 2013a). Case studies demonstrate that regional and long-range transport of smoke causes elevated column and surface concentrations of aerosols and trace gases over extensive (continental) regions of the U.S., and the smoke can have implications for atmospheric composition over relatively long temporal scales (weeks) (Creamean et al., 2016; Park et al., 2003, 2007; Val Martin et al., 2013a; Vedral and Dutton, 2006).

In this paper, we show how smoke data from the National Environmental Satellite, Data and Information Service (NESDIS) Hazard Mapping System (HMS) can be used to provide context for the growing number of case studies linking compromised air quality or visibility to smoke. As an introductory example, Fig. 1 shows that during summer (June – September) over the Contiguous U.S. North Dakota, South Dakota, and Minnesota have more smoke plumes overhead than any other states, averaging between 8 and 12 days per month between June and September. The location with the most smoke overhead is approximately co-located with Fargo North Dakota. Figure 1 also incorporates data from PM_{2.5} monitors. Fargo North Dakota lacks continuous ground level PM_{2.5} observations. Nearby monitors in the north east, south east and west of Minnesota show that approximately 10% of these plume days are days where ground level PM_{2.5} is one standard deviation above average summertime concentrations, approximately one day per summer month in these areas. In contrast, Washington and Oregon, both states with major summertime wildfire activity, average six plume days per month. On ~30% of days with smoke plumes in the atmospheric column (~two days per month), ground level PM_{2.5} concentrations are one standard deviation above the summertime average. [Figure 1 is not intended to validate the HMS smoke product. This figure is meant to set the stage for interpreting the analysis presented in later sections, i.e. a smoke plume overhead does not necessarily ensure elevated ground-level PM_{2.5} concentrations.](#)

The aggregate view provided by Fig. 1 ~~is unique because it is observationally grounded. There are a number of challenges associated with using a chemical transport model (CTM) to produce an analogous representation of Fig. 1. Rastigejev et al. (2010) show that CTMs have difficulty representing plume dispersion, but the plan view result of this~~

- Deleted:** is important because it cannot currently be produced using chemical transport model
- Deleted:** s
- Deleted:** .
- Deleted:** Rastigejev et al. (2010)
- Deleted:** this

process is captured in the HMS smoke plume analysis. There are other factors contributing to the modelling challenge (e.g. Lassman et al., 2017 and references within). For example, there have been a number of advances made in estimating the emissions inputs by improving burned area products (e.g. Randerson et al., 2012) and combining these with emission factors for a wider range of trace species (e.g. Akagi et al., 2011; Wiedinmyer et al., 2011). However, incorporating the full suite of emitted species into models and simulating the rapid chemical evolution of smoke remains a challenge (Alvarado et al., 2015), as is proper treatment of injection height (Paugam et al., 2016) and the timing of emissions (Saide et al., 2015). Models are also subject to uncertainty associated with meteorological inputs (Garcia-Menendez et al., 2013). Finally, running and analyzing a chemical transport model at the fine grid resolution appropriate to simulate all the individual smoke plumes of interest from North American fires over the scale of a decade is currently too computationally expensive to be practical. Thus other lenses are needed to examine how the smoke from North American fires is transported and dispersed in the atmosphere over seasonal and interannual timescales.

- Deleted: A
- Deleted:
- Deleted: have recently been
- Deleted: (e.g
- Deleted: (Randerson et al., 2012)
- Deleted: (e.g.
- Deleted:)

The two primary goals of this study are to 1) present the distribution and seasonality of fires that initiate National Weather Service (NWS) smoke forecasts, and 2) develop a regional climatology of smoke transport in the U.S. using operational data from the NESDIS HMS combined with forward trajectory calculations. Based on the subset of fires initiating smoke forecasts, HMS observations of smoke in the atmospheric column and trajectory calculations, we present an estimate of the relative frequency that smoke observed over U.S. regions is associated with fires throughout North America.

Deleted: trigger

Deleted: triggering

2 Data

2.1 Description of operational fire and smoke products

The HMS is an interactive environmental satellite image display and graphical interface system that was developed by NESDIS. Trained satellite analysts use the HMS to generate a daily operational list of fire locations and outline areas of smoke. As a part of this process, analysts manually compare automated fire detections to the mid-wave infrared (MWIR) images used to produce them to ensure each fire exists (Ruminski et al., 2006). Schroeder et al. (2008) assessed the automatic detections and estimated they have a false alarm rate of about (~2%) in the conterminous U.S. As in all satellite-based fire detection systems, small fires are more difficult to detect and are under-reported (e.g. Hu et al., 2016). Detections deemed to be false are removed, and fires that are not automatically detected are added manually. Visible satellite imagery is also used by analysts to identify fires that may be too small to be automatically detected, either because they do not produce sufficient heat or because they are obscured by a tree canopy (Rolph et al., 2009). In these cases, a smoke plume may be the only indication of a fire. The number of fire detections added manually can be significant. For example, over 50% of the total fire detections were added manually during a 12-month period in 2002-2003 examined by (Ruminski et al., 2006). Land-cover data and power-plant locations compliment satellite imagery to help HMS analysts confirm whether automatic

- Deleted: ,
- Deleted: ; there are
- Deleted: small false alarm rates

detections are fires (Ruminski et al., 2006). The HMS office makes a distinction between all detected fires (hereafter HMS hotspots) and fires an HMS analyst has confirmed to produce a substantial amount of smoke (hereafter HYSPLIT points).

HYSPLIT points are a subset of the HMS hotspots; they are fire detections where an analyst also visually confirms the presence of smoke using visible satellite imagery. HYSPLIT points are human-vetted because they are used to initialize the NWS smoke forecasts (Rolph et al., 2009; Ruminski et al., 2006). Each HYSPLIT point is assigned a latitude, longitude, date, time, and duration. The locations of HYSPLIT points are estimated to be accurate to within 2-3 km. GOES visible band and polar orbiting satellites used by the HMS have 1 km resolution at nadir. The 2-3 km accuracy of the location of HYSPLIT points is an estimate based on the additional uncertainties introduced by navigation errors and loss of resolution for observations made away from nadir. Visible satellite imagery was available every 30 minutes during the study period, HMS analysts estimate that this makes the start time of smoke emissions accurate to within 1-2 hours. However, fires can continue to generate smoke after sunset when visible imagery is no longer available. Single fires that produce notable amounts of smoke are associated with a cluster of co-located, or nearly co-located, HYSPLIT points assigned roughly in proportion to the amount of smoke observed. The intended operational consequence of designating HYSPLIT points this way is to allow the NWS smoke forecast model to generate more smoke for large fires and less smoke for smaller fires.

The HMS office does not make any distinctions between sources of smoke. HYSPLIT points can be associated with agricultural burning, prescribed burning, or wildfires (Ruminski et al., 2006). The number of HYSPLIT points analyzed, multiplied by their respective duration (Smoke Production Duration Hours or SPDH) is proportional to visual smoke produced for the land cover in which it is burning, and the analyst determines this relationship. The relationship between smoke quantity (as defined by particulate matter concentration [$\mu\text{g m}^{-3}$] or kg of emissions for example) and HYSPLIT points is variable and does not account for land cover. Large wildfires are represented by dozens of HYSPLIT points spread over many square kilometers. These are typically in the western U.S., Canada, and Alaska. The start times of HYSPLIT points can vary within the cluster of points. Operationally, this serves to represent the variability in the amount of smoke observed at different times of the day. For example, during a large wildfire event, analysts may create several HYSPLIT points with a 24-hr duration starting at 08 UTC (middle of the night local time). They also create another set of HYSPLIT points in the vicinity that are assigned a shorter duration and a start time of 20 UTC (early afternoon local time). The operational intention of this strategy is to force the NWS smoke forecast model to produce more smoke in the afternoon and evening and less overnight to replicate observed diurnal trends. HYSPLIT points can also be proxies for unobservable smoke producing fires. When analysts see a large number of HMS hotspots, but due to cloud cover do not directly observe smoke, they create HYSPLIT points in order to initiate the NWS smoke forecast model. This occurs most frequently in Kansas, Oklahoma, the Northern Plains (Dakotas), and the lower Mississippi Valley (eastern Arkansas, eastern Louisiana, western Mississippi). The Servicio Meteorológico Nacional (SMN, the Mexican National Weather Service) provides most HYSPLIT points over Mexico. These locations are merged with the HMS product. Occasionally the HMS office will perform fire-

Deleted: The accuracy of the duration is a bit more uncertain since many of the

Deleted: However, it is believed that the duration accuracy for most HYSPLIT points is within 2 hours.

Deleted: Single fires that produce notable amounts of smoke are associated with a cluster of co-located, or nearly co-located, HYSPLIT points in proportion to the amount of smoke observed. The intended operational consequence of designating HYSPLIT points in proportion to the amount of smoke observed is to allow the NWS smoke forecast model to generate more smoke for large fires and less smoke for smaller fires.

Deleted: There is a relationship between the number of HYSPLIT points and the amount of smoke produced by fires, and the analyst determines this relationship.

Deleted: P

detection analysis in parts of Northern Mexico. The archives of smoke and fire locations spans from August 2005 to present day; but the analysis presented here spans 2007–2014. These archives include text files for HYSPLIT points and HMS hotspots and GIS shapefiles for smoke plumes.

This analysis uses data from 2007–2014 for two reasons. First, prior to April 2006 HYSPLIT points did not have duration or start-time estimates. Second, the HMS implemented a system that automatically generates HYSPLIT points in Northern Canada, Mexico, and Central America in the fall of 2014. This change in procedure resulted in more HYSPLIT points than each of the prior years, and there were many more instances of HYSPLIT points assigned durations of 24 hours. The majority of fires in Northern Canada are wildfires in boreal forests, so each of these automated HYSPLIT points is assigned a duration of 24 hours whereas prior to this it would have received a mix of 24 hour and lesser durations. The intention of the automated system was to reduce the workload of analysts. A similar automated system was implemented for Alaska in 2009. However, this implementation did not lead to a significant change in the proportion of HYSPLIT points with durations of 24 hours analyzed in North America. Prior to Fall 2014 the HYSPLIT points in Mexico and Central America were intended to be generated by SMN, but at some point in the years prior to 2014 SMN began performing HYSPLIT point analysis inconsistently. As a result, NESDIS developed an automated system based on HMS hotspots. The durations for these HYSPLIT points are estimated using the difference between the latest and earliest time for hotspots aggregated into a 20 km grid.

HYSPLIT points are sometimes analyzed at hours when no visible satellite imagery is available to confirm smoke production. This only occurs when the thermal signal in the MWIR imagery is significant in terms of intensity and duration (e.g. strong downslope winds at night can cause significant nighttime fire activity). Wildfires can burn for weeks or even months. For the long-lived wildfire scenario, HMS analysts will get two looks daily at a fire from a given polar satellite. One look overnight (in the Western U.S. between 08 – 10 UTC) and another in the afternoon (20 – 22 UTC). Analysts will add HYSPLIT points at both of those times. For the nighttime pass, fires are often not burning as actively (fewer hotspots). Analysts will add HYSPLIT points based on the fewer number of hotspots and typically assign them a 24-hr duration (i.e. total hours smoke production observed), creating a baseline for emissions. In the afternoon, fires are more active and generate more smoke so analysts will add additional HYSPLIT points based on the afternoon satellite data. In this case, they only assign durations of 10 or 12 hours. The operational significance of these procedures is to attempt to account for the diurnal variations in smoke production in initializing smoke forecasts.

HYSPLIT Points are analyzed in all 50 U.S. States as well as all Canadian Provinces and Territories. Figure 2 shows the location of all HYSPLIT points analyzed between 2007–2014 shaded by the analyzed duration. Dense clusters of 24-hour duration HYSPLIT points are analyzed in regions with active wildfire seasons (e.g. Rocky Mountains, Cascade Mountains, Northern California, Northwest Territories). The Midwest, Great Plains, and Southeast U.S. have many smaller short-lived fires where most HYSPLIT point durations are 12 hours or less. The smoke observed from small short-lived fires

Deleted: result

Deleted: short lived

in the Mississippi River valley is consistent with other studies that consider burn area from small fires (Randerson et al., 2012).

2.2 Description of HMS smoke analysis

After identifying HYSPLIT points, HMS analysts use imagery from multiple NOAA and NASA satellites to identify the geographic extent of smoke-plumes (Rolph et al., 2009; Ruminski et al., 2006). Smoke detection is done with visible-band imagery occasionally assisted by infrared to distinguish between clouds and smoke when possible (Ruminski et al., 2006). Geostationary GOES imagery, with its frequent refresh rate (typically every 15 minutes for each spacecraft), is used almost exclusively for smoke detection, although on rare occasions polar orbiting satellite imagery is used. Given the limitations of the satellite data (mostly obscuration of smoke due to cloud cover), the number and extent of smoke plumes within this dataset represents a conservative estimate. Due to the limitations of visible satellite imagery and time constraints, no information about the vertical location or extent of smoke plumes is provided. In 2006 HMS analysts began providing estimates of smoke-plume concentrations (e.g. 5 $\mu\text{g}/\text{m}^3$, 16 $\mu\text{g}/\text{m}^3$, and 27 $\mu\text{g}/\text{m}^3$). These plumes of varying concentrations are often nested (e.g. 27 $\mu\text{g}/\text{m}^3$ within 16 $\mu\text{g}/\text{m}^3$ and 16 $\mu\text{g}/\text{m}^3$ within 5 $\mu\text{g}/\text{m}^3$). Smoke plumes vary in size considerably; small plumes cover areas < 100 km² and others cover several western states. Between 5 August 2005 and 21 December 2015 there are only 80 days (~2%) where there are either no smoke plume GIS files available or no smoke-plumes analyzed. Most of these days occur during winter months. Rolph et al. (2009) used the HMS smoke plumes to validate NOAA's operational smoke forecasting system. There is no published validation of the HMS smoke plume extent data. It could have systematic biases because discrimination of smoke is easier over some areas, seasons, and under certain synoptic weather conditions. For our aggregate smoke plume analysis, the largest uncertainty is at the edges of the plumes. The temporal information is also a source of uncertainty. During the day, the extent can be assessed hourly. However, this is not possible overnight. Smoke is sometimes transported to areas with anthropogenic haze pollution. In some cases the smoke will mix with and become indistinguishable from the anthropogenic haze pollution. The greater the distance travelled by a smoke plume, the more challenging it is to distinguish between smoke and anthropogenic haze. This challenge is particularly pronounced for aged smoke impacting the Southeastern U.S. For this work, we use the archived GIS smoke-plume files available at the following URL <ftp://satepsanone.nesdis.noaa.gov/FIRE/HMS/GIS/>.

Deleted: Smoke is sometimes transported to areas with anthropogenic haze pollution. In some cases the smoke will mix with and become indistinguishable from the anthropogenic haze pollution. The greater the distance traveled by a smoke plume, the more challenging it is to distinguish between smoke and anthropogenic haze. This challenge is particularly pronounced for aged smoke impacting the south-eastern

Deleted: traveled

Deleted: south-eastern

2.3 Description of land cover characteristics database

We assign each HYSPLIT point a land cover type using land-cover classifications from the U.S. Geological Survey (USGS) 2002 North American Land-Cover Characteristics 1 km grid-spacing dataset, created by the National Center for Earth Resources Observation and Science (EROS) as part of the Global Land Cover Characterization Project (Brown, 2016). Land-cover characteristics are assessed using 1 km Advanced Very High Resolution Radiometer (AVHRR) data between 1992 and

1993 using the methods described in (Anderson et al., 1976). For this work, we use the GeoTIFF file projected to latitude-longitude grid as a geospatial raster (Brown, 2016). The latitudinal extent is 18°N - 72°N and 66°W - 172°W. We assign land-cover classifications to HYSPLIT points based on the nearest grid-point center that is not classified as urban or water. When urban or water is the closet grid-point, we substituted the assigned land-cover type with the most common other land-cover classification in the surrounding 0.06 degrees (~5 km) land-cover grid-cells. If all surrounding grid cell land-cover classifications are urban or water, no land-cover assessment is made. Data are available at https://nationalmap.gov/small_scale/mld/landevi.html. We point readers to Hansen et al. 2000 for a discussion of the weaknesses of the 1992 land-cover dataset. We have also completed a comparison to a 2010 land-cover dataset, and this comparison is available in the Supplemental Information Sect 9.

Comment [4]: The URL that used to be here is no longer active. It looks like USGS now hosts data to download with Amazon. I am providing this URL which describes the data and has a link to download the exact 2002 data used in this analysis. Linking to the exact download URL is probably not a good long term solution for people being able to find these data.

Deleted: <https://www.sciencebase.gov/catalog/item/535fe572e4b078dca33ae61f>.

3 Comparison to Global Fire Emissions Database Version 4s (GFED4s)

The number of HYSPLIT points assigned to a fire is intended to be proportional to the amount of smoke observed. We gridded HYSPLIT points and compared them to the Global Fire Emissions Inventory Database (GFED; <http://www.globalfiredata.org/data.html>) version 4s (Giglio et al., 2013; Randerson et al., 2012; van der Werf et al., 2010). To compare HMS emissions to GFED4s we count the total duration associated with all HYSPLIT points that fall within each GFED4s grid cell for each month between 2007 and 2014. The units of our new gridded emission inventory are thus duration hours per 0.25° x 0.25° grid box, hereafter referred to as HMS smoke production duration hours (SPDH). GFED4s produces emissions estimates in kg of carbon. Figure 3 shows a comparison of the cumulative gridded SPDH and monthly GFED4s kg carbon emissions over North America for June to September 2007 to 2014 (32 months). The dark red areas in Fig. 3 show the locations where SPDH and GFED4s kg carbon emissions have maximum cumulative values for this time period. Figure 3 shows agreement between the two datasets for the locations of their respective maxima in summer, with some notable differences. For example, GFED4s shows the lower Mississippi river valley as an area with significant fire emissions, but this area is not as prominent in the HMS derived dataset. The HMS dataset also show larger extents of local maximums of fire activity compared to GFED4s (e.g. North Central Idaho, North Cascades, Gila National Forest). The spatial agreement for locations with maximum emissions holds when we compare individual summers between 2007 and 2014 (not shown). For example, both emission inventories agree on the geographical location and extent of the 2013 Quebec fires, an anomalously high fire year for Quebec.

Figure 3c presents the cumulative June through September 2007 to 2014 SPDH (Fig. 3a) divided by GFED4s kg of carbon (Fig. 3b) for each grid cell. Areas represented by the same color can be interpreted as locations where the total HMS smoke production duration hours assigned to observed fires is consistent with a given quantity of carbon emitted according to GFED4s. Fig. 3c shows that the relationship between SPDH and GFED4s kg of carbon varies by several orders of

Deleted: As expected based on varying emission factors for different ecosystems,

magnitude. The largest ratios are observed in North Dakota and southern Manitoba, the southern Mississippi River Valley, Sinaloa Mexico, and over interior Alaska. [The GFED4s estimate of grams of carbon emitted is a function of the estimated burn area, combustion efficiency, soil moisture, land cover type, fuel loading, and emission factors \(Giglio et al., 2013; Randerson et al., 2012; van der Werf et al., 2017\).](#) The observed difference between SPDH and GFED4s total grams of carbon emitted could be due to any of these factors.

Deleted: the estimated

Deleted: , fuel moisture content

When considering the entire North American domain (15 - 80°N, 50 - 170°W), summed monthly emissions of both SPDH and GFED4s kg of carbon time series, we observe that the magnitudes of the two inventories are also correlated temporally. Figure 4 shows the normalized domain summed monthly time series for all months between 2007 and 2014. The Pearson correlation coefficient for the two time series is 0.842, confirming that at large scales the two emission inventories are well-correlated. In 2007 and 2008 the normalized HMS duration hours greatly exceed normalized GFED4s emissions. The difference in 2007 is due to large smoke production in the Northwest and Rocky Mountain regions present in the HMS data. In 2008 extreme smoke production associated with fires in the Southwest are responsible for the discrepancy. Figure 5 shows the Pearson correlation coefficient for the monthly 8-year time series for each grid cell. Locations with large wildfires (Fig. 2) are well correlated between the two datasets ($r > 0.90$). Locations with small fires like the Southeast, Southern Plains, and Northern Great Plains have lower correlation values ($r < 0.20$). [Small fires are difficult to detect from satellite.](#) The high correlation between SPDH and GFED4s kg carbon demonstrate that [spatial and temporal aggregates of](#) the duration field of HYSPLIT points is roughly proportional to the amount of smoke produced by analyzed fires, though that proportionality varies.

4 HYSPLIT point regional distributions

Figure 6 designates 10 U.S. regions that closely align, but do not exactly overlap, with EPA regions. Figure 7a presents the total number of HYSPLIT points aggregated for each region. The largest numbers of HYSPLIT points are identified in the Southwest, Northwest, Northwest Territories, and Southeast regions. Figure 7b shows the total SPDH produced by each region and the percentage of SPDH that are produced by HYSPLIT points analyzed on cropland. For most regions over the course of the entire year, the percent of SPDH owed to cropland is less than 5%. However, the relative importance of cropland fires has a strong seasonality. Notable exceptions are the U.S. Southeast and the Southern Plains, where the SPDH from cropland > 25%. Figure 8 presents the seasonality of North American HYSPLIT points between 2007-2014, and it shows that the majority of HYSPLIT points are identified between June and August. During these months, the dominant land cover classification for HYSPLIT points is evergreen needleleaf forest, followed by a nearly equal share of scrubland and mixed forest. When viewed in aggregate, the contribution to HYSPLIT points from cropland is largest in the months of April, September, and October. [When we assess the land cover classification of HYSPLIT points using a 2010 land cover](#)

Deleted: Planes

Deleted:

dataset, the most common alternative assignment for the most abundant cropland assignment type (“cropland/grassland mosaic”) is “temperate subpolar grassland”. Regional differences for alternative assignments exist. For example, in the U.S. Midwest and Great Plains, the most common alternative land cover assignment for cropland is “temperate subpolar grassland” while in the Southeast U.S. the most common alternatives are “temperate subpolar needleleaf forests” and “wetland”. These 2010 data show that the most common alternative land cover assignment for forested lands in North America is “subpolar shrubland”. Maps and bar graphs showing the differences in land cover assignments for HYSPLIT points between the 1992 and 2010 data are available in the Supplemental Information Sect 9.

Figure 9 shows the locations, seasonality, and duration of HYSPLIT points in the 9 contiguous U.S. regions shown in Fig. 8 between 2007 and 2014. The land cover classification for the seasonality and duration histograms is indicated by color using the same color scheme as Fig. 8. HYSPLIT points with durations of 24 hours are usually associated with wildfires. HYSPLIT points with shorter durations represent smaller fires, and often occur on cropland. At the national scale shown in Fig. 8, grassland and cropland land cover classifications make up a small proportion of the total HYSPLIT points throughout the year. However as discussed above at the regional scale, grassland and cropland HYSPLIT points can represent a significant fraction or even dominate the total number of HYSPLIT points. Figure 9 shows this is the case for the Great Plains, Midwest, and Southern Plains. These regions also have the fewest HYSPLIT points analyzed in the summer months, whereas regions dominated by evergreen forest have a minimum in the winter. The Southwest has more HYSPLIT points than any other U.S. region, followed by the Northwest, Southeast, and Southern Plains. The Northeast has the fewest HYSPLIT points, which occur mostly on cropland in southern New Jersey. The Mississippi river valley has some of the most densely analyzed HYSPLIT points in the U.S, and these points are located most commonly on forest and cropland. These points are split between the Southeast and Southern Plains regions. The same HYSPLIT point duration and monthly histograms presented in Fig. 9 are available for all regions in the supplemental information.

There are more HYSPLIT points analyzed in the Southern Plains (n=41,846) than there are in the Rocky Mountains region (n=35,371). However, this does not indicate that the Southern Plains generate more smoke, because the number of points does not include information on fire duration or land cover (discussed in Sect 2.1 and 3.0). The total smoke produced in a region should be roughly proportional to the number of HYSPLIT points multiplied by their respective durations (Fig. 7b). Most of the fires in the Southern Plains have durations less than nine hours while the most-common duration of HYSPLIT points in the Rocky Mountains region is 24 hours. Alaska (not shown) is an extreme example. Almost all of the HYSPLIT points in Alaska have 24-hour durations. This is by design, since 2009 all HYSPLIT points in Alaska have been assigned 24-hour durations, which is consistent with the types of fires that occur within the state.

Deleted: 3.0

5 Smoke-transport analysis

5.1 Forward trajectories

Forward HYSPLIT trajectories are initialized from each of the HYSPLIT points over the duration of the fires and they represent likely smoke transport pathways. We initialize HYSPLIT trajectories at three different altitudes that span the range of injection heights expected for North American fires based on a prior analysis. Val Martin et al. (2010) present a climatology of smoke-plume heights by land biome for North America. The smoke-plume heights were estimated with the Multi-angle Imaging SpectroRadiometer (MISR) data, and thus could represent an underestimate of the actual injection height due to the timing of the MISR overpass. A given fire can inject smoke into the atmosphere at many different altitudes. We initialize each HYSPLIT trajectory start hour at three different altitudes spanning the range of injection heights in Val Martin et al. (2010): 500, 1500, and 2500 m amgl. In total, 3,925,932 trajectories are associated with the 517,214 HYSPLIT points analyzed between 2007 and 2014. For this analysis, trajectories are only considered for the hours that the calculated height above ground level is > 0 . Each trajectory was run using the Global Data Assimilation System (GDAS) 1-degree meteorology data and the Eta Data Assimilation System (EDAS) 40km meteorology data. Further specifics on the meteorology data, the HYSPLIT model, and how we ran trajectories for this analysis can be found in Sect S1 of the Supplemental Information.

Deleted: ,

Deleted: ,

5.2 Combined analysis of HYSPLIT points and forward trajectories

To build smoke source-receptor relationships for 10 U.S. regions, we define a “smoke hour” as an hourly latitude-longitude HYSPLIT trajectory location (hereafter trajectory point) that overlaps a HMS smoke plume. We use these smoke hours to represent the relative abundance of probable smoke transport pathways. Smoke plume overlap assessments are made using a two-step process which reduces the number of trajectories included in the analysis initialized at heights that do not represent the smoke injection height of a given fire. Spatial overlap analysis is performed using the R Sp package *over* function (Pebesma et al., 2016). This code and further information on the procedure used can be found in Supplemental Information Sect S3 and S11.

1) We confirm that at least one of the first 49 trajectory points (2 days + start hour) overlap a smoke plume analyzed for the same two dates. If none of the first 49 trajectory points overlap a smoke plume, the trajectory is immediately discarded. If any of the first 49 trajectory points overlap a smoke plume, plume-overlap analysis is performed for the entire trajectory (145 trajectory points). We determine the relevance of a trajectory using two days of smoke plumes because smoke plumes only represent smoke perimeters during daylight hours. By including the next-dates smoke plumes in the test, trajectories associated with fires that start in the afternoon are not evaluated more stringently than trajectories associated with

HYSPLIT points for fires in the morning. The results do not change significantly when validating trajectories with only the first-days smoke plumes.

2) When trajectories meet our first criteria, a point over polygon calculation is done for each matching date trajectory point and smoke plume. There are two weaknesses to this approach: 1) Smoke-plume boundaries are only representative of smoke-plume perimeters during daylight hours, while trajectories exist at both day and night. 2) Some HMS smoke plumes on individual days are very large; during extreme-smoke events plumes can cover most of the continental U.S., and thus this criteria is not always meaningful. Smoke plumes with different concentration estimates are often nested. For this analysis, these smoke plumes are merged, so a trajectory point can only overlap a single plume and contribute one smoke hour. Each trajectory smoke hour is associated with the source region and land cover classification from its initialization point, allowing a source region and land classification analysis of the total number of smoke hours impacting or emanating from a region. This methodology does not provide information about smoke concentration ($\mu\text{g}/\text{m}^3$), and we have not placed additional altitude constraints on the trajectories. [A further weaknesses of smoke hours is that they have no way of accounting for secondary organic aerosol particle formation, which previous studies have shown can be significant \(e.g. Janhäll et al., 2010; Sakamoto et al., 2015, 2016\). However, these processes remain poorly understood and represented in chemical transport models, so an appreciation for the fact that these processes exist, but not attempting to account for them, is sufficient for understanding the results presented in this work.](#)

5.3 Smoke production and frequency by region

Figure 10 shows the total number of smoke hours produced by and present over each region. Years with elevated fire activity in each region can be easily identified using Fig. 10. This figure provides context for isolated case studies of smoke transport associated with extreme periods including the summer 2013 Quebec wildfires (Laffineur et al., 2014), the summer 2012 wildfires in the Rocky Mountain region (Val Martin et al., 2013b), and the 2008 California wildfires (SW Region) (Gyawali et al., 2009). Supplemental Table S3 shows the total smoke hours produced by and over each U.S. region and the differences between using the GDAS and EDAS meteorology datasets for the trajectory calculations.

5.4 Smoke transport climatology: Attribution, age and altitude

Figure 11 shows a summary of smoke transport to contiguous U.S. regions between 2007 and 2014 for the months of June, July, August, and September. The first histogram associated with each region shows the distribution of the age (hour in HYSPLIT trajectory) of smoke hours in the atmospheric column above each region separated by the region of origin. The second histogram associated with each region shows the distribution of the height of the smoke in the column above each region (height of the HYSPLIT trajectories). For a given fire, older smoke is more likely to deliver lower $\text{PM}_{2.5}$ concentrations than smoke that is only a few hours old. For example, the Great Plains region has more smoke hours (12.3

Deleted: s

million hours) than the Northwest (12.1 million hours) and more than the Southwest (10.1 million); however, the average age of smoke hours over the Great Plains is ~one day older than in the Northwest and Southwest.

On average regions that produce the most smoke hours during the summer have more smoke at lower altitudes (*e.g.* Northwest and Rocky Mountains), and the smoke is located at higher altitudes over regions far downwind of summertime fire activity (*e.g.* Northeast). The impact of our choices of 500, 1500, and 2500 m trajectory starting height is apparent in the panels showing trajectory altitude; the majority of the smoke-hours defined over every U.S. region are between these altitudes. There are clear maxima in the number of smoke hours defined at 500, 1500, and 2500 m over source regions that are not receptors of aged smoke hours.

Regions with the largest number of HYSPLIT points tend to contribute the largest proportion of the total smoke hours within their own borders. For example, the smoke impacting the Southwest originates almost exclusively within the Southwest. Smoke present over the Northwest is nearly equally likely to be associated with fires from the Northwest or Southwest. Regions with comparatively little local fire activity have a diverse set of source regions contributing to their total column smoke hour budgets; examples include the Southern Plains, the Northeast, and the Midwest. Due to the difficulty in detecting small fires, it is possible that the smoke hour budget in these regions underestimates local contributions of smoke in these regions. The Northwest, Southwest, and Rocky Mountains dominate most other regions total smoke hours; fires in Canada make a major contribution to smoke hours, particularly over the Midwest and the Northeast. The only regions where the three largest contributors of smoke hours are not the Southwest, Northwest, and Rocky Mountains, are the Southeast, Northeast, the Southern Plains and Alaska (not shown). The only regions that contribute more smoke hours to their own total budget than any outside region are the Southwest, the Northwest, and the Southeast. When the analysis presented in Fig. 11 is generated with trajectories run using EDAS meteorology data, the interpretation of the results is nearly identical and they are available in Sect S7 of the Supplemental Information.

Deleted: are

5.5 Common regional smoke transport pathways

The Northwest, Southwest, and Rocky mountains produce more smoke hours than any other U.S. regions (Fig. 10). Figure 12 shows the average smoke-transport pathways for fires in these regions for June to September between 2007 and 2014, and it was generated by summing smoke hours. This figure is not a simple trajectory climatology, rather it is a trajectory climatology when smoke-producing fires occur. Smoke produced by fires in California is transported most frequently over Northern California and Eastern Oregon (Fig. 12b). Based on our analysis of the HYSPLIT points these fires occur primarily in evergreen needleleaf forests. Smoke originating from fires in the Northwest is transported most frequently over Eastern Washington, Eastern Oregon, Northern Idaho, and Montana (Fig. 12a). Smoke from fires in Alaska impact every U.S. and Canadian region (not shown). The dominant transport pathway for the smoke crosses Alaska, the Northwest Territories, and

Deleted:

Yukon Territory. Smoke traveling from Alaska to Texas has been observed previously (Morris et al., 2006), but this situation is relatively rare when viewed in an aggregate context (Supplemental Information Fig. S3a).

Figure 13 summarizes the climatology of the abundance of smoke hour transport for U.S. regions between June and September 2007 to 2014. The Northwest, Southwest, and Rocky Mountains are responsible for the majority of U.S. summertime smoke hour production. They are also among the smokiest regions by measure of smoke hours overhead and smoke hour age. These three regions also dominate the total smoke hours overhead for all U.S. regions excluding the Southeast and Alaska.

Figure 1 shows that the U.S. Midwest has more smoke plumes overhead than the Northwest and Southwest while Fig. 13 shows that the Northwest and Southwest are the largest U.S. producers and receptors of smoke hours. This occurs because smoke hours are proportional to total smoke while the plumes in Fig. 1 represent the total count of overhead plumes and contains no information about smoke concentration. This contrast shows that there are many dilute smoke plumes over the Midwest since it is downwind of so many smoke producing regions. The Northwest and Southwest by comparison have fewer plumes overhead but are located much closer to fire activity. Plumes over the Northwest and Southwest represent higher smoke concentrations than the plumes observed over Midwest.

6 Conclusions

This work moves a new dataset from a daily operational setting to a research context. We define smoke hours, a quantity designed to be proportional to total column smoke, by linking observed smoke plumes to observed fires using HYSPLIT trajectories. [The location of smoke hours is restricted to locations where HMS analysts have drawn smoke plumes while the height is estimated from HYSPLIT forward trajectories emanating from HYSPLIT points.](#) This work shows that the Southwest, Northwest, and Northwest Territories [initiate](#) the most air quality forecasts, and produce more smoke than any other North American region by measure of the number of HYSPLIT points [analyzed](#), the duration of those HYSPLIT points, and the total number of smoke hours produced (Fig. 3, 10-13). This dataset confirms that there is a substantial amount of smoke-producing fire activity in the Southeast, particularly along the lower Mississippi River Valley. [This is likely an underestimate of the contribution of small fires to smoke abundance in this region given that small fires within this region can be substantially under-detected \(Hu et al., 2016\). In addition, it can be challenging to differentiate anthropogenic haze from smoke in this region.](#)

During the summer wildfire season, the largest smoke [plume](#) source regions are located in the west, while receptor regions for smoke [plumes](#) are primarily located in the east. The majority of smoke [plumes](#) located over western source regions [are](#) less than 24 hours old. During summer, our analysis implies that the receptor regions have very little smoke less than 24 hours old with most smoke in the column older than 48 hours. The Southeast is a unique exception. There is an

Deleted: trigger

Deleted:

Deleted: is

abundance of fresh smoke [hours](#) (peak near zero hours in Fig. 11) due to the numerous small fires within the region, and this region receives aged smoke [hours](#) (<48 hours of atmospheric aging) from several upwind regions. [Due to the challenge of distinguishing aged smoke plumes from anthropogenic haze in the Southeast, the abundance of aged smoke hours is likely underestimated in this region.](#) Though not the focus of the paper, this dataset shows that the Northeast and Mid Atlantic receive more smoke from fires in Canada than regions in the U.S. Midwest.

We present a smoke transport climatology for the summer wildfire season. Based on our metric of smoke hours, the U.S. regions that produce the most smoke are the Northwest, Southwest, and Rocky Mountains (Fig. 10 and 13). Heavily populated locations in the eastern U.S. (Northeast, Mid Atlantic, Southeast) are routinely impacted by wildland fire smoke from western regions. [Thus](#), changes to the frequency or intensity of fires in the U.S. west or Canada is likely to impact the entire U.S. airshed.

7 Code availability

All analysis code associated with this project is available online at the following subversion repository: <http://salix.atmos.colostate.edu/svn/smokeSource/>. The code for the Python module used to execute HYSPLIT Trajectories is available at the following GitHub repository: <https://github.com/samatwood/HYSPLITm/>. All figures were created using R and Python. Scripts used to make figures can be identified by a leading “plot” in script names (e.g. R/plotRegionSmokeTotals.R). These scripts explicitly reference the data files used to create the plots.

8 Data availability

All data for this project are publicly available at the URLs specified in Sect 2. Formatted analysis level data and the code used to format the raw data described in Sect 2, are available in the subversion code repository.

9 Author contributions

S. Brey and E. Fischer prepared the manuscript with contributions from all co-authors. E. Fischer was the leader of this research project. S. Brey performed the majority of analysis, including writing analysis code, creating figures, and executing HYSPLIT trajectories. M. Ruminski is responsible for creating, describing, and properly interpreting Hazard Mapping System HYSPLIT points and smoke plume data. S. Atwood wrote the Python module used to run HYSPLIT Trajectories and served as our expert for best practices in the use of HYSPLIT source-receptor analysis.

10 Competing interests

The authors declare that they have no conflict of interest.

11 Acknowledgements

5 [This publication was developed under Assistance Agreement No. 83588401 awarded by the U.S. Environmental Protection Agency to Emily V. Fischer. It has not been formally reviewed by EPA. The views expressed in this document are solely those of the authors and do not necessarily reflect those of the Agency. EPA does not endorse any products or commercial services mentioned in this publication.](#) Bonne Hotmann made significant science and style contributions to Fig. 1. We gratefully acknowledge the skill and dedication of NESDIS Hazard Mapping System analysts; their careful operations are responsible for the dataset presented in this paper. The authors would like to thank Ana Rappold for her work using HMS, 10 which strengthened and guided the early stages of this analysis, and for a brainstorming phone call in January 2016 which helped spark the authors interest in performing this work. Parts of this work were included in Steven Brey's masters thesis. His graduate committee, Elizabeth Barnes, Jeffery Pierce, and Monique Rocca made this work stronger. The authors gratefully acknowledge Matt Bishop for his help in enabling us to execute millions of HYSPLIT trajectories on our local computer cluster. The authors gratefully acknowledge the NOAA Air Resources Laboratory (ARL) for the provision of the 15 HYSPLIT transport and dispersion model and READY website used in this paper. The authors would also like to thank the core development teams of R and Python for making open source languages that are free and help advance scientific discovery.

References

- 20 [Akagi, S. K., Yokelson, R. J., Wiedinmyer, C., Alvarado, M. J., Reid, J. S., Karl, T., Crouse, J. D. and Wennberg, P. O.: Emission factors for open and domestic biomass burning for use in atmospheric models, *Atmos Chem Phys*, 11\(9\), 4039–4072, doi:10.5194/acp-11-4039-2011, 2011.](#)
- 25 [Alvarado, M. J., Lonsdale, C. R., Yokelson, R. J., Akagi, S. K., Coe, H., Craven, J. S., Fischer, E. V., McMeeking, G. R., Seinfeld, J. H., Soni, T., Taylor, J. W., Weise, D. R. and Wold, C. E.: Investigating the links between ozone and organic aerosol chemistry in a biomass burning plume from a prescribed fire in California chaparral, *Atmos Chem Phys*, 15\(12\), 6667–6688, doi:10.5194/acp-15-6667-2015, 2015.](#)
- [Anderson, J. R., Hardy, E. E., Roach, J. T. and Witmer, R. E.: A land use and land cover classification system for use with remote sensor data, USGS Numbered Series. \[online\] Available from: <http://pubs.er.usgs.gov/publication/pp964> \(Accessed 23 August 2016\), 1976.](#)

Deleted: -

... 11

- Baker, K. R., Woody, M. C., Tonnesen, G. S., Hutzell, W., Pye, H. O. T., Beaver, M. R., Pouliot, G. and Pierce, T.: Contribution of regional-scale fire events to ozone and PM_{2.5} air quality estimated by photochemical modeling approaches, *Atmos. Environ.*, 140, 539–554, doi:10.1016/j.atmosenv.2016.06.032, 2016.
- 5 Brey, S. J. and Fischer, E. V.: Smoke in the City: How Often and Where Does Smoke Impact Summertime Ozone in the United States?, *Environ. Sci. Technol.*, 50(3), 1288–1294, doi:10.1021/acs.est.5b05218, 2016.
- Brown, J.: USGS Small-scale Dataset - North American Land Cover Characteristics - 1-Kilometer Resolution 200212 GeoTIFF - ScienceBase-Catalog. [online] Available from: <https://www.sciencebase.gov/catalog/item/535fe572e4b078deca33ae61f> (Accessed 12 July 2016), 2016.
- 10 Creamean, J. M., Neiman, P. J., Coleman, T., Senff, C. J., Kirgis, G., Alvarez, R. J. and Yamamoto, A.: Colorado air quality impacted by long range transport: A set of case studies during the 2015 Pacific Northwest fires, *Atmospheric Chem. Phys. Discuss.*, 1–35, doi:10.5194/acp-2016-280, 2016.
- Dennekamp, M. and Carey, M.: Air quality and chronic disease: why action on climate change is also good for health, *New South Wales Public Health Bull.*, 21(5–6), 115–121, doi:10.1071/NB10026, 2010.
- 15 Dennis, A., Fraser, M., Anderson, S. and Allen, D.: Air pollutant emissions associated with forest, grassland, and agricultural burning in Texas, *Atmos. Environ.*, 36(23), 3779–3792, doi:10.1016/S1352-2310(02)00219-4, 2002.
- Forrister, H., Liu, J., Scheuer, E., Dibb, J., Ziemba, L., Thornhill, K. L., Anderson, B., Diskin, G., Perring, A. E., Schwarz, J. P., Campuzano-Jost, P., Day, D. A., Palm, B. B., Jimenez, J. L., Nenes, A. and Weber, R. J.: Evolution of brown carbon in wildfire plumes, *Geophys. Res. Lett.*, 42(11), 2015GL063897, doi:10.1002/2015GL063897, 2015.
- 20 Garcia-Menendez, F., Hu, Y. and Odman, M. T.: Simulating smoke transport from wildland fires with a regional-scale air quality model: Sensitivity to uncertain wind fields, *J. Geophys. Res. Atmospheres*, 118(12), 6493–6504, doi:10.1002/jgrd.50524, 2013.
- Giglio, L., Randerson, J. T. and van der Werf, G. R.: Analysis of daily, monthly, and annual burned area using the fourth-generation global fire emissions database (GFED4), *J. Geophys. Res. Biogeosciences*, 118(1), 317–328, doi:10.1002/jgrg.20042, 2013.
- 25 Gyawali, M., Arnott, W. P., Lewis, K. and Moosmüller, H.: In situ aerosol optics in Reno, NV, USA during and after the summer 2008 California wildfires and the influence of absorbing and non-absorbing organic coatings on spectral light absorption, *Atmos Chem Phys*, 9(20), 8007–8015, doi:10.5194/acp-9-8007-2009, 2009.
- 30 Haikerwal, A., Akram, M., Monaco, A. D., Smith, K., Sim, M. R., Meyer, M., Tonkin, A. M., Abramson, M. J. and Dennekamp, M.: Impact of Fine Particulate Matter (PM_{2.5}) Exposure During Wildfires on Cardiovascular Health Outcomes, *J. Am. Heart Assoc.*, 4(7), e001653, doi:10.1161/JAHA.114.001653, 2015.
- Hansen, M. C., Defries, R. S., Townshend, J. R. G. and Sohlberg, R.: Global land cover classification at 1 km spatial resolution using a classification tree approach, *Int. J. Remote Sens.*, 21(6–7), 1331–1364, doi:10.1080/014311600210209, 2000.

- Hu, X., Yu, C., Tian, D., Ruminski, M., Robertson, K., Waller, L. A. and Liu, Y.: Comparison of the Hazard Mapping System (HMS) fire product to ground-based fire records in Georgia, USA, *J. Geophys. Res. Atmospheres*, 121(6), 2015JD024448, doi:10.1002/2015JD024448, 2016.
- 5 Hurteau, M. D., Westerling, A. L., Wiedinmyer, C. and Bryant, B. P.: Projected Effects of Climate and Development on California Wildfire Emissions through 2100, *Environ. Sci. Technol.*, 48(4), 2298–2304, doi:10.1021/es4050133, 2014.
- Jaffe, D., Chand, D., Hafner, W., Westerling, A. and Spracklen, D.: Influence of fires on O-3 concentrations in the western US, *Environ. Sci. Technol.*, 42(16), 5885–5891, doi:10.1021/es800084k, 2008.
- Janháňal, S., Andreae, M. O. and Pöschl, U.: Biomass burning aerosol emissions from vegetation fires: particle number and mass emission factors and size distributions, *Atmos Chem Phys*, 10(3), 1427–1439, doi:10.5194/acp-10-1427-2010, 2010.
- 10 Jimenez, J., Wu, C.-F., Claiborn, C., Gould, T., Simpson, C. D., Larson, T. and Sally Liu, L.-J.: Agricultural burning smoke in eastern Washington—part I: Atmospheric characterization, *Atmos. Environ.*, 40(4), 639–650, doi:10.1016/j.atmosenv.2005.09.071, 2006.
- 15 Keywood, M., Kanakidou, M., Stohl, A., Dentener, F., Grassi, G., Meyer, C. P., Torseth, K., Edwards, D., Thompson, A. M., Lohmann, U. and Burrows, J.: Fire in the Air: Biomass Burning Impacts in a Changing Climate, *Crit. Rev. Environ. Sci. Technol.*, 43(1), 40–83, doi:10.1080/10643389.2011.604248, 2013.
- Laffineur, Q., Delcloo, A., De Backer, H., Adam, M. and Klugmann, D.: Observation of an intercontinental smoke plume over Europe on June 2013: some ambiguity in the determination of the source, vol. 16, p. 2173. [online] Available from: <http://adsabs.harvard.edu/abs/2014EGUGA..16.2173L> (Accessed 22 August 2016), 2014.
- 20 Lassman, W., Ford, B., Gan, R. W., Pfister, G., Magzamen, S., Fischer, E. V. and Pierce, J. R.: Spatial and temporal estimates of population exposure to wildfire smoke during the Washington state 2012 wildfire season using blended model, satellite, and in situ data, *GeoHealth*, 1(3), 2017GH000049, doi:10.1002/2017GH000049, 2017.
- 25 Liu, J., Scheuer, E., Dibb, J., Diskin, G. S., Ziemba, L. D., Thornhill, K. L., Anderson, B. E., Wisthaler, A., Mikoviny, T., Devi, J. J., Bergin, M., Perring, A. E., Markovic, M. Z., Schwarz, J. P., Campuzano-Jost, P., Day, D. A., Jimenez, J. L. and Weber, R. J.: Brown carbon aerosol in the North American continental troposphere: sources, abundance, and radiative forcing, *Atmos Chem Phys*, 15(14), 7841–7858, doi:10.5194/acp-15-7841-2015, 2015.
- Liu, Y.: A Regression Model for Smoke Plume Rise of Prescribed Fires Using Meteorological Conditions, *J. Appl. Meteorol. Climatol.*, 53(8), 1961–1975, doi:10.1175/JAMC-D-13-0114.1, 2014.
- McCart, J. L., Korontzi, S., Justice, C. O. and Loboda, T.: The spatial and temporal distribution of crop residue burning in the contiguous United States, *Sci. Total Environ.*, 407(21), 5701–5712, doi:10.1016/j.scitotenv.2009.07.009, 2009.
- 30 Miller, D. J., Sun, K., Zondlo, M. A., Kanter, D., Dubovik, O., Welton, E. J., Winker, D. M. and Ginoux, P.: Assessing boreal forest fire smoke aerosol impacts on U.S. air quality: A case study using multiple data sets, *J. Geophys. Res. Atmospheres*, 116(D22), D22209, doi:10.1029/2011JD016170, 2011.
- Morris, G. A., Hersey, S., Thompson, A. M., Pawson, S., Nielsen, J. E., Colarco, P. R., McMillan, W. W., Stohl, A., Turquety, S., Warner, J., Johnson, B. J., Kucsera, T. L., Larko, D. E., Oltmans, S. J. and Witte, J. C.: Alaskan and Canadian

- forest fires exacerbate ozone pollution over Houston, Texas, on 19 and 20 July 2004, *J. Geophys. Res. Atmospheres*, 111(D24), D24S03, doi:10.1029/2006JD007090, 2006.
- Park, R. J., Jacob, D. J., Chin, M. and Martin, R. V.: Sources of carbonaceous aerosols over the United States and implications for natural visibility, *J. Geophys. Res. Atmospheres*, 108(D12), 4355, doi:10.1029/2002JD003190, 2003.
- 5 Park, R. J., Jacob, D. J. and Logan, J. A.: Fire and biofuel contributions to annual mean aerosol mass concentrations in the United States, *Atmos. Environ.*, 41(35), 7389–7400, doi:10.1016/j.atmosenv.2007.05.061, 2007.
- Paugam, R., Wooster, M., Freitas, S. and Val Martin, M.: A review of approaches to estimate wildfire plume injection height within large-scale atmospheric chemical transport models, *Atmos Chem Phys*, 16(2), 907–925, doi:10.5194/acp-16-907-2016, 2016.
- 10 Pebesma, E., Bivand, R., Rowlingson, B., Gomez-Rubio, V., Hijmans, R., Sumner, M., MacQueen, D., Lemon, J. and O'Brien, J.: *sp: Classes and Methods for Spatial Data*. [online] Available from: <https://cran.r-project.org/web/packages/sp/index.html> (Accessed 8 July 2016), 2016.
- Pfister, G. G., Wiedinmyer, C. and Emmons, L. K.: Impacts of the fall 2007 California wildfires on surface ozone: Integrating local observations with global model simulations, *Geophys. Res. Lett.*, 35(19), L19814, doi:10.1029/2008GL034747, 2008.
- 15 Randerson, J. T., Chen, Y., van der Werf, G. R., Rogers, B. M. and Morton, D. C.: Global burned area and biomass burning emissions from small fires, *J. Geophys. Res. Biogeosciences*, 117(G4), G04012, doi:10.1029/2012JG002128, 2012.
- Rappold, A. G., Stone, S. L., Cascio, W. E., Neas, L. M., Kilaru, V. J., Carraway, M. S., Szykman, J. J., Ising, A., Cleve, W. E., Meredith, J. T., Vaughan-Batten, H., Deyneka, L. and Devlin, R. B.: Peat Bog Wildfire Smoke Exposure in Rural North Carolina Is Associated with Cardiopulmonary Emergency Department Visits Assessed through Syndromic Surveillance, *Environ. Health Perspect.*, 119(10), 1415–1420, doi:10.1289/ehp.1003206, 2011.
- 20 Rastigejev, Y., Park, R., Brenner, M. P. and Jacob, D. J.: Resolving intercontinental pollution plumes in global models of atmospheric transport, *J. Geophys. Res. Atmospheres*, 115(D2), D02302, doi:10.1029/2009JD012568, 2010.
- Rolph, G. D., Draxler, R. R., Stein, A. F., Taylor, A., Ruminski, M. G., Kondragunta, S., Zeng, J., Huang, H.-C., Manikin, G., McQueen, J. T. and Davidson, P. M.: Description and Verification of the NOAA Smoke Forecasting System: The 2007 Fire Season, *Weather Forecast.*, 24(2), 361–378, doi:10.1175/2008WAF2222165.1, 2009.
- 25 Ruminski, M., Kondragunta, S., Draxler, R. and Zeng, J.: Recent changes to the Hazard Mapping System, 15th Int. Emiss. Inventory Conf. (Reinventing Inventories) [online] Available from: <https://www.researchgate.net/publication/228625934> Recent changes to the Hazard Mapping System (Accessed 8 July 2016), 2006.
- 30 Russell, A. R., Valin, L. C. and Cohen, R. C.: Trends in OMI NO₂ observations over the US: Effects of emission control technology and the economic recession, *Atmospheric Chem. Phys.*, 12(6), 15419–15452, doi:10.5194/acpd-12-15419-2012, 2012.
- 35 Saide, P. E., Peterson, D. A., da Silva, A., Anderson, B., Ziemba, L. D., Diskin, G., Sachse, G., Hair, J., Butler, C., Fenn, M., Jimenez, J. L., Campuzano-Jost, P., Perring, A. E., Schwarz, J. P., Markovic, M. Z., Russell, P., Redemann, J., Shinzuka,

- Y., Streets, D. G., Yan, F., Dibb, J., Yokelson, R., Toon, O. B., Hyer, E. and Carmichael, G. R.: Revealing important nocturnal and day-to-day variations in fire smoke emissions through a multiplatform inversion, *Geophys. Res. Lett.*, 42(9), 2015GL063737, doi:10.1002/2015GL063737, 2015.
- 5 Sakamoto, K. M., Allan, J. D., Coe, H., Taylor, J. W., Duck, T. J. and Pierce, J. R.: Aged boreal biomass-burning aerosol size distributions from BORTAS 2011, *Atmos Chem Phys*, 15(4), 1633–1646, doi:10.5194/acp-15-1633-2015, 2015.
- Sakamoto, K. M., Laing, J. R., Stevens, R. G., Jaffe, D. A. and Pierce, J. R.: The evolution of biomass-burning aerosol size distributions due to coagulation: dependence on fire and meteorological details and parameterization, *Atmos Chem Phys*, 16(12), 7709–7724, doi:10.5194/acp-16-7709-2016, 2016.
- 10 Scholze, M., Knorr, W., Arnell, N. W. and Prentice, I. C.: A climate-change risk analysis for world ecosystems, *Proc. Natl. Acad. Sci.*, 103(35), 13116–13120, doi:10.1073/pnas.0601816103, 2006.
- Schroeder, W., RUMINSKI, M., CSISZAR, I., GIGLIO, L., GIGLIO, E., SCHMIDT, C. and MORISETTE, J.: Validation analyses of an operational fire monitoring product: The Hazard Mapping System, *Int. J. Remote Sens.*, 29(20), 6059–6066, 2008.
- 15 Stein, A. F., Rolph, G. D., Draxler, R. R., Stunder, B. and Ruminski, M.: Verification of the NOAA Smoke Forecasting System: Model Sensitivity to the Injection Height, *Weather Forecast.*, 24(2), 379–394, doi:10.1175/2008WAF2222166.1, 2009.
- Val Martin, M., Logan, J. A., Kahn, R. A., Leung, F.-Y., Nelson, D. L. and Diner, D. J.: Smoke injection heights from fires in North America: analysis of 5 years of satellite observations, *Atmos Chem Phys*, 10(4), 1491–1510, doi:10.5194/acp-10-1491-2010, 2010.
- 20 Val Martin, M., Heald, C. L., Ford, B., Prenni, A. J. and Wiedinmyer, C.: A decadal satellite analysis of the origins and impacts of smoke in Colorado, *Atmos Chem Phys*, 13(15), 7429–7439, doi:10.5194/acp-13-7429-2013, 2013a.
- Val Martin, M., Heald, C. L., Ford, B., Prenni, A. J. and Wiedinmyer, C.: A decadal satellite analysis of the origins and impacts of smoke in Colorado, *Atmos Chem Phys*, 13(15), 7429–7439, doi:10.5194/acp-13-7429-2013, 2013b.
- 25 Val Martin, M., Heald, C. L., Lamarque, J.-F., Tilmes, S., Emmons, L. K. and Schichtel, B. A.: How emissions, climate, and land use change will impact mid-century air quality over the United States: a focus on effects at national parks, *Atmos Chem Phys*, 15(5), 2805–2823, doi:10.5194/acp-15-2805-2015, 2015.
- Vedal, S. and Dutton, S. J.: Wildfire air pollution and daily mortality in a large urban area, *Environ. Res.*, 102(1), 29–35, doi:10.1016/j.envres.2006.03.008, 2006.
- 30 Washenfelder, R. A., Attwood, A. R., Brock, C. A., Guo, H., Xu, L., Weber, R. J., Ng, N. L., Allen, H. M., Ayres, B. R., Baumann, K., Cohen, R. C., Draper, D. C., Duffey, K. C., Edgerton, E., Fry, J. L., Hu, W. W., Jimenez, J. L., Palm, B. B., Romer, P., Stone, E. A., Wooldridge, P. J. and Brown, S. S.: Biomass burning dominates brown carbon absorption in the rural southeastern United States, *Geophys. Res. Lett.*, 42(2), 2014GL062444, doi:10.1002/2014GL062444, 2015.
- 35 van der Werf, G. R., Randerson, J. T., Giglio, L., Collatz, G. J., Mu, M., Kasibhatla, P. S., Morton, D. C., DeFries, R. S., Jin, Y. and van Leeuwen, T. T.: Global fire emissions and the contribution of deforestation, savanna, forest, agricultural, and peat fires (1997–2009), *Atmos Chem Phys*, 10(23), 11707–11735, doi:10.5194/acp-10-11707-2010, 2010.

- van der Werf, G. R. van der, Randerson, J. T., Giglio, L., Leeuwen, T. T. van, Chen, Y., Rogers, B. M., Mu, M., Marle, M. J., E. van, Morton, D. C., Collatz, G. J., Yokelson, R. J. and Kasibhatla, P. S.: Global fire emissions estimates during 1997–2016, *Earth Syst. Sci. Data*, 9(2), 697–720, doi:<https://doi.org/10.5194/essd-9-697-2017>, 2017.
- 5 Westerling, A. L.: Increasing western US forest wildfire activity: sensitivity to changes in the timing of spring, *Phil Trans R Soc B*, 371(1696), 20150178, doi:10.1098/rstb.2015.0178, 2016.
- Westerling, A. L., Hidalgo, H. G., Cayan, D. R. and Swetnam, T. W.: Warming and Earlier Spring Increase Western U.S. Forest Wildfire Activity, *Science*, 313(5789), 940–943, doi:10.1126/science.1128834, 2006.
- 10 Wiedinmyer, C., Quayle, B., Geron, C., Belote, A., McKenzie, D., Zhang, X., O’Neill, S. and Wynne, K. K.: Estimating emissions from fires in North America for air quality modeling, *Atmos. Environ.*, 40(19), 3419–3432, doi:10.1016/j.atmosenv.2006.02.010, 2006.
- Wiedinmyer, C., Akagi, S. K., Yokelson, R. J., Emmons, L. K., Al-Saadi, J. A., Orlando, J. J. and Soja, A. J.: The Fire INventory from NCAR (FINN): a high resolution global model to estimate the emissions from open burning, *Geosci. Model Dev.*, 4(3), 625–641, doi:10.5194/gmd-4-625-2011, 2011.
- 15 Yue, X., Mickley, L. J., Logan, J. A. and Kaplan, J. O.: Ensemble projections of wildfire activity and carbonaceous aerosol concentrations over the western United States in the mid-21st century, *Atmospheric Environ. Oxf. Engl.* 1994, 77, 767–780, doi:10.1016/j.atmosenv.2013.06.003, 2013.

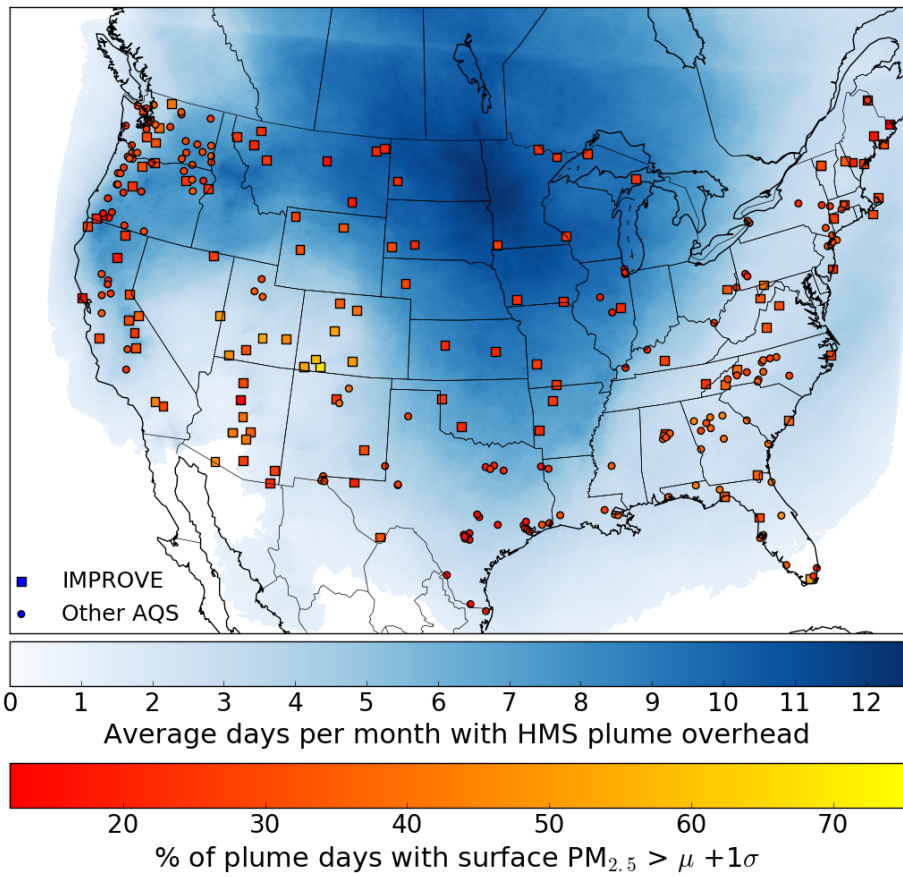
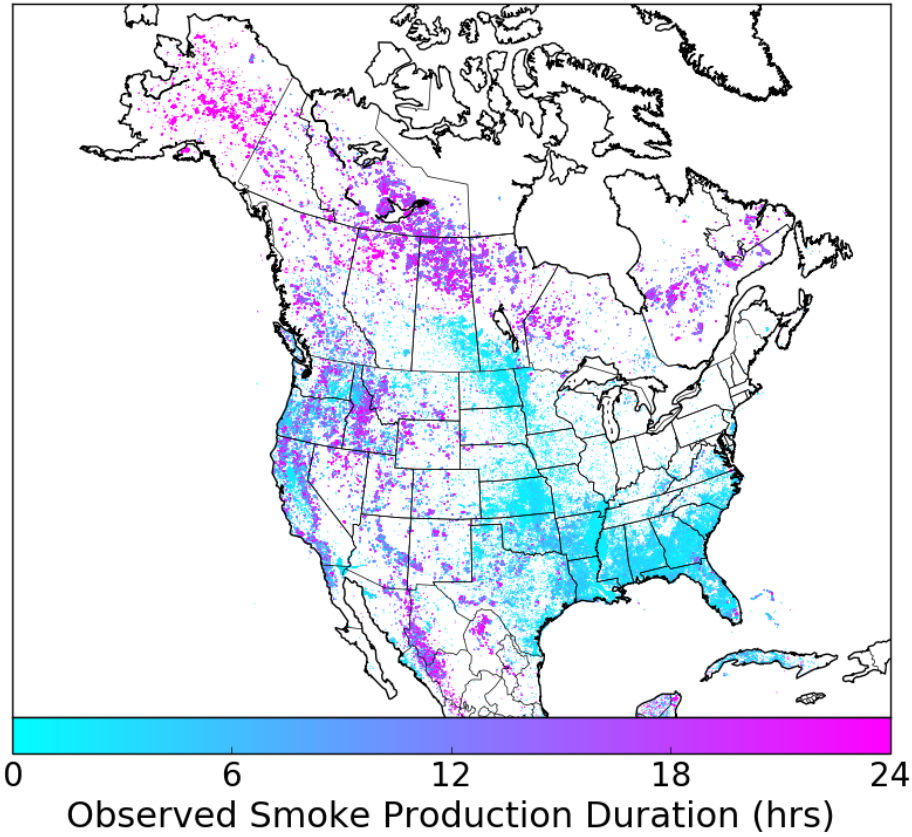


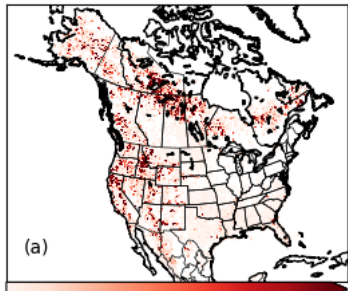
Figure 1: North American smoke climatology for June-September 2007-2014. Blue shading indicates the average days per month HMS smoke plumes are analyzed overhead. Markers show non FRM (Federal Reference Method) $PM_{2.5}$ monitors shaded by the percent of plume days where surface 24-hr average $PM_{2.5}$ is greater than the mean (μ) plus one standard deviation (σ) value for the monitors mean value in June-September. Only monitors with data on 90% of days between June-September 2007-2014 are presented. IMPROVE monitors are marked by squares; all other monitors from the EPA Air Quality System (AQS) are marked by circles. IMPROVE monitors record data every third day. We make the assumption that smoke plumes are equally likely to occur on measurement days as non-measurement days, and thus multiply the number of ground level smoke-impacted plume days

at IMPROVE sites by three. Monitors that fall within white areas are influenced by smoke < 1 day per month. The climatology presented here does not relate to smoke plume or ground level PM_{2.5} concentrations, only the presence of smoke in the column and proportion of those days when surface PM_{2.5} is elevated.

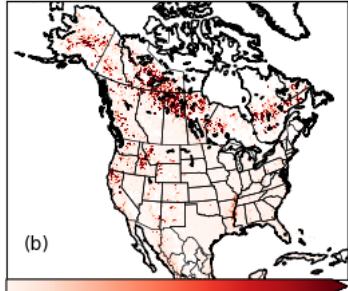


5

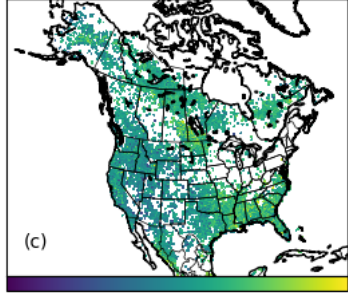
Figure 2: The locations of all HYSPLIT points analyzed between 2007-2014 shaded by the duration assigned by the analyst. HYSPLIT Points are assigned a duration between 1 and 15, or 24 hours.



(a)
0 200 400 600 800 1000 1200 1400
Total HMS SPDH



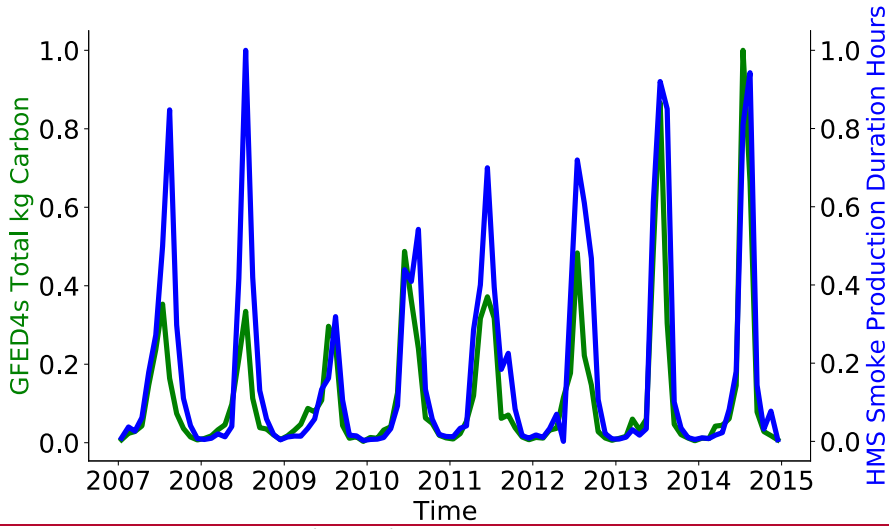
(b)
0.0 0.3 0.6 0.9 1.2
GFED4s kg Carbon Emissions (10^8)



(c)
 10^2 10^3 10^4 10^5 10^6 10^7
(GFED4s kg Carbon) / (HMS SPDH)

Figure 3: (a) Cumulative June-September 2007-2014 HMS smoke production duration hours (SPDH) and (b) GFED4s kg carbon per 0.25° x 0.25° grid cell. Both emission inventories color bars saturate (darkest red) at the 99th percentile of non-zero values, meaning all values above the 99th percentile value for both datasets are represented by the darkest color on the color bar. (c) Total GFED4s kg of carbon emitted divided by the total HMS smoke production duration hours per grid cell for months June-September 2007-2014. The color bar shows the values on a log₁₀ scale where yellow values represent grid cells with more GFED4s kg of carbon per HYSPLIT Point smoke production duration hour and purple indicate fewer. Locations where either GFED4s or HMS emissions are equal to zero are not plotted. The mean kg carbon per HYSPLIT Point smoke production duration hour is 300,123.

5



10

Figure 4: Time series of monthly domain (20-30° N, 50-170° W) summed kg carbon (left axis) and HMS-hours (right axis). Monthly totals have been divided by the maximum monthly value observed between 2007-2014. The Pearson correlation coefficient for the presented monthly time series is 0.842.

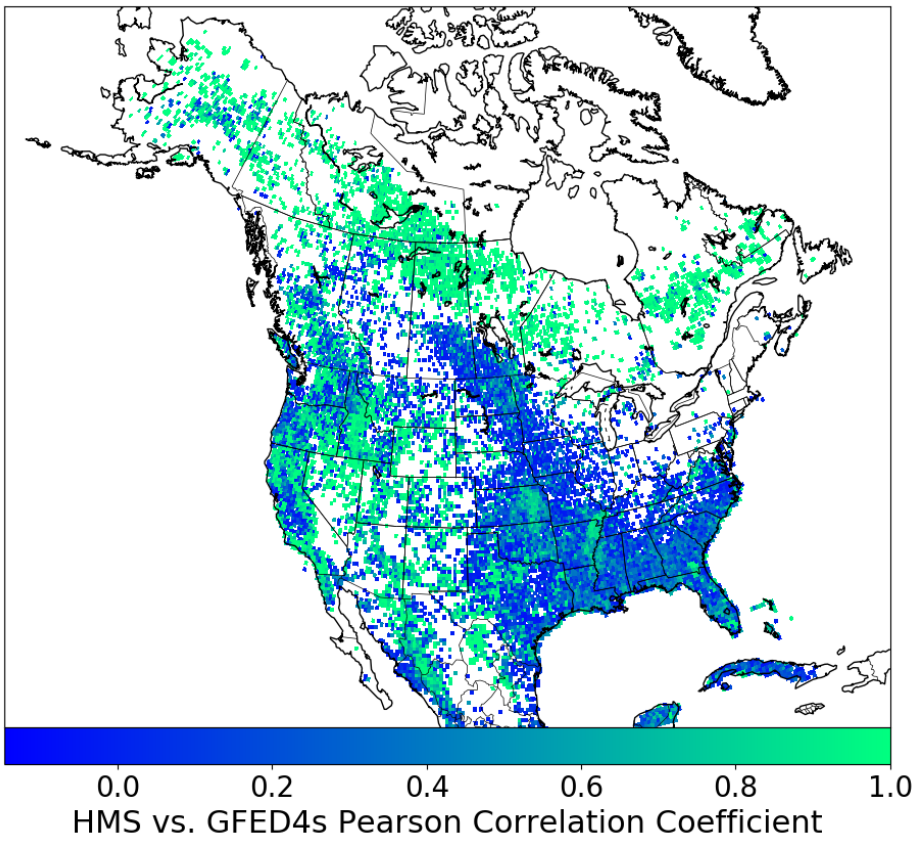


Figure 5: Plan view monthly time series Pearson correlation coefficient for monthly HMS-hours and GFED4s kg carbon for each 0.25 x 0.25 degree grid cell. White grid cells are locations where one or both of the inventories have zero emissions for all 96 months.

5

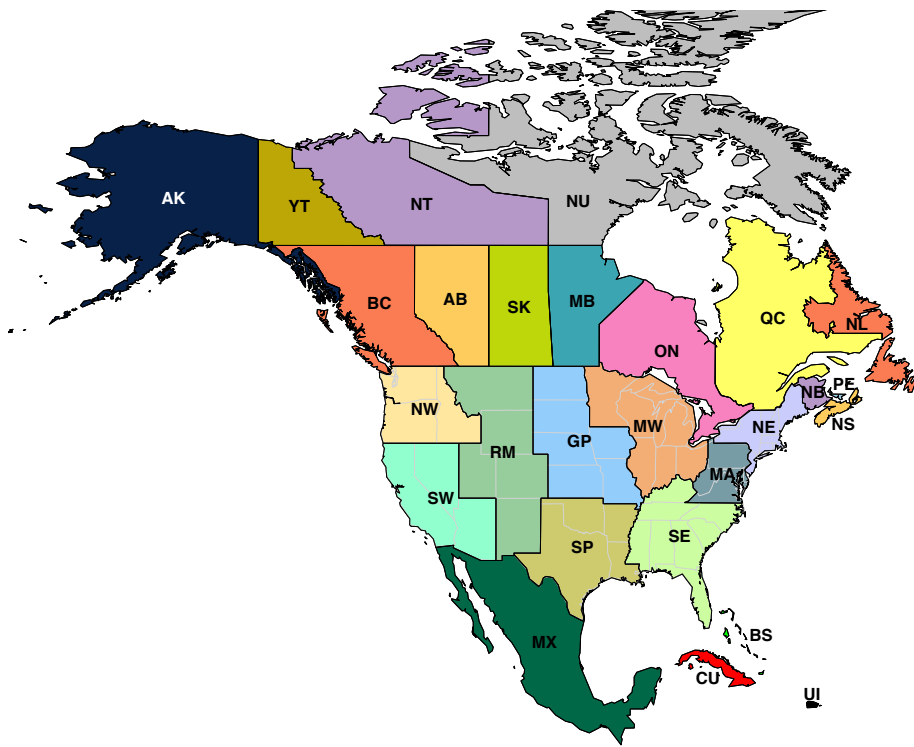


Figure 6: Smoke source and receptor regions used in this analysis. Northeast (NE), Mid Atlantic (MA), Southeast (SE), Midwest (MW), Southern Plains (SP), Great Plains (GP), Rocky Mountains (RM), Southwest (SW), Northwest (NW), Alaska (AK), U.S. Islands (UI), Mexico (MX), Quebec (QC), Nova Scotia (NS), Saskatchewan (SK), Alberta (AB), Newfoundland and Labrador (NL), British Columbia (BC), New Brunswick (NB), Prince Edward Island (PE), Yukon Territory (YT), Manitoba (MB), Ontario (ON), Nunavut (NU), Northwest Territories (NT), Cuba (CU), and Bahamas (BS).

5

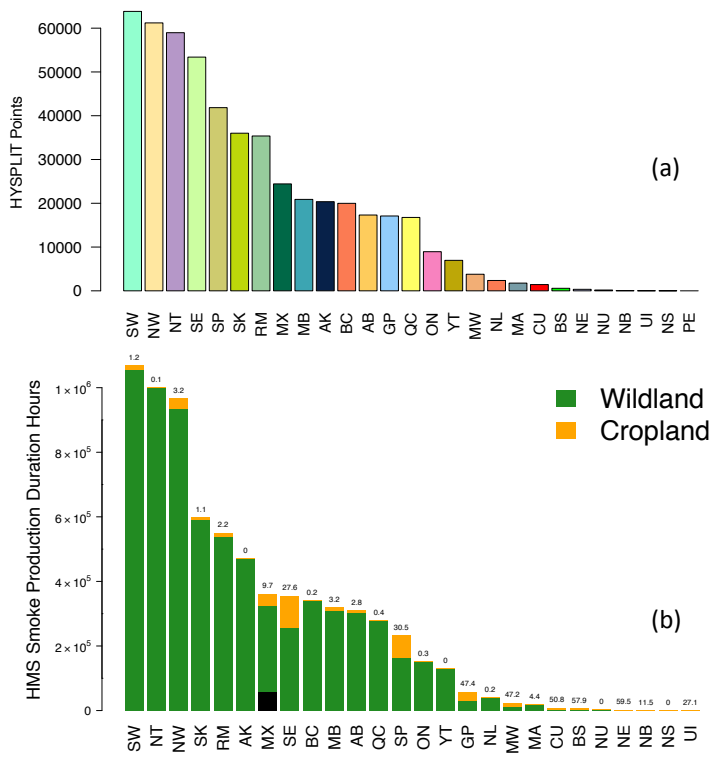
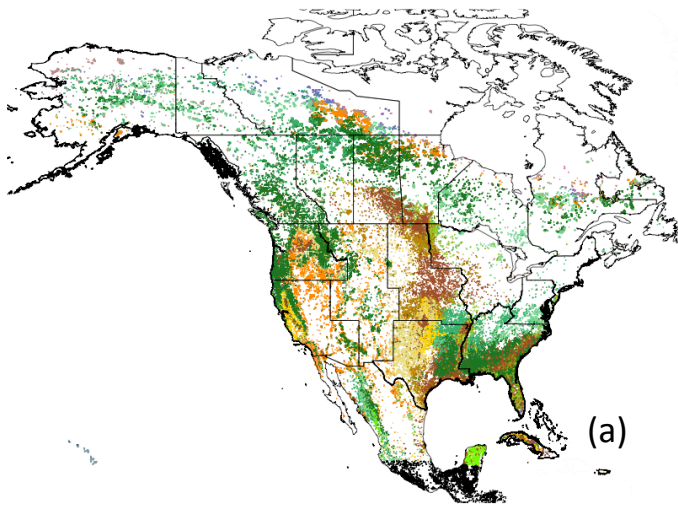
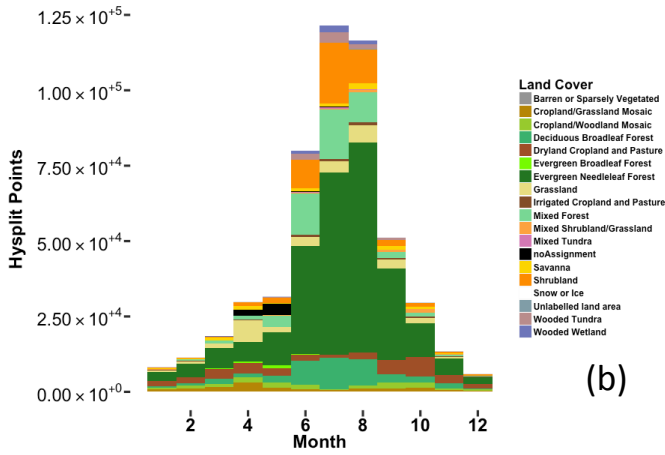


Figure 7: (a) Total HMS HYSPLIT point detections for all regions and months between 2007-2014. Region colors and abbreviations are defined in Fig. 6. (b) Total HMS smoke production duration hours (SPDH) for the same time period. The number on top of each bar indicates the percentage of SPDH that are from croplands. The black portion of Mexico (MX) represents fires that occurred on land outside of the land cover data extent used in this analysis.

5



(a)



(b)

Figure 8: Location, (a) seasonality, (b) and land cover classification assignment (color) for all HYSPLIT points analyzed over North America between 2007-2014 (n=517,214). No land cover assignment is made for Southern Mexico (MX) and U.S. Islands (UI) due to the latitudinal range of land cover data.

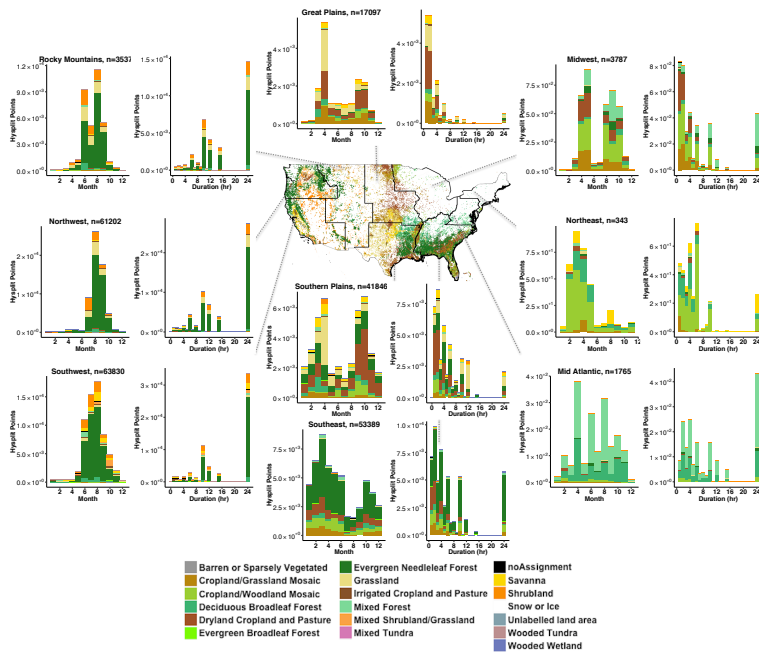


Figure 9: HYSPLIT point locations and land cover classification for the nine continental U.S. regions. The map in the middle shows the regions and the locations of all HYSPLIT points analyzed between 2007 and 2014. The HYSPLIT points are shaded by land cover classification. Two histograms are shown for each region. The total number of HYSPLIT points analyzed each month is shown on the left histograms. The HYSPLIT point duration and land cover classification is shown on the right. The bars for both histograms are shaded by the land cover classification assigned to the HYSPLIT points. Non U.S. regions and Alaska are available in the supplemental information.

5

10

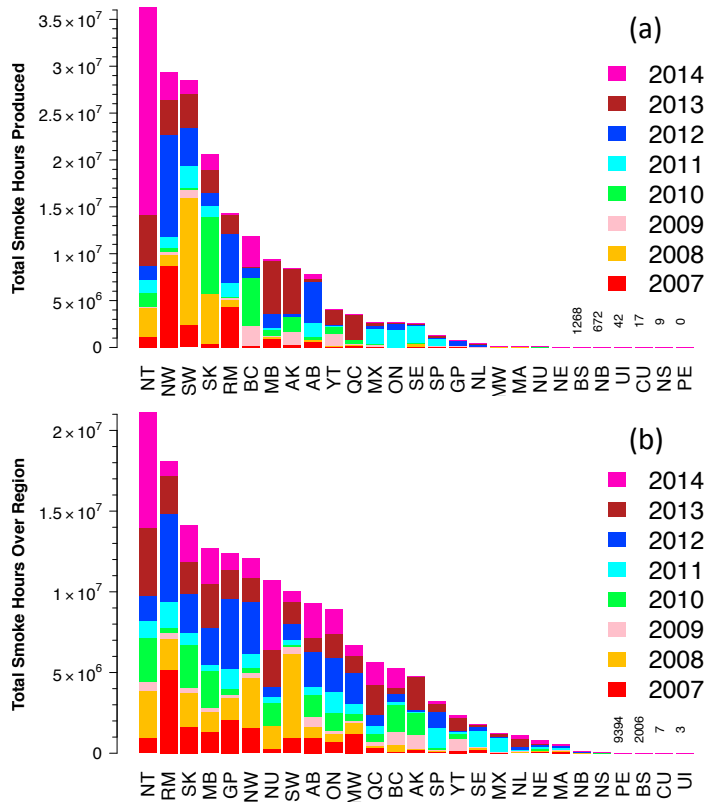


Figure 10: (a) Total number of smoke hours produced (anywhere) by each region for months June-September between 2007 and 2014 using GDAS1 meteorology. (b) Total number of smoke hours over each region for months June-September between 2007 and 2014 using GDAS1 meteorology.

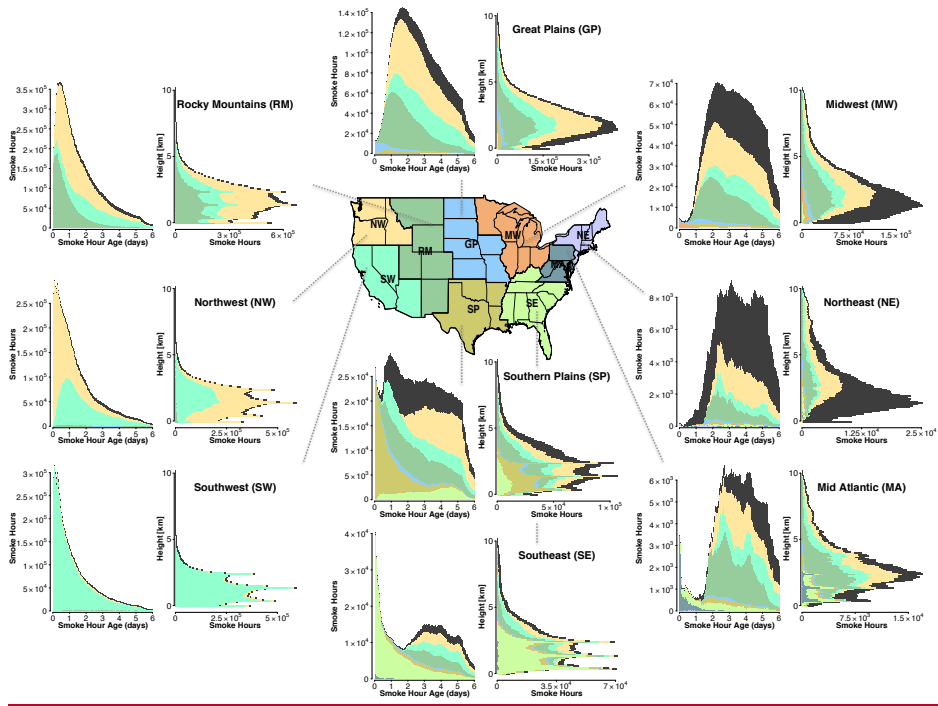


Figure 11: Summertime (June-September) regional smoke hour transport summaries for the nine continental U.S. regions between 2007 and 2014 using GDASI meteorology. Two histograms are shown for each region. The histogram on the left shows the distribution of smoke hour age. The color of the smoke hours matches the region of origin as indicated by the map in the center. Column 2 shows the distribution of smoke hour height segregated by source region color. Smoke hours contributed by regions outside of the continental U.S. are dark gray. Histograms of smoke hour age, height, and region of origin for all regions shown in Fig. 6 are available in the supplemental information.

5

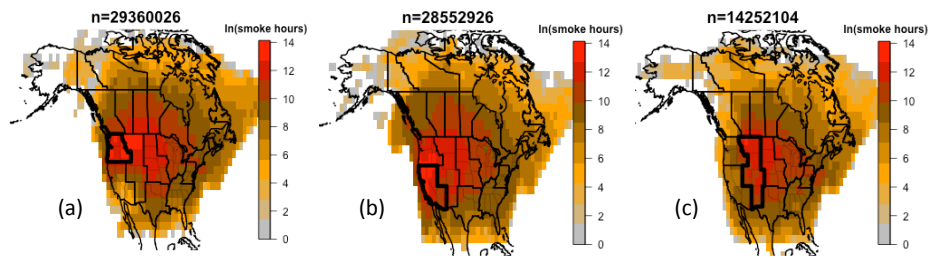


Figure 12: Summertime (June-September) regional smoke hour transport heat maps for the Northwest (a), Southwest (b), and Rocky Mountains (c). Each column shows the count of smoke hours produced by each region on a 2° by 2° degree grid with a consistent color bar for all three regions. The grid spans $18-180^\circ$ W and $18-90^\circ$ N, a domain covering all five sectors where HMS analyzes smoke plumes (only a subset plotted). Shaded values are the natural log of the number of smoke hours in each grid cell (min=1, max=1.2 million). All figures were generated using GDAS1 meteorology data.

5

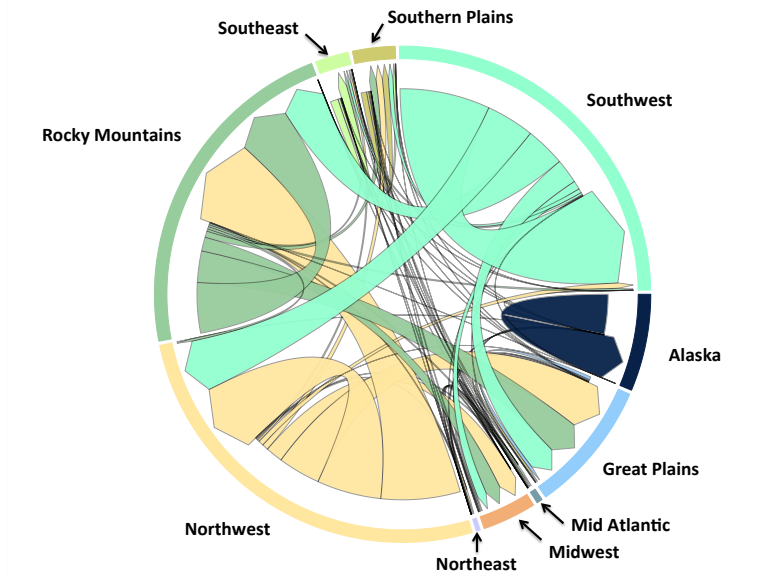


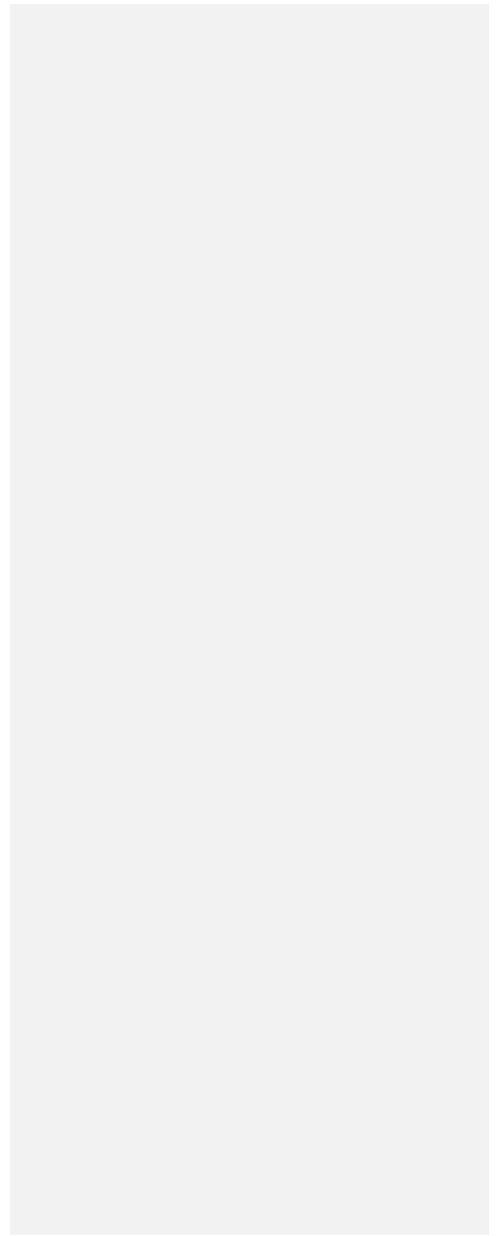
Figure 13: U.S. regions smoke hour climatology for June-September 2007-2014 using GDAS1 meteorology. Arrows indicate the smoke hours source region and destination region. The width of arrows are proportional to total smoke hours transported between regions. Each of the 10 U.S. regions makes up a fraction of the total circumference of the circle, which is proportional to the total

10

Comment [B6]: Previous version of this figure misspelled "Great Plains" as "Great Planes".

Deleted:

smoke hours over and produced by all U.S. regions. The widths of the arrows are proportional to the number of smoke hours in a given transport pathway. The colors of the arrows match the source region of the smoke hours (Fig. 6). This figure places the individual histogram of Fig. 11 into context.



Support for this work was provided by the Environmental Protection Agency Award Number 83588401.

S1 HYSPLIT Trajectories detailed description

The HYSPLIT (Hybrid Single Particle Lagrangian Integrated Trajectory) trajectory model simulates air parcel movement by wind advection using spatially and temporally gridded meteorology data, and it is used to establish source-receptor relationships [Draxler and Hess, 1998; Stein et al., 2015]. The model computational method is a hybrid between Lagrangian and Eulerian reference frames [Stein et al., 2015]. HYSPLIT has been used extensively to model the transport of smoke (e.g., [Stein et al., 2015]). The model executable is available for download on the NOAA Air Resources Laboratory (ARL) webpage http://ready.arl.noaa.gov/hyreg/HYSPLIT_pchysplit.php.

Based on numerical and physical limitations of the model, the error in the location of a trajectory is approximately 15-30% of the distance traveled by the air parcel [Draxler, 2008]. The physical error is related to how well the numerical values (e.g. u and v winds) represent the true state of the atmosphere. The numerical error arises from integration error, truncation, and the fact that calculations of continuous variables are being done on a discrete grid [Draxler, 2008]. We present results generated using the 32 bit Windows PC executable version of the trajectory model (`hyts_std.exe`) on a Debian Unix cluster at Colorado State University using the WINE (Wine Is Not an Emulator; <https://www.winehq.org>) compatibility layer. A Python based HYSPLIT manager system allows each available core to independently call the HYSPLIT trajectory executable. Six-day (144-hr) forward trajectories are calculated for each HMS HYSPLIT point using meteorological data from the GDAS (Global Data Assimilation System) archive, which has a time step of 3-hours, horizontal grid spacing of 1° latitude by 1° longitude (120 km), and a vertical grid spacing of 23 pressure surfaces between 1000 and 20 hPa. Vertical layers 1-5 are separated by 25 hPa. All higher layers (with the exception of the top layer) are separated by 50 hPa [Kanamitsu, 1989]. The GDAS 1-degree archived data is available for download at: <ftp://arlftp.arlhq.noaa.gov/pub/archives/gdas1>. Six-day trajectories are also calculated for each HYSPLIT point in the data domain (excludes Alaska, parts of Canada and Mexico) using meteorological data from the EDAS (Eta Data Assimilation System) archive. This data has a 3-hour time step, horizontal grid spacing of 40 km x 40 km, and 26 pressure surfaces between 1000 and 50 hPa. EDAS40 archived data is available for download at: <ftp://arlftp.arlhq.noaa.gov/pub/archives/edas40>.

In this work, forward HYSPLIT trajectories are initialized from each of the HYSPLIT points over the duration of the fires to represent likely smoke transport. Practically, this means that for HYSPLIT points assigned durations of 0 - 6 hours, one trajectory is initialized at the middle hour between the first and last hour. For HYSPLIT points with durations of 7 - 12 hours, two trajectories are initialized at the 25th and 75th percentile of the span of hours over the duration of the fire. For durations of 13 - 18 hours, three trajectories are initialized at the 20th, 50th, and 80th percentile of the span of hours between start time and end time. For durations of 19 - 24 hours, four trajectories are initialized at the 20th, 40th, 60th, and 80th percentile of the span of hours. Trajectories are not initialized at the start or finish hours because many of the HYSPLIT points have durations of 24 hours, last multiple days, and are re-detected daily, so initializing trajectories at the time fires are detected would overweight early morning hours when HYSPLIT points are first detected with visible satellite imagery. This is a concern because the most common duration for the HYSPLIT points is 24 hours (manuscript Fig. 2 & 9).

Table S1: Trajectories initialized for GDAS1 HYSPLIT runs following the strategy outlined in Sect S1. The third column is the percent of initiated trajectories that reach 0 m within the 6 day calculation. These trajectories are subset and only considered for the hours before they reach 0 m. The minimum number of trajectories that can be run for a HYSPLIT point is 3 (heights); the maximum is 12 (4 start times for a 24-hour duration at 3 initialization heights). The number of trajectories for each year includes all months.

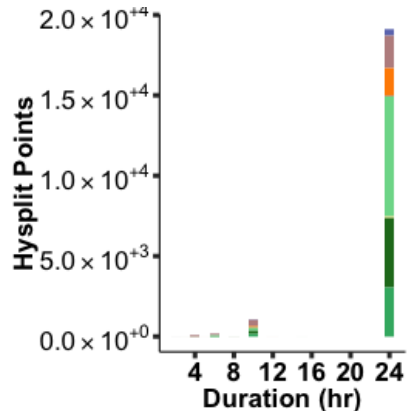
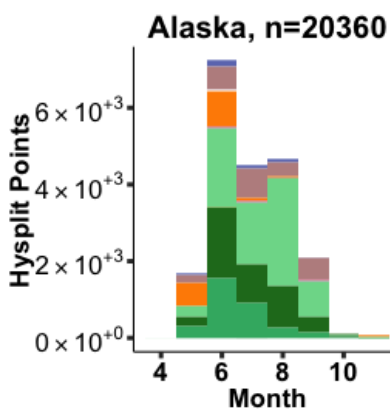
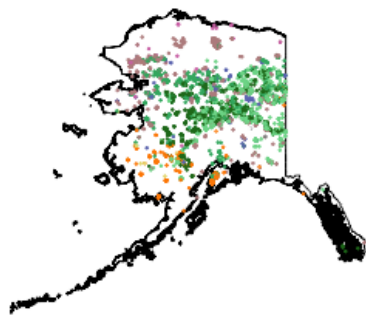
Year	Unique trajectories (total with duplicates)	% reaching 0 m
2007	460209 (546377)	4.2
2008	433671 (482816)	4.9
2009	210089 (226872)	5.9
2010	379568 (417395)	8.2
2011	494375 (563040)	8.3
2012	481438 (563915)	9.7
2013	544463 (598368)	8.5
2014	494320 (527149)	8.0

Table S2: Same as Table S1 but for EDAS 40 km meteorology data. Fewer trajectories were run due to the limited domain of EDAS 40 km. Parts of Alaska, Northern Canada, and Southern Mexico are not included in this reanalysis dataset. The number of trajectories for each year includes all months.

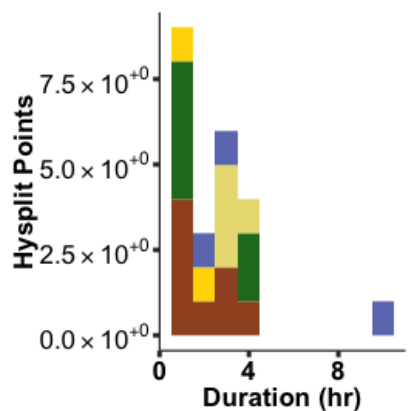
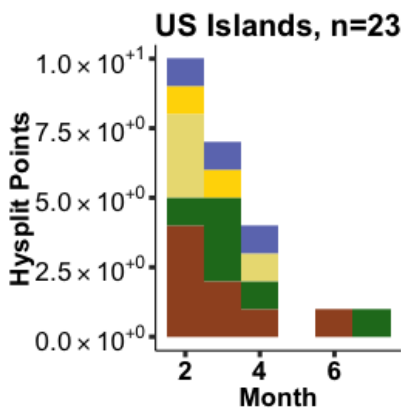
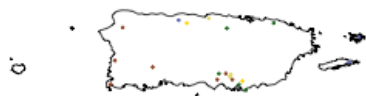
Year	Unique trajectories (total with duplicates)	% reaching 0 m
2007	412930 (496592)	3.4
2008	356785 (397645)	3.1
2009	156219 (169415)	4.3
2010	255939 (287771)	7.6
2011	451102 (525644)	9.3
2012	427541 (506334)	19.7
2013	375993 (423159)	17.3
2014	215841 (231218)	15.6

S2 HYSPLIT point seasonality and location figures for non-CONUS regions:

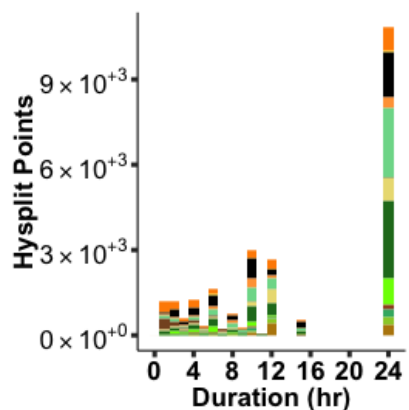
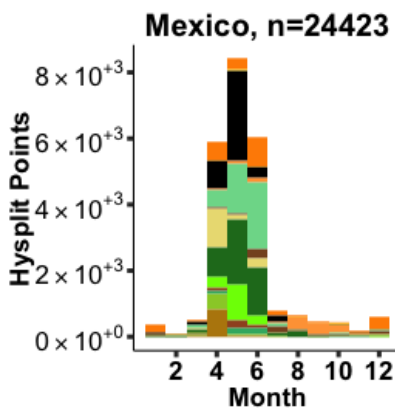
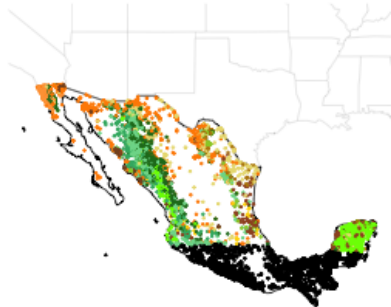
Manuscript Fig. 9 shows only U.S. regions. Here we provide versions of these figures for all regions shown in Fig. 6. All figures were generated using the same methodology described in Sect 4 of the manuscript.



(a)

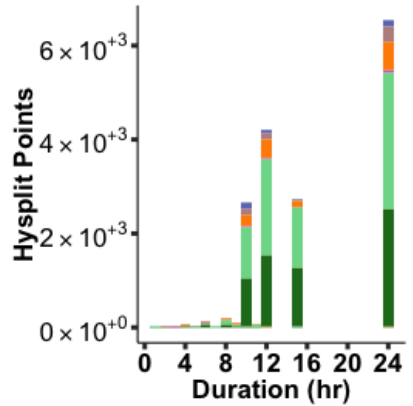
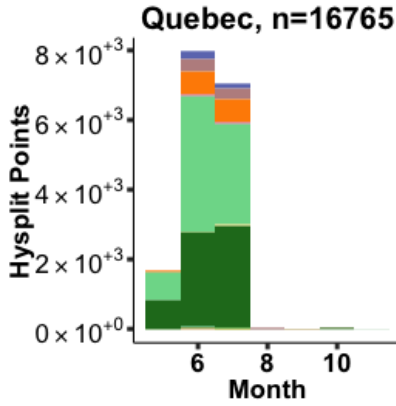
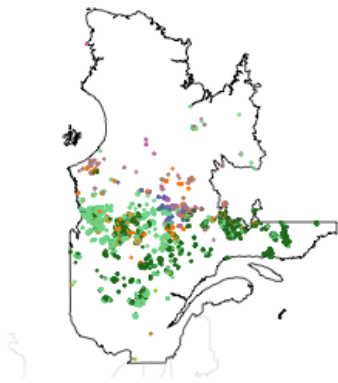


(b)

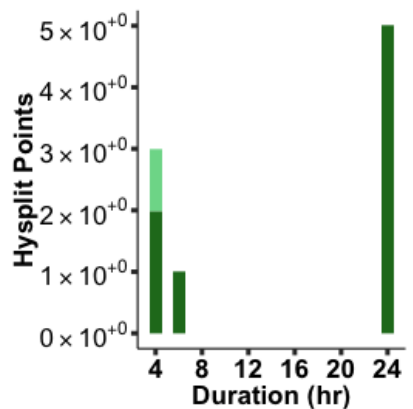
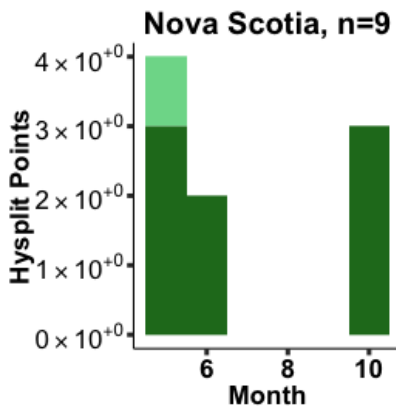


(c)

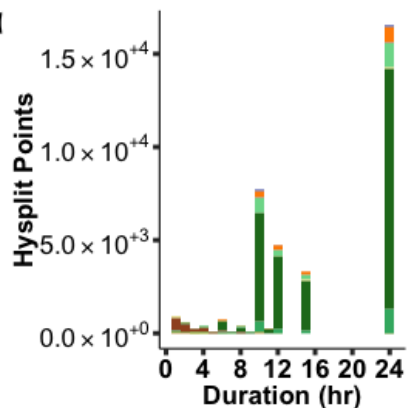
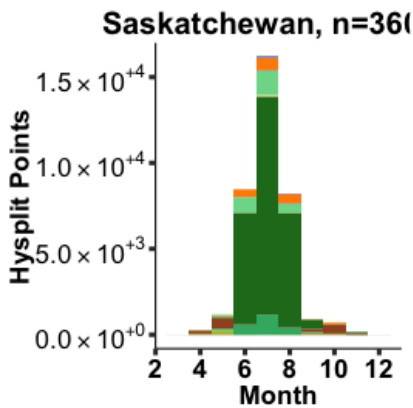
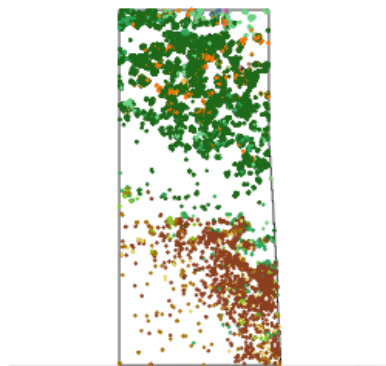




(d)

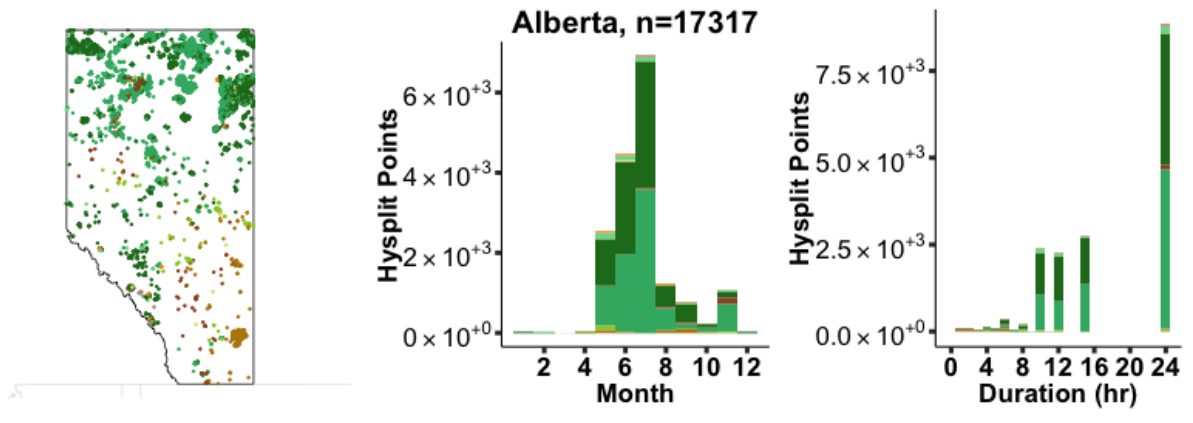


(e)

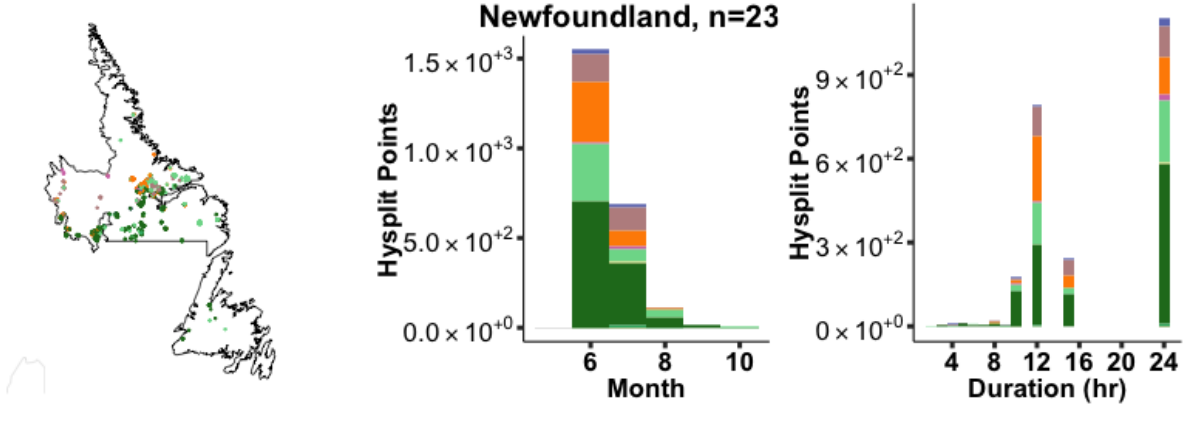


(f)

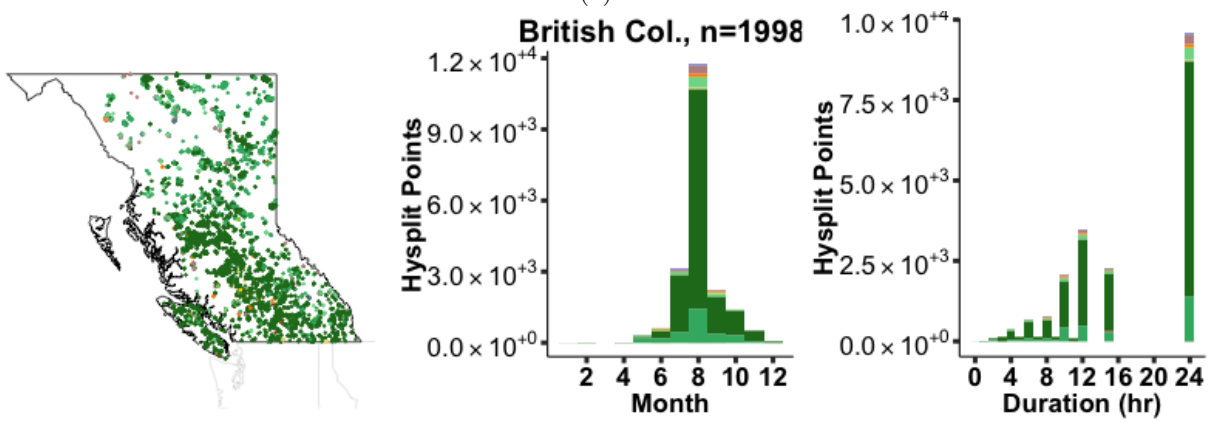




(g)



(h)

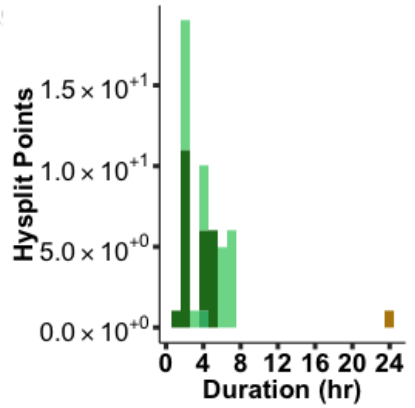
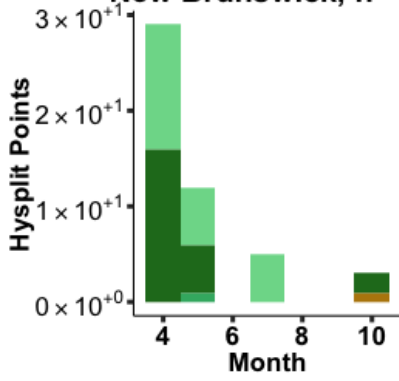


(i)





New Brunswick, n=4



(j)

Prince Edward Island, n=0



Hysplit Points

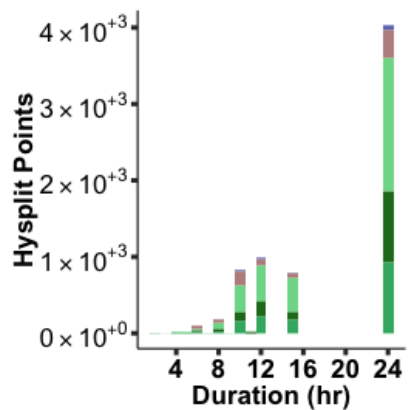
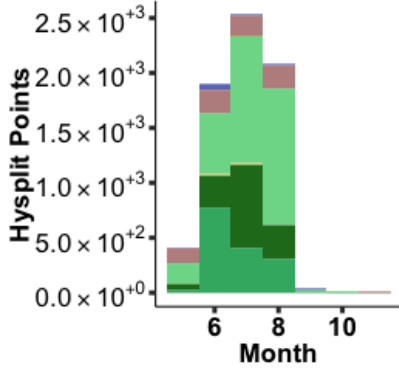
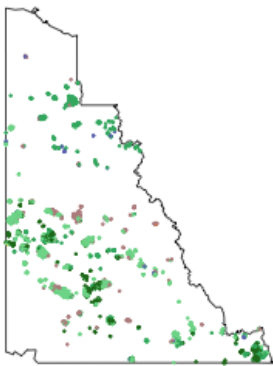
Hysplit Points

Month

Duration (hr)

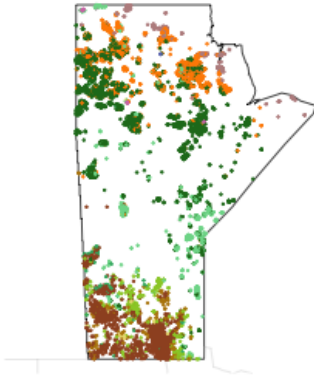
(k)

Yukon, n=6962

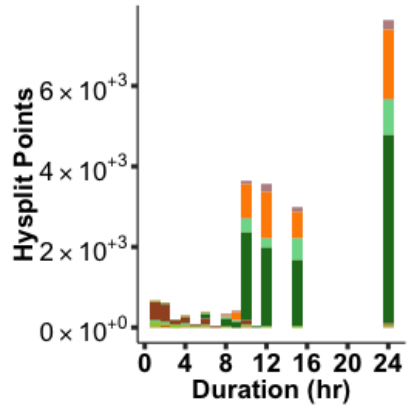
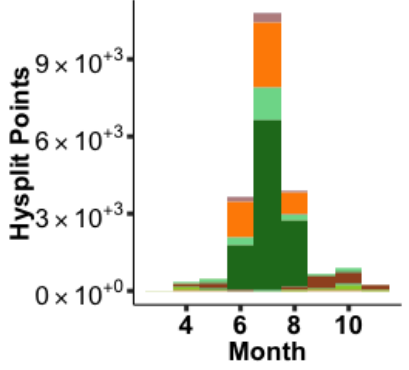


(l)

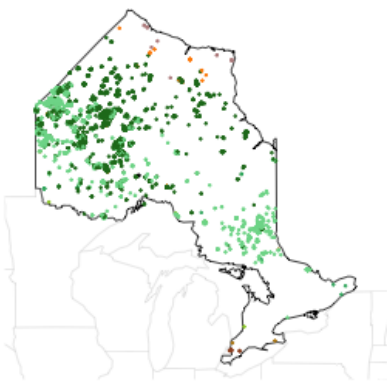




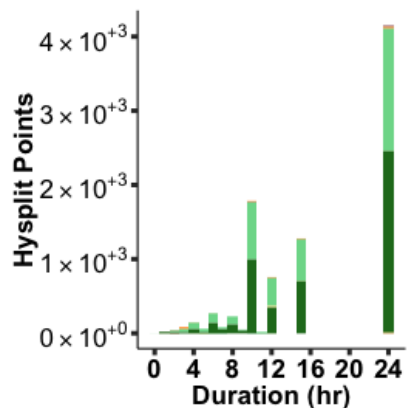
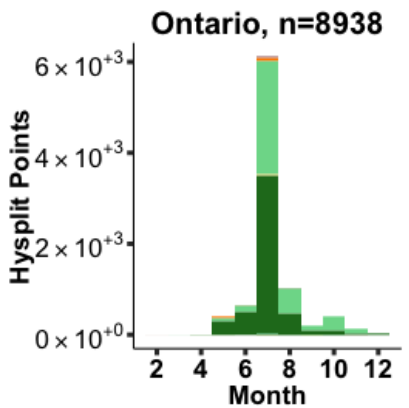
Manitoba, n=20888



(m)



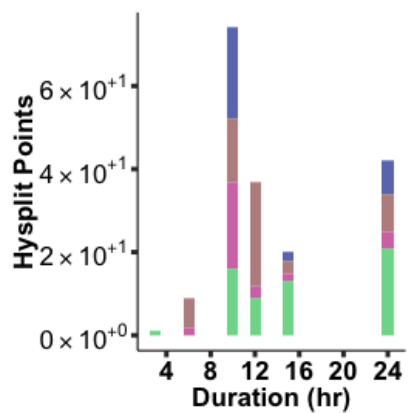
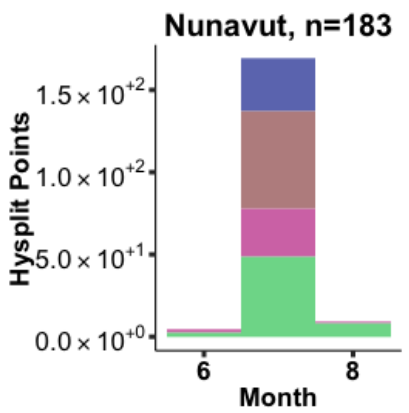
Ontario, n=8938



(n)



Nunavut, n=183



(o)



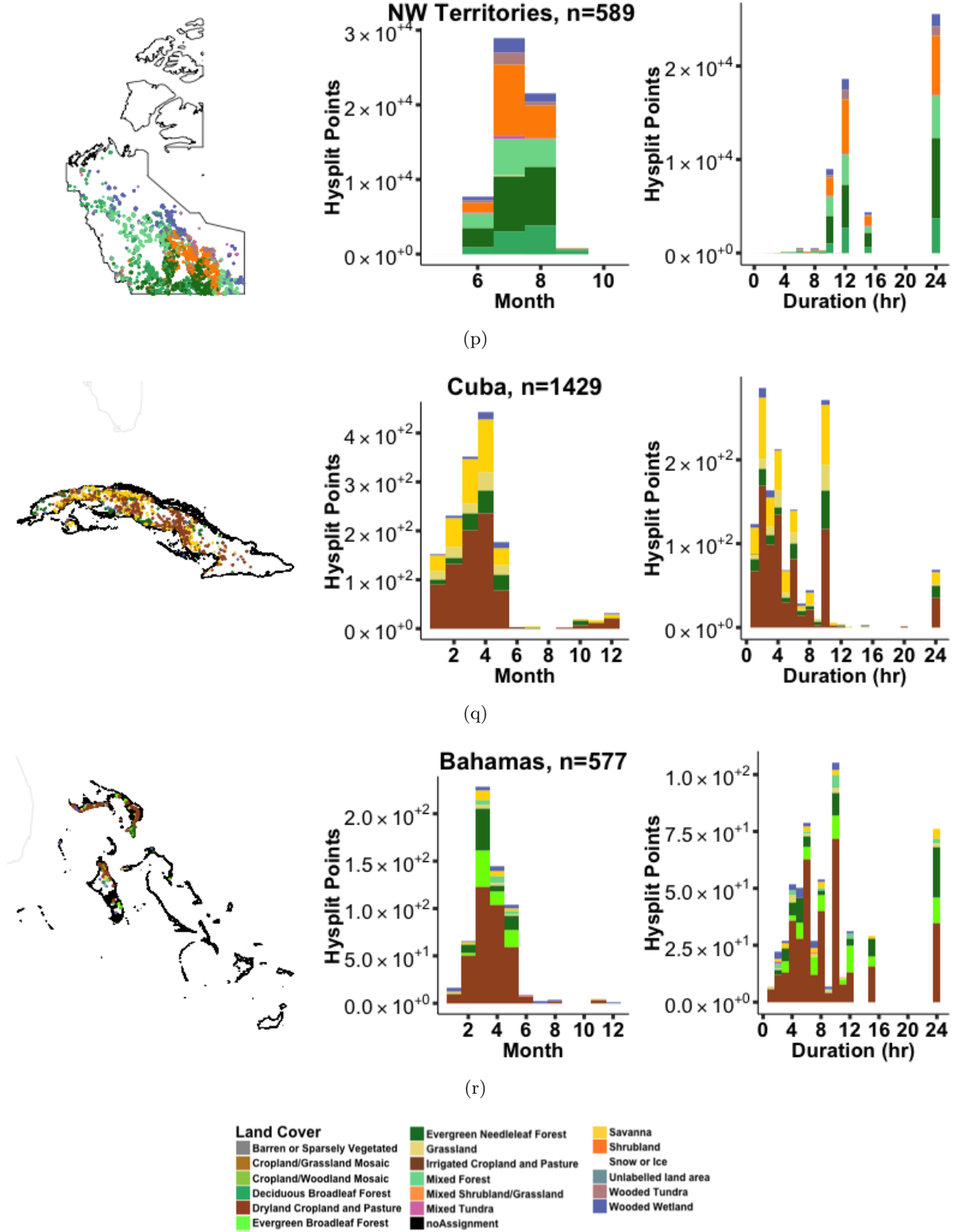


Figure S1: HYSPLIT Points locations and land cover classification represented by color (left), total number of occurrence by month and land cover classification (middle), duration and land cover classification (right).

S3 Overlapping trajectories with HMS smoke plumes:

HMS smoke plumes are analyzed using visible satellite imagery. During the summer months most latitudes of North America experience daylight hours that span two different dates in UTC time. For example, on the summer solstice (June 20) in Seattle (47 degrees North) the sun sets at approximately 9:11 PM local time (PDT) which is 04:11 UTC June 21. However, operationally HMS stores daily smoke plume data for a single date relative to North America, though technically these files contain smoke plumes from two different UTC dates. In order to make the daily overlap analysis more relevant to the daylight hours over North America (when the smoke is observed), our overlap analysis shifted HYSPLIT trajectory times backwards by 6 hours. Had we not done this HYSPLIT Points with analyzed start times late in the afternoon could never overlap that dates smoke plumes since those trajectories occur after 24 UTC (next date). The adjustment allows more trajectories UTC dates to better overlap the daylight analysis date of the smoke plumes (including early morning). The results presented in Chapter 1 are highly insensitive to whether or not the 6 hour adjustment was applied. Previous versions of the figures and analysis prior to the 6 hour adjustment are nearly identical.

Validating the trajectories using only the first day of smoke would make it more likely that HYSPLIT points analyzed in the morning would overlap a plume than HYSPLIT points analyzed later in the day. Due to the visible daylight imagery limitations placed on analyzed smoke plumes, fires that start later in the day are less likely to overlap the matching dates smoke plumes than fires that start early in the day.

S4 EDAS and GDAS smoke hours summaries for U.S. regions

The biggest difference in smoke hours between EDAS and GDAS can be seen in Alaska, since only the southeast portion of the state is within the EDAS domain. Regions that receive smoke from high latitudes generally have more smoke-hours when the GDAS data is used (Mid Atlantic, Midwest, Northeast). Regardless of the meteorological dataset used for the trajectory calculations, the Northwest, Rocky Mountains, and Southwest are the largest smoke-source regions. They also have more smoke-hours over their regions when EDAS meteorology is used. This suggests that the higher-resolution EDAS meteorology results in more trajectories that overlap smoke plumes within the first 49 hours than trajectories run with GDAS meteorology. Thus the consequence of using EDAS meteorology is for regions to contribute more smoke-hours within their own borders and fewer downwind.

Table S3: Summary of smoke hours produced by and over each U.S. region for each meteorology dataset. Numbers show June-September totals between 2007-2014.

Region	GDAS Produced	EDAS Produced	GDAS Over	EDAS Over
Alaska	8,412,383	2	4,785,421	10,685
Great Plains	781,704	757,094	12,382,290	10,539,018
Mid Atlantic	115,583	108,265	563,442	497,545
Midwest	143,343	145,691	6,684,312	5,282,670
Northeast	6,723	8,784	782,790	541,174
Northwest	29,360,026	29,120,925	12,083,168	12,890,475
Rocky Mt.	14,252,104	13,703,437	18,066,760	19,064,474
Southeast	2,553,898	2,378,645	1,799,372	1,745,907
Southern Plains	1,286,888	1,296,988	3,206,060	3,437,671
Southwest	28,552,926	28,255,271	10,069,858	10,084,839

S5 Smoke hour false positives

Our intent is for smoke hours to represent the advection of smoke; however, trajectory points can overlap smoke plumes that are not associated with the correct fires, and this creates smoke hours that are false positives. There are a number of possible scenarios that could lead to a smoke-hour false positive; to illustrate this we will highlight two possible scenarios here. 1) Trajectory points could be validated on the

first two days when they overlap a smoke plume that has been advected from upwind. These trajectory points could then travel with that existing smoke plume and be incorrectly classified as smoke hours. This scenario does not necessarily mean that the fire associated with the trajectory does not produce smoke. It is possible that the trajectory misses the plume created by its associated HYSPLIT point due to being initialized at the wrong injection height. 2) Trajectory points could overlap smoke for the first day, then no smoke for a couple of days, then overlap an unrelated smoke plume very far downwind. Both of these types of false positives have been observed in developing our definition for smoke hours.

Currently the best way we have of identifying false-positive smoke hours is sorting trajectories into smaller aggregates (individual years and seasons) and observing the heat maps associated with these subsets of trajectories. The second type of false positive described above would be visible in these types of maps as disconnected smoke hours. The long-range transport of smoke hours originating in the Northwest during winter months provides ideal conditions to test the methods described in Sect 5.2. In winter months there are fewer and smaller fires and fewer smoke plumes analyzed by HMS. Additionally, fires that occur in the winter have lower smoke-injection altitudes on average compared to their summer counterparts (Val Martin et al., 2010; Paugam et al., 2016). All of these factors will tend to reduce the long-range transport of smoke during winter months. The Northwest has very-little fire activity for the first three months of the year. In contrast, January, February, and March have a significant amount of local fire activity in the Southeast as indicated by the number of HYSPLIT points for these months. These conditions create an ideal environment for trajectories that originate in the Northwest to travel to the Southeast without advecting any smoke and create false positive smoke hours. When we plot the heat map for the Northwest for these months we see two disconnected hot spots (Fig. S2), which almost certainly represent false positives far downwind. Figure S2 shows how the Northwest contributes smoke hours to the Northwest and Southeast without impacting the Rocky Mountain region. This strongly suggests that the smoke hours over the Southeast are false positives. During the summer there is very little local fire activity in the Southeast so it is likely this problem dominates the summer smoke hour transport climatologies shown in Fig. 13 of the manuscript. This type of evidence for false positive smoke hours is not apparent in summertime data; however, the very large smoke plumes analyzed during the summer may not allow for disconnection. Even for individual-year heat maps, we do not observe disconnected areas of smoke impact far downwind of source regions. Winter smoke-hour transport figures for all regions are shown in Fig. S7.

HMS analysts observe that fires in the Great Plains, Southern Plains, and Midwest, generally produce short duration smoke plumes that quickly dissipate. It is unusual for smoke produced in these regions to persist long enough to reach areas of Northern Canada or the Canadian Maritimes. Thus the long range transport smoke hour impact from these regions shown in manuscript Fig. S6 may be examples of trajectories overlapping HMS smoke plumes that originated in other source regions.

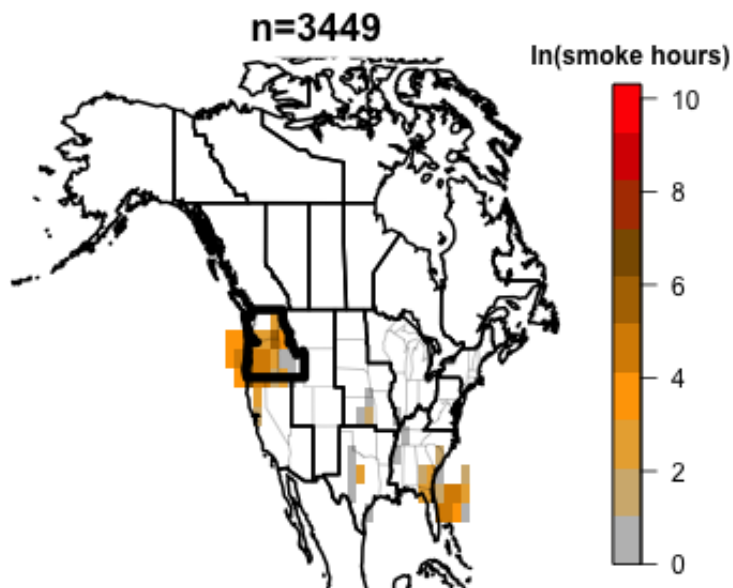
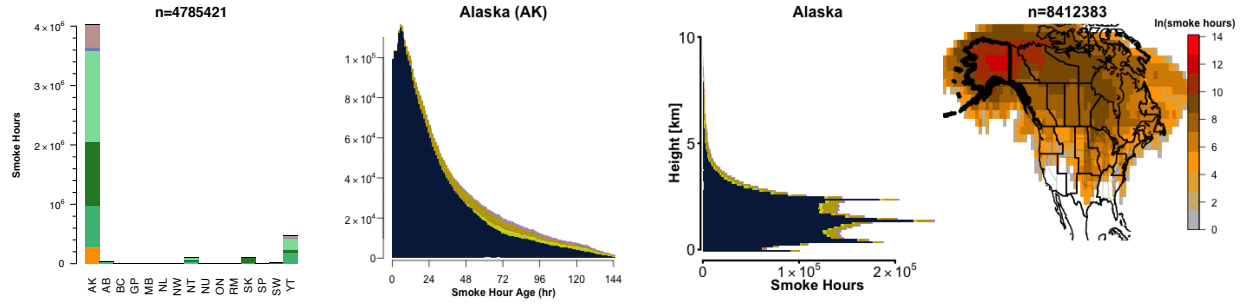


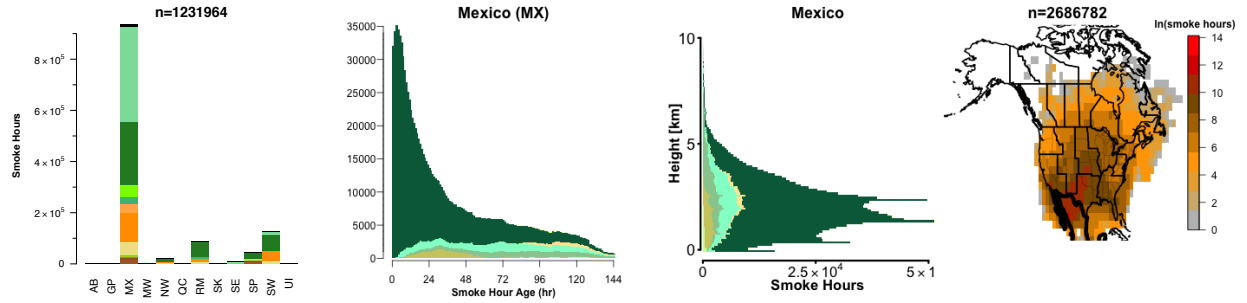
Figure S2: Total number of smoke hours produced by the Northwest region for months January-March between 2007 and 2014 using GDAS1 meteorology.

S6 Smoke hour transport figures for non-CONUS regions:

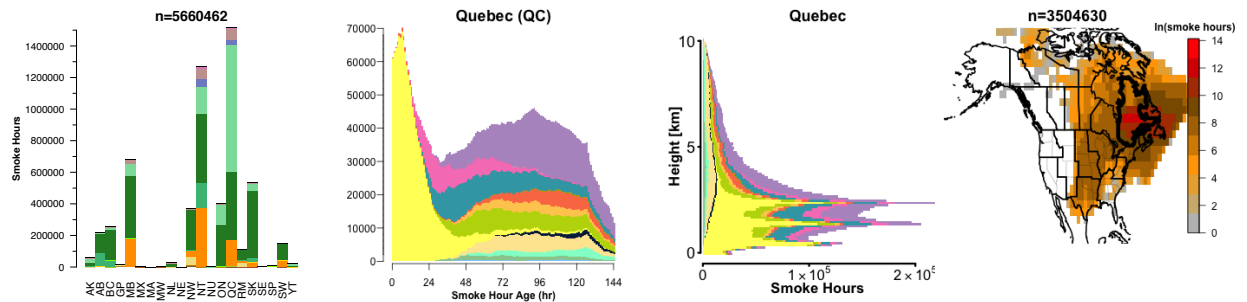
Here we present the GDAS1 smoke hour transport figures (similar to Fig 11) for regions outside of CONUS. The U.S Islands and Cuba are not included due to limited smoke-hours over these regions.



(a)



(b)



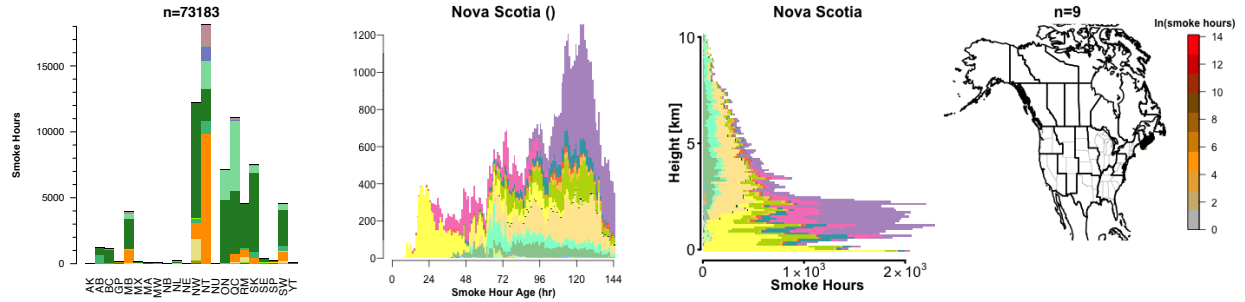
(c)

Land Cover

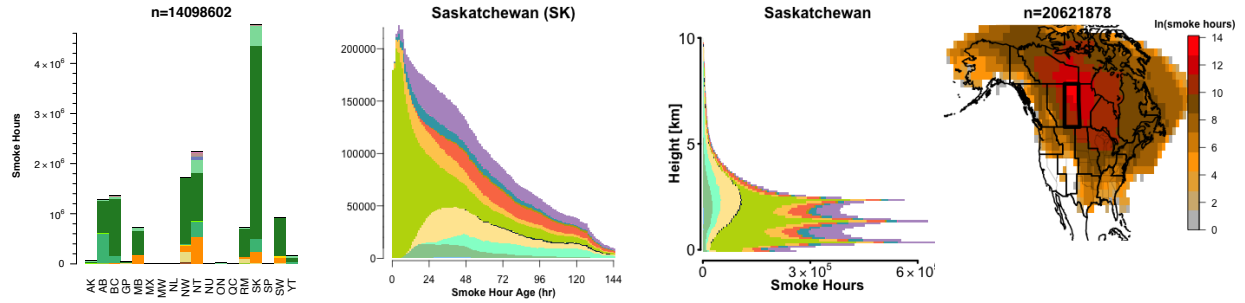
- Barren or Sparsely Vegetated
- Cropland/Grassland Mosaic
- Cropland/Woodland Mosaic
- Deciduous Broadleaf Forest
- Dryland Cropland and Pasture
- Evergreen Broadleaf Forest
- Evergreen Needleleaf Forest
- Grassland
- Irrigated Cropland and Pasture
- Mixed Forest
- Mixed Shrubland/Grassland
- Mixed Tundra
- noAssignment
- Savanna
- Shrubland
- Snow or Ice
- Unlabelled land area
- Wooded Tundra
- Wooded Wetland

Region

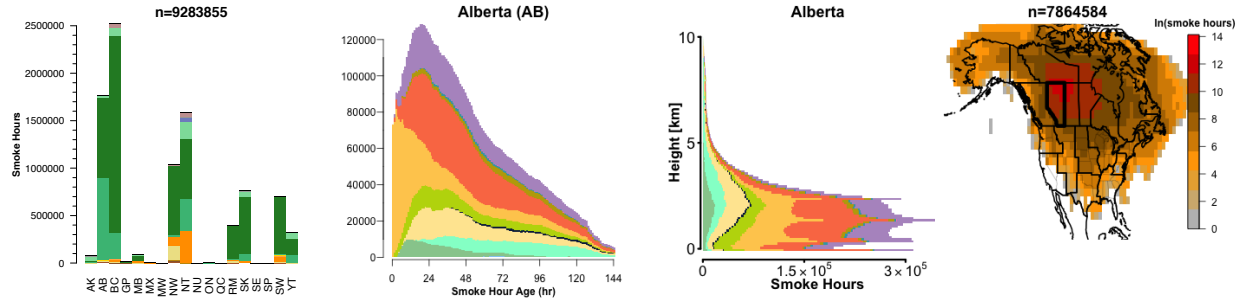
- GP
- MX
- BC
- NU
- NE
- RM
- QC
- NB
- NT
- MA
- SW
- NS
- PE
- SE
- NW
- SK
- YT
- MW
- AK
- AB
- MB
- SP
- UI
- NL
- ON
- CU
- BS



(d)



(e)



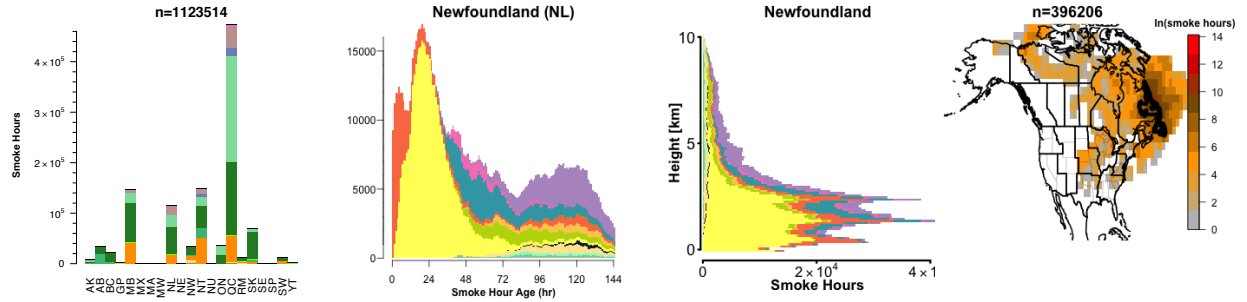
(f)

Land Cover

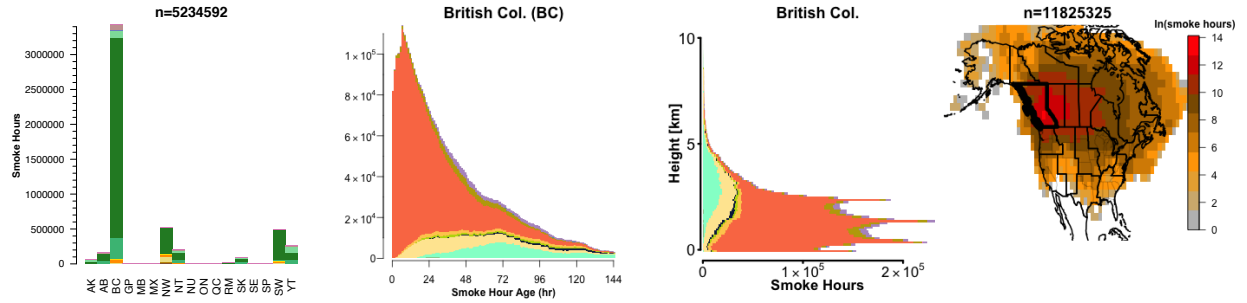
- Barren or Sparsely Vegetated
- Cropland/Grassland Mosaic
- Cropland/Woodland Mosaic
- Deciduous Broadleaf Forest
- Dryland Cropland and Pasture
- Evergreen Broadleaf Forest
- Evergreen Needleleaf Forest
- Grassland
- Irrigated Cropland and Pasture
- Mixed Forest
- Mixed Shrubland/Grassland
- Mixed Tundra
- noAssignment
- Savanna
- Shrubland
- Snow or Ice
- Unlabelled land area
- Wooded Tundra
- Wooded Wetland

Region

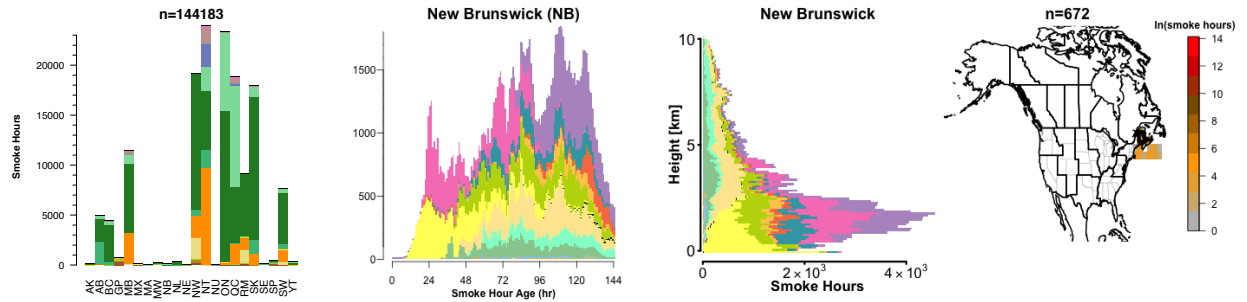
- GP
- NE
- MA
- SE
- MW
- SP
- MX
- RM
- SW
- NW
- AK
- UI
- BC
- QC
- NS
- SK
- AB
- NL
- NU
- NB
- PE
- YT
- MB
- ON
- CU
- BS



(g)



(h)



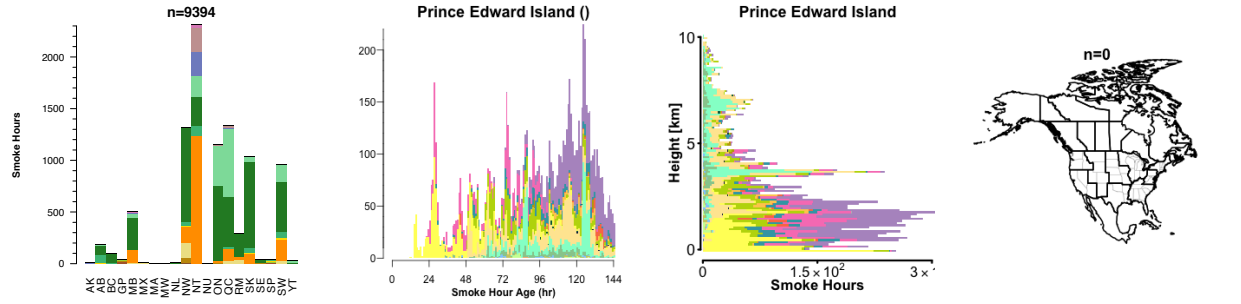
(i)

Land Cover

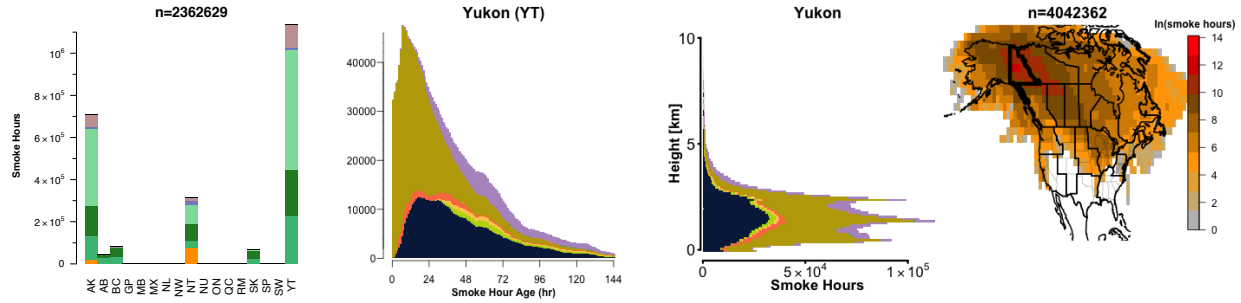
- Barren or Sparsely Vegetated
- Cropland/Grassland Mosaic
- Cropland/Woodland Mosaic
- Deciduous Broadleaf Forest
- Dryland Cropland and Pasture
- Evergreen Broadleaf Forest
- Evergreen Needleleaf Forest
- Grassland
- Irrigated Cropland and Pasture
- Mixed Forest
- Mixed Shrubland/Grassland
- Mixed Tundra
- noAssignment
- Savanna
- Shrubland
- Snow or Ice
- Unlabelled land area
- Wooded Tundra
- Wooded Wetland

Region

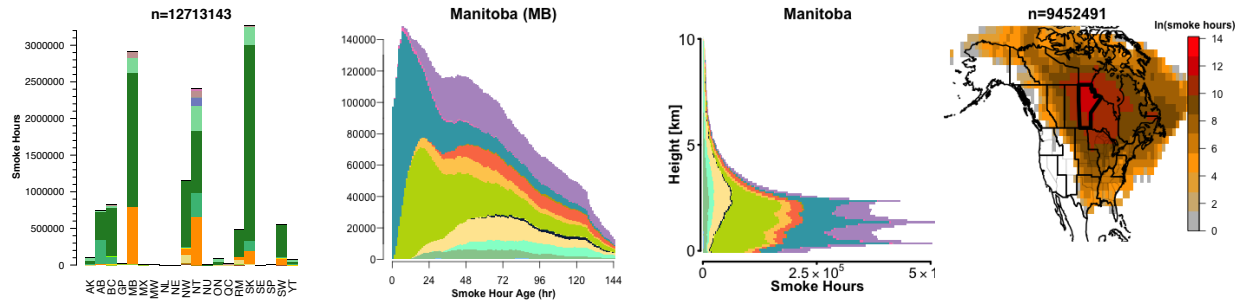
- GP
- NE
- MA
- SE
- MW
- SP
- MX
- RM
- SW
- NW
- AK
- UI
- BC
- QC
- NS
- SK
- AB
- NL
- NU
- NB
- PE
- YT
- MB
- ON
- CU
- BS



(j)



(k)



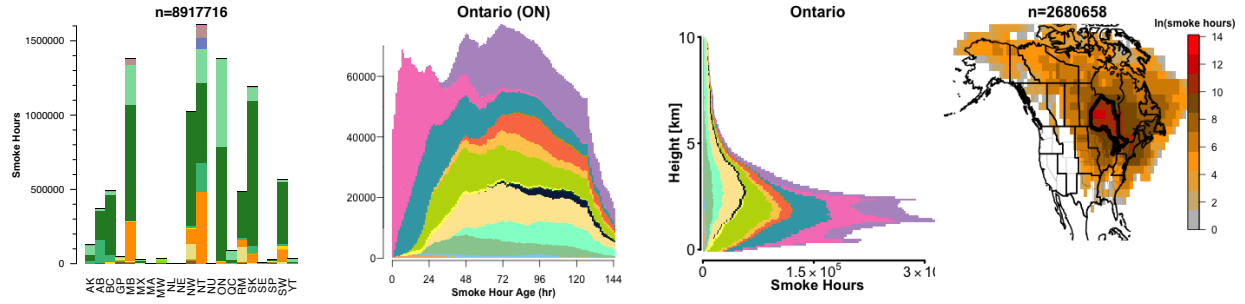
(l)

Land Cover

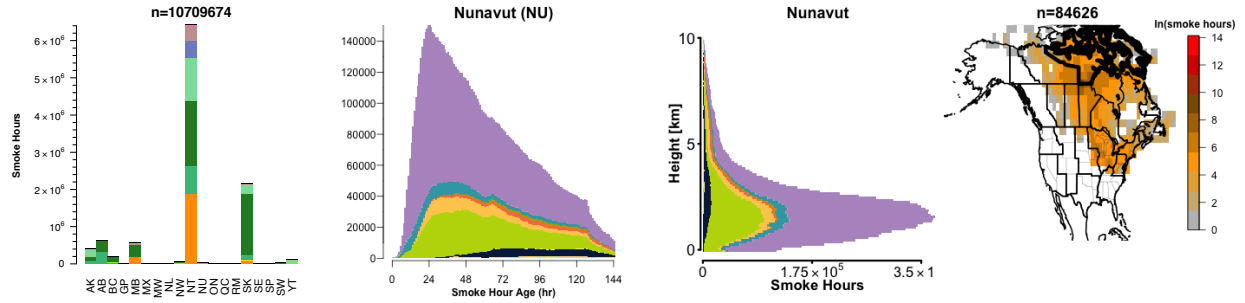
- Barren or Sparsely Vegetated
- Cropland/Grassland Mosaic
- Cropland/Woodland Mosaic
- Deciduous Broadleaf Forest
- Dryland Cropland and Pasture
- Evergreen Broadleaf Forest
- Evergreen Needleleaf Forest
- Grassland
- Irrigated Cropland and Pasture
- Mixed Forest
- Mixed Shrubland/Grassland
- Mixed Tundra
- noAssignment
- Savanna
- Shrubland
- Snow or Ice
- Unlabelled land area
- Wooded Tundra
- Wooded Wetland

Region

- GP
- MX
- BC
- NU
- NE
- RM
- QC
- NB
- NT
- MA
- SW
- NS
- PE
- CU
- SE
- NW
- SK
- YT
- BS
- MW
- AK
- AB
- MB
- SP
- UI
- NL
- ON



(m)



(n)



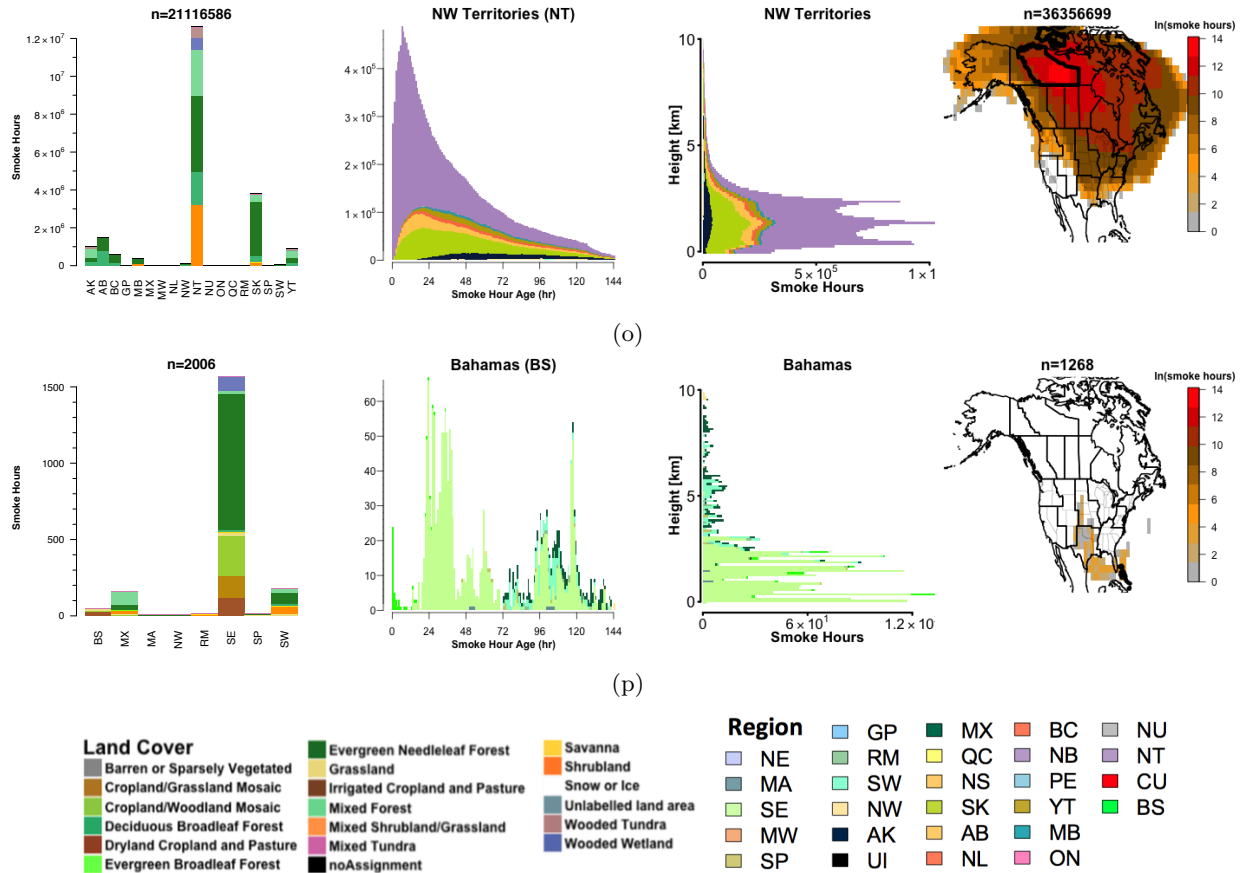


Figure S3: June-September 2007-2014 regional smoke hour transport summaries for non-CONUS regions. Column 1 shows the number of smoke hours in the region by source region and land cover classification. Only source regions with non-zero smoke hour contributions are shown. Column 2 shows the distribution of smoke hour age segregated by source region using the colors from manuscript Fig. 6. Column 3 shows the distribution of smoke hour height segregated by source region using the colors from manuscript Fig. 6. Column 4 shows the count of smoke hours produced by a region on a $2^\circ \times 2^\circ$ degree grid with consistent color bar for all regions. The grid spans $18^\circ - 180^\circ$ W and $18^\circ - 90^\circ$ N, a domain covering all five sectors where HMS analyzes smoke plumes (only a subset plotted). Shaded values are the natural logarithm of the number of smoke hours in each grid cell. All figures were generated using GDAS1 meteorology.

S7 EDAS meteorology versions of manuscript figures:

Figures 10 & 11 of the manuscript is driven by GDAS1 meteorology data. This section provides these figures when EDAS40 meteorology data is used to run HYSPLIT trajectories.

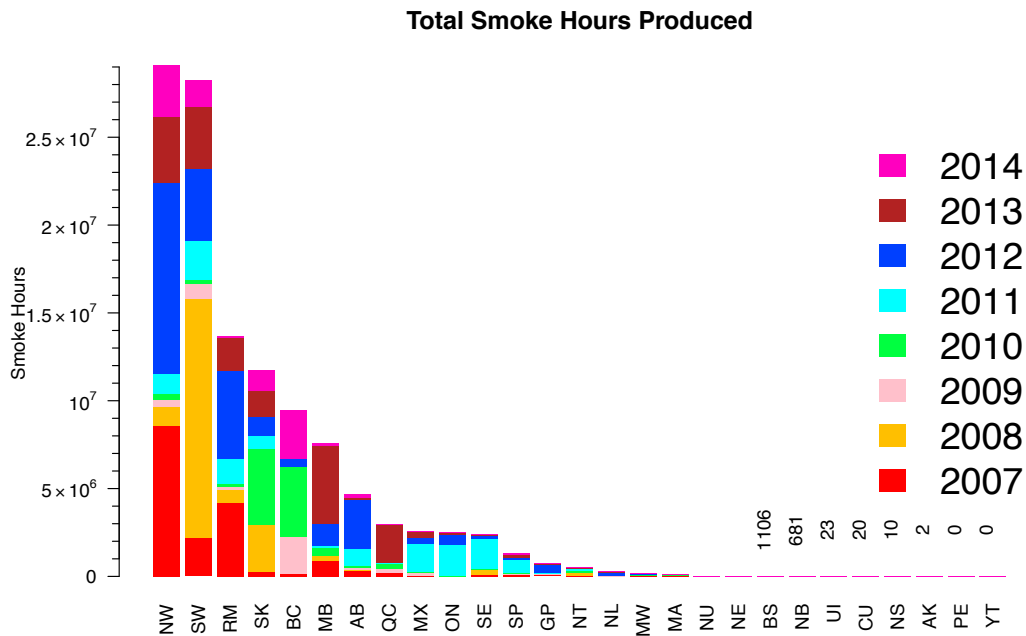


Figure S4: Total number of smoke hours produced (anywhere) by each region for months June-September between 2007 and 2014 using EDAS40 meteorology.

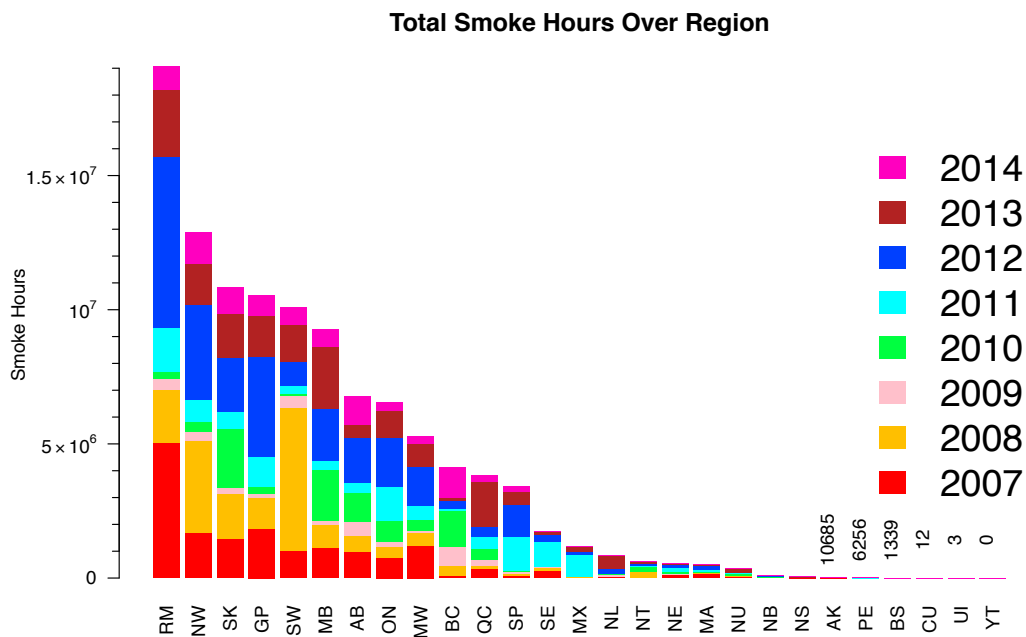
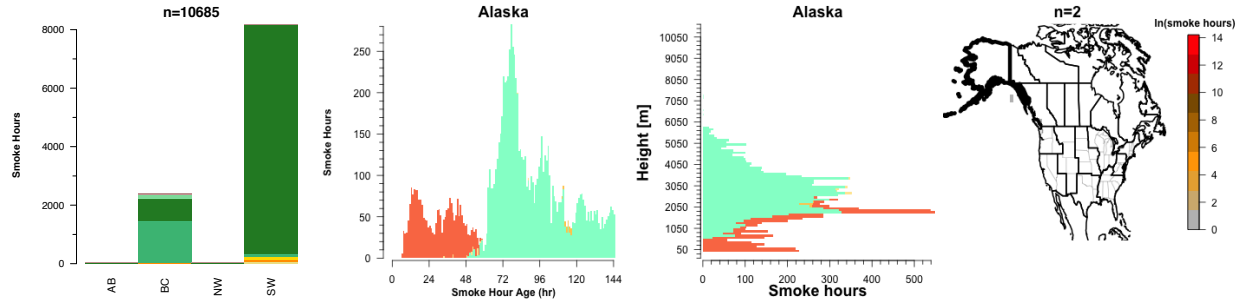
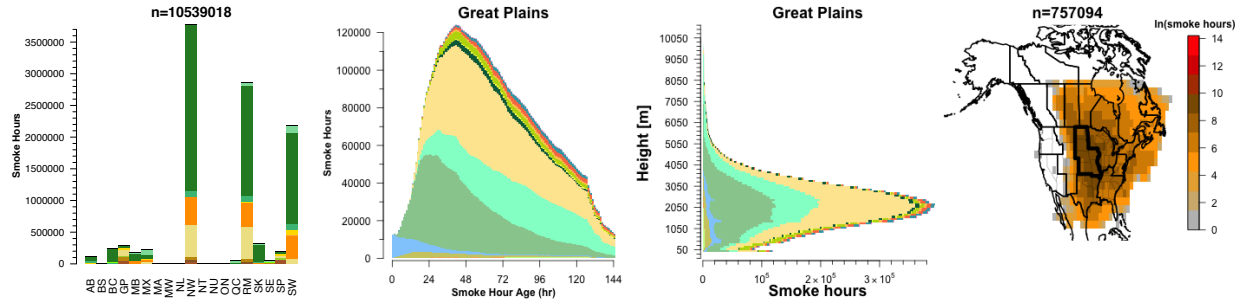


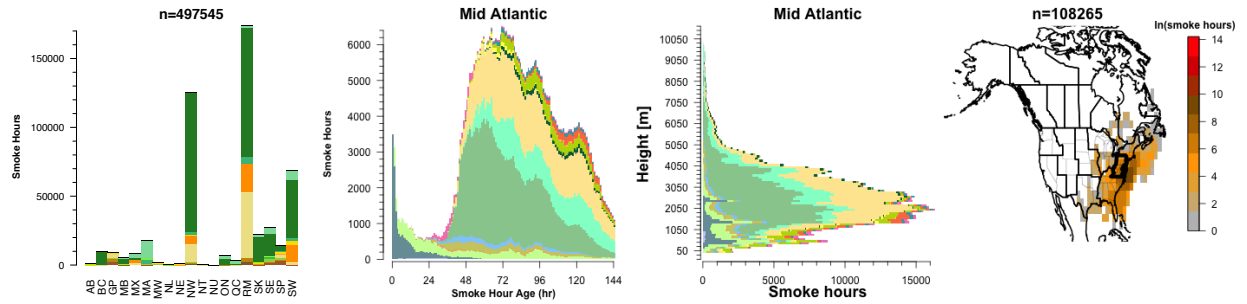
Figure S5: Total number of smoke hours over each region sorted from highest to lowest for months June-September between 2007 and 2014 using EDAS40 meteorology.



(a)



(b)



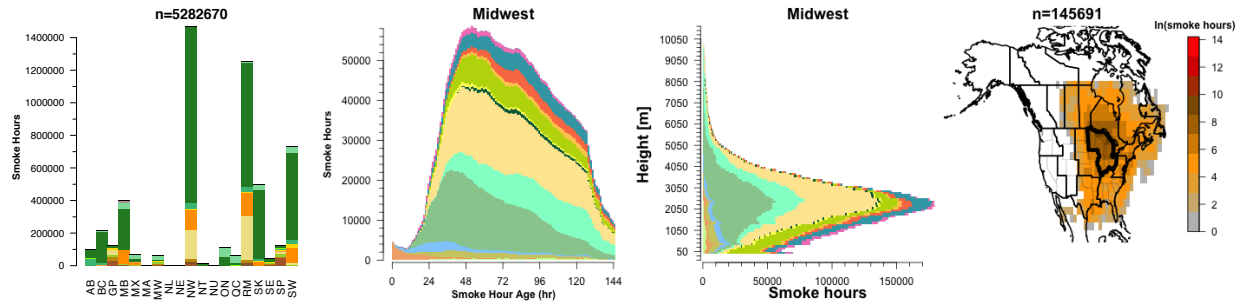
(c)

Land Cover

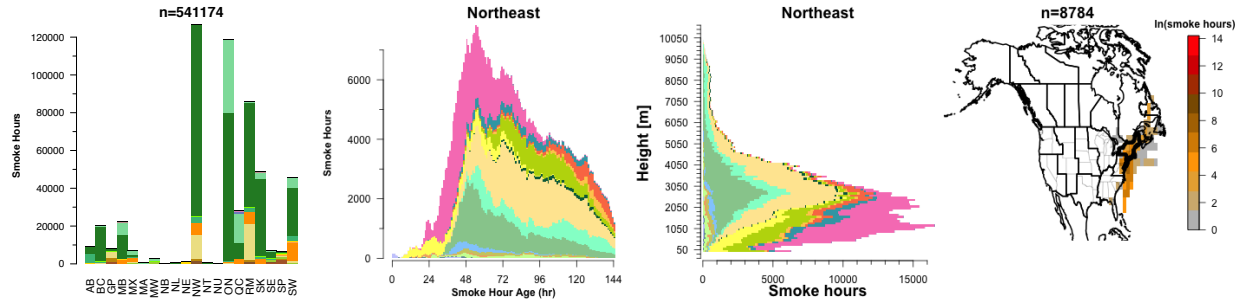
- Barren or Sparsely Vegetated
- Cropland/Grassland Mosaic
- Cropland/Woodland Mosaic
- Deciduous Broadleaf Forest
- Dryland Cropland and Pasture
- Evergreen Broadleaf Forest
- Evergreen Needleleaf Forest
- Grassland
- Irrigated Cropland and Pasture
- Mixed Forest
- Mixed Shrubland/Grassland
- Mixed Tundra
- noAssignment
- Savanna
- Shrubland
- Snow or Ice
- Unlabelled land area
- Wooded Tundra
- Wooded Wetland

Region

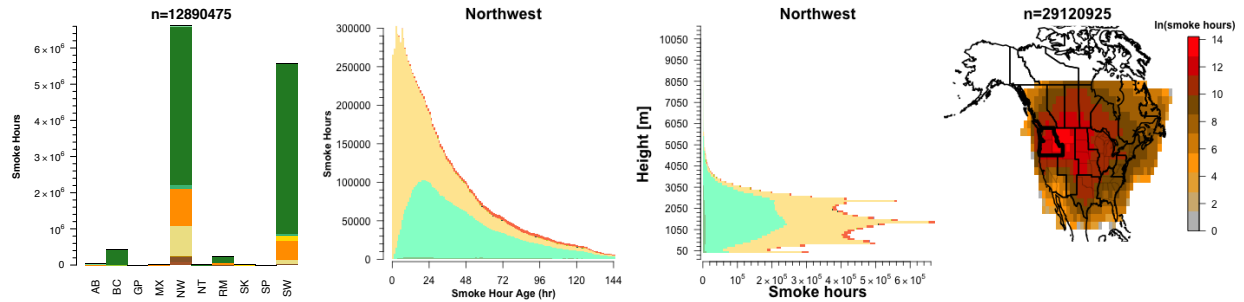
- GP
- NE
- MA
- SE
- MW
- SP
- RM
- SW
- NW
- AK
- UI
- MX
- QC
- NS
- SK
- AB
- NL
- BC
- NB
- PE
- YT
- MB
- ON
- NU
- NT
- CU
- BS



(d)



(e)



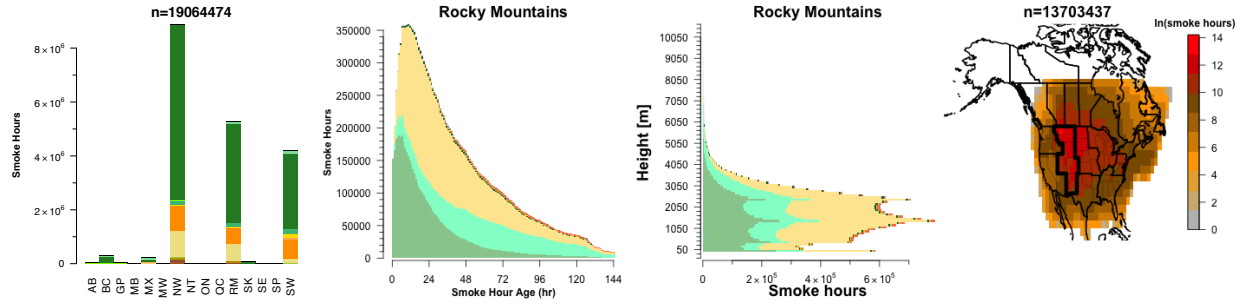
(f)

Land Cover

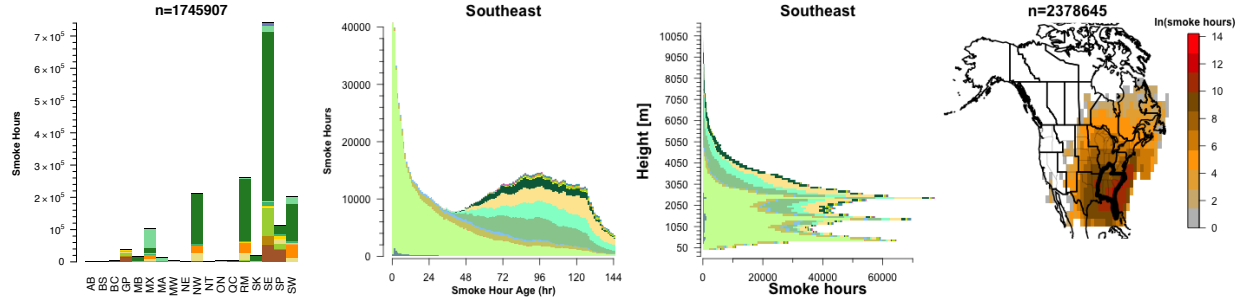
- Barren or Sparsely Vegetated
- Cropland/Grassland Mosaic
- Cropland/Woodland Mosaic
- Deciduous Broadleaf Forest
- Dryland Cropland and Pasture
- Evergreen Broadleaf Forest
- Evergreen Needleleaf Forest
- Grassland
- Irrigated Cropland and Pasture
- Mixed Forest
- Mixed Shrubland/Grassland
- Mixed Tundra
- noAssignment
- Savanna
- Shrubland
- Snow or Ice
- Unlabelled land area
- Wooded Tundra
- Wooded Wetland

Region

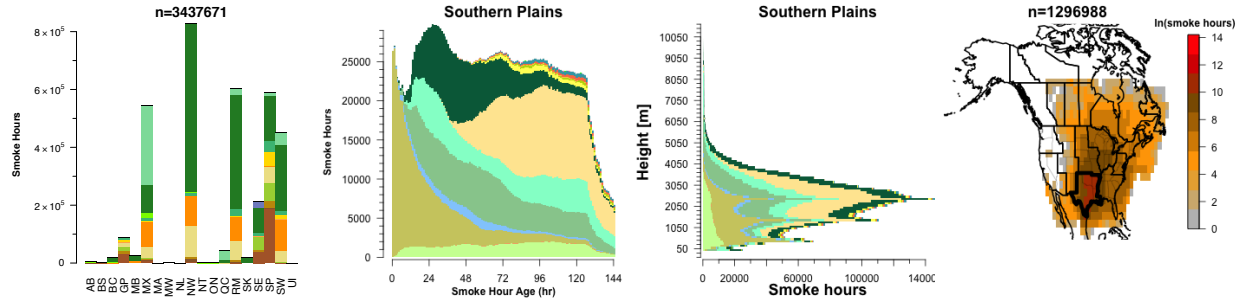
- GP
- NE
- MA
- SE
- MW
- SP
- MX
- RM
- SW
- NW
- AK
- UI
- BC
- QC
- NS
- SK
- AB
- NL
- NU
- NB
- PE
- YT
- MB
- ON
- CU
- BS



(g)



(h)



(i)

Land Cover

- Barren or Sparsely Vegetated
- Cropland/Grassland Mosaic
- Cropland/Woodland Mosaic
- Deciduous Broadleaf Forest
- Dryland Cropland and Pasture
- Evergreen Broadleaf Forest
- Evergreen Needleleaf Forest
- Grassland
- Irrigated Cropland and Pasture
- Mixed Forest
- Mixed Shrubland/Grassland
- Mixed Tundra
- noAssignment
- Savanna
- Shrubland
- Snow or Ice
- Unlabelled land area
- Wooded Tundra
- Wooded Wetland

Region

- GP
- NE
- MA
- SE
- MW
- SP
- MX
- RM
- SW
- NW
- AK
- UI
- BC
- QC
- NS
- SK
- AB
- NL
- NU
- NB
- PE
- YT
- MB
- ON
- CU
- BS

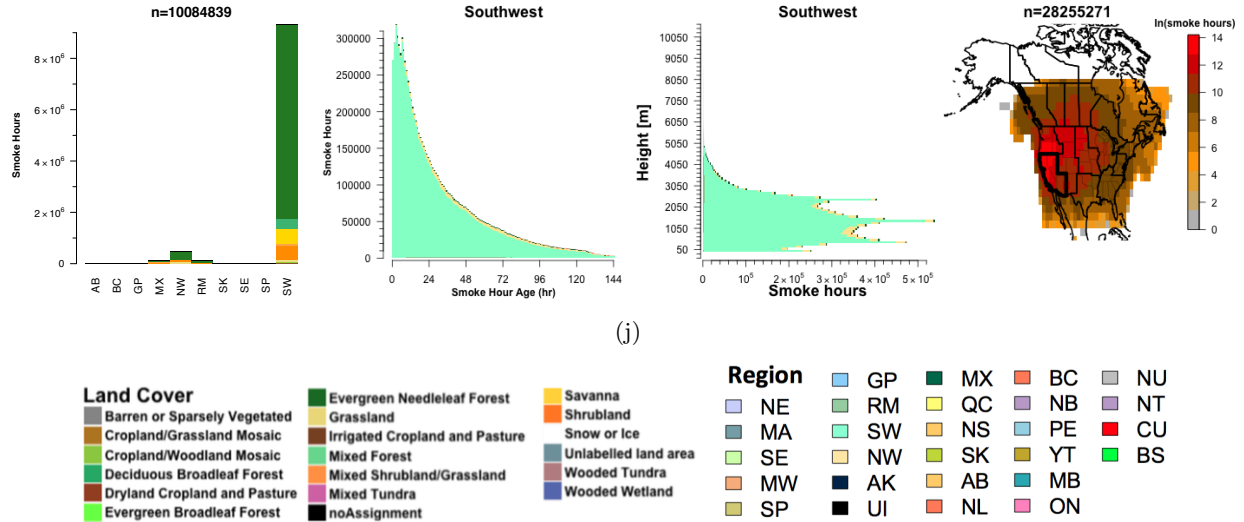
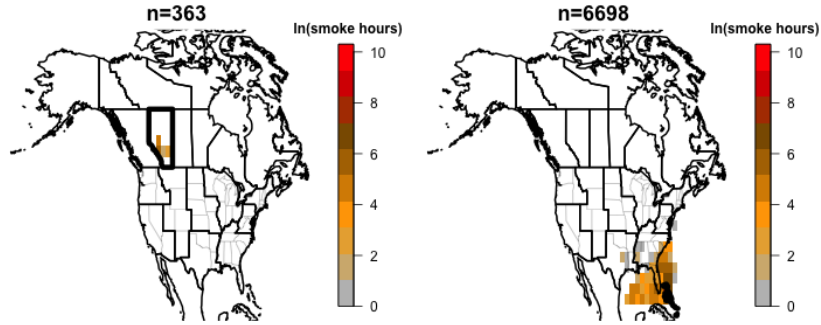


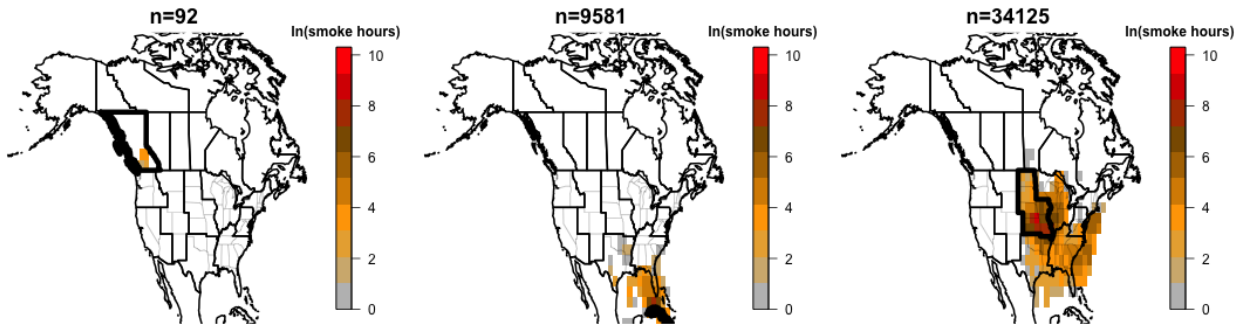
Figure S6: June-September 2007-2014 regional smoke hour transport summaries. Column 1 shows the number of smoke hours in the region by source region and land cover classification. Only source regions with non-zero smoke hour contributions are shown. Column 2 shows the distribution of smoke age segregated by source region. Column 3 shows the distribution of smoke hour height segregated by source region. Column 4 shows the count of smoke hours produced by a region on a $2^\circ \times 2^\circ$ degree grid with consistent colorbar for all regions. The grid spans $18^\circ - 180^\circ$ W and $18^\circ - 90^\circ$ N, a domain covering all five sectors where HMS analyzes smoke plumes (only a subset plotted). Shaded values are the natural log of the number of smoke hours in each grid cell. All figures generated using EDAS meteorology.

S8 Winter heat maps for all regions:

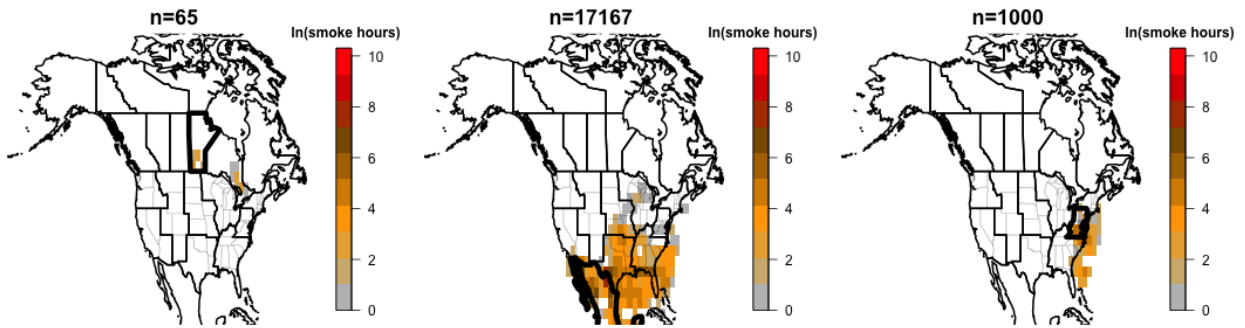
This section contains smoke hour heat maps for all regions with non-zero smoke hours produced in the months January through March years 2007 through 2014. The intention of these figures is to highlight possible smoke-hour false alarms, which are indicated by disconnected regions of smoke hours.



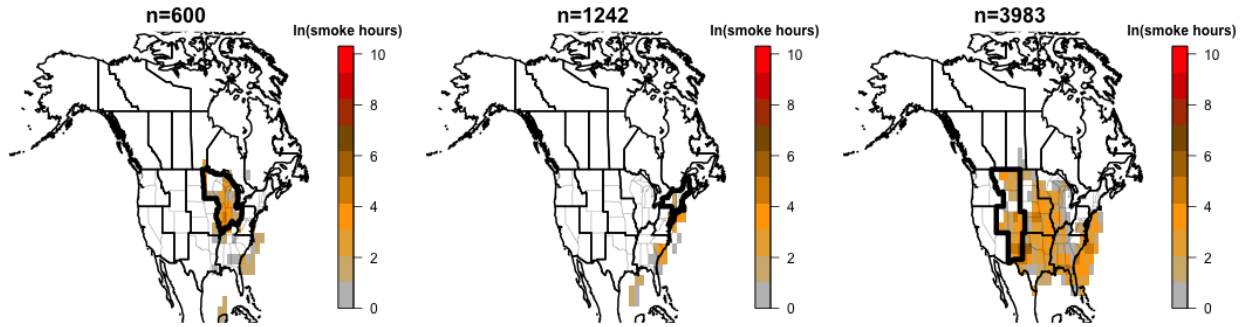
(a)



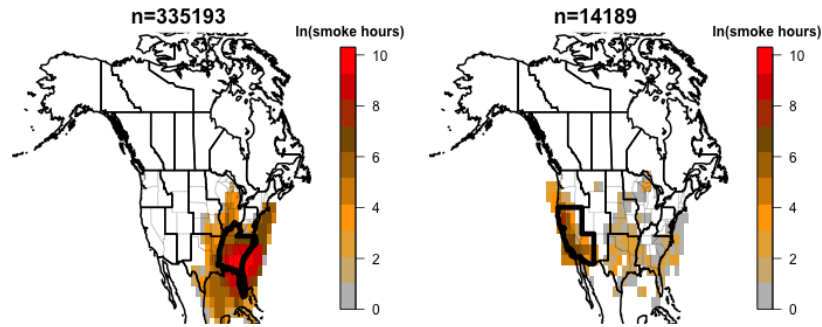
(b)



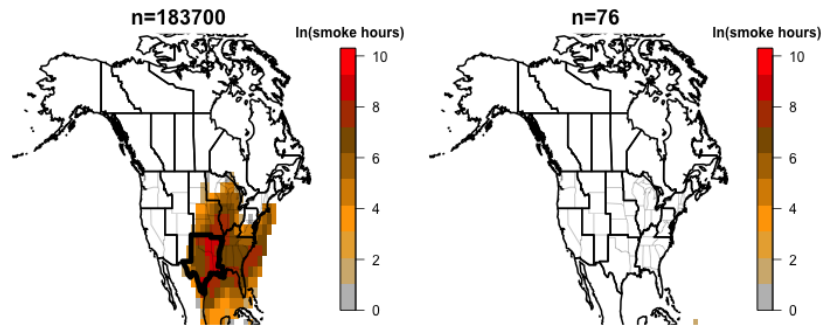
(c)



(d)



(e)



(f)

Figure S7: Total number of smoke hours produced by regions for months January-March between 2007 and 2014 using GDAS1 meteorology. Only regions with more than zero smoke hours produced are shown. Region labels are as follows; row A: (left to right) Alberta, Bahamas. Row B: British Columbia, Cuba, Great Plains. Row C: Manitoba, Mexico, Mid Atlantic. Row D: Midwest, Northeast, Rocky Mountains. Row E: Southeast, Southwest. Row F: Southern Plains, U.S. Islands.

S9 Description of observed weaknesses in land cover classification assignments:

S9.1 Comparison of 1990 AVHRR land cover data to 2010 MODIS/TERRA land cover data

In this section we assign HYSPLIT points land cover using a dataset from the North American Land Cover Change Monitoring System. The specific dataset we choose to use within this system was the 2010 Land Cover of North America at 250 meters data published in 2013 by the Commission for Environmental Cooperation in Montreal, Quebec, Canada (<http://www.cec.org/tools-and-resources/map-files/land-cover-2010>). These data are based on the Moderate Resolution Imaging Spectroradiometer (MODIS/TERRA) seven land spectral bands top of atmosphere reflectance. These data were created primarily to assess North America land cover changes between 2005 and 2010. Approximately 1% of land area land cover classifications changed during this time period.

Overall we find that the differences between the two datasets are driven by an inconsistent list of land cover classifications between the 1992 and 2010 data. Comparing the two different land cover classifications is challenging and requires subjectivity due to the fact that the land cover classification categories are not the same between the 1992 and 2010 data. For example, when assessing whether the two datasets agree on land cover for a given location there needs to be a decision as to whether “Temperate or subpolar needleleaf forest” and “Evergreen Needleleaf Forest” count as a match. Instead of making this decision we show what land cover assignment would have been made for each HYSPLIT point had we used the 2010 data rather than the 1992 data using the same methods described in Sect 2.3 of the manuscript. The only difference is that we allow “Urban” land cover assignments to be made, as these updated data were created after many of the fires in our analysis occurred.

Figures S8 through S24 show what the 2010 land cover data would have assigned to HYSPLIT points for each type of 1992 land cover classification made. For example, Fig. S8 shows the location of HYSPLIT points where the 1992 data assigned the land cover type “cropland/grassland mosaic” and color codes them by the land cover that would have been assigned had we used the 2010 data. The bar graphs on the left shows the abundance of each 2010 data classification.

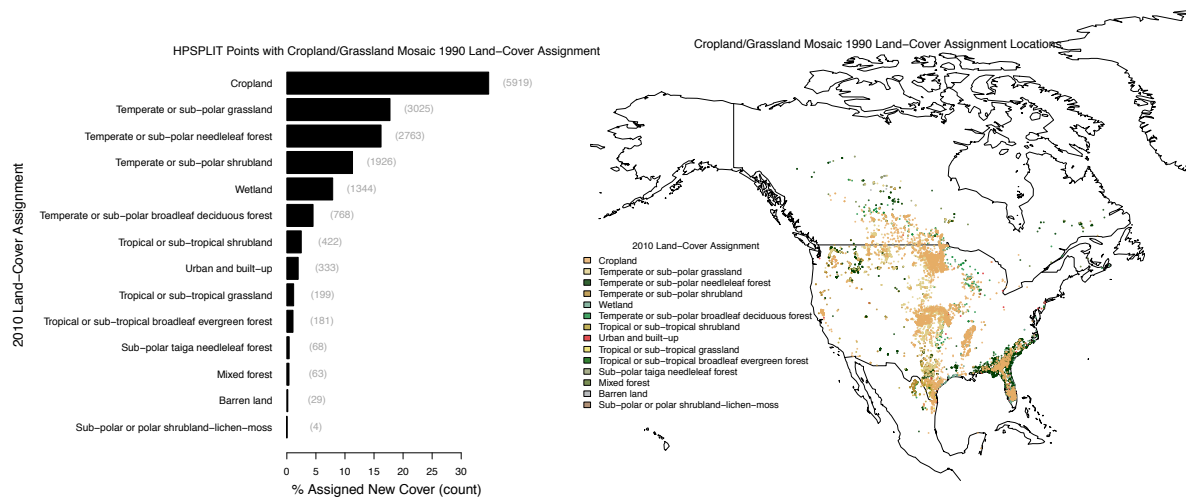


Figure S8

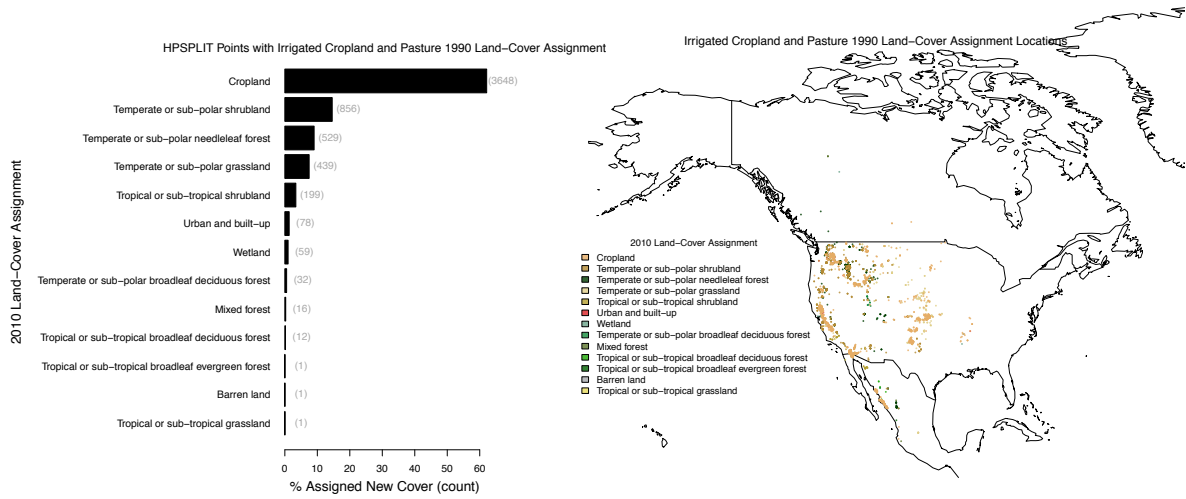


Figure S9

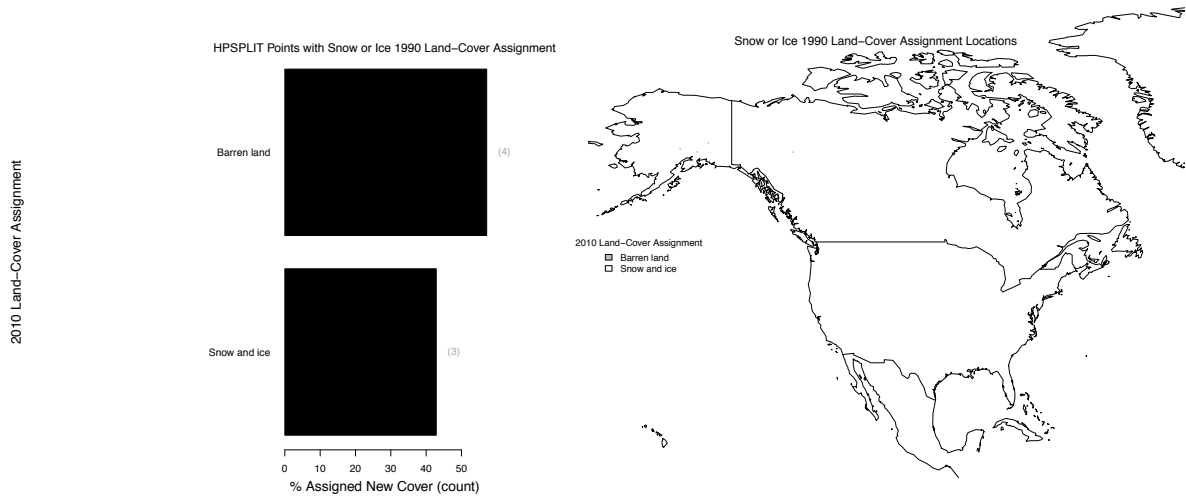


Figure S10

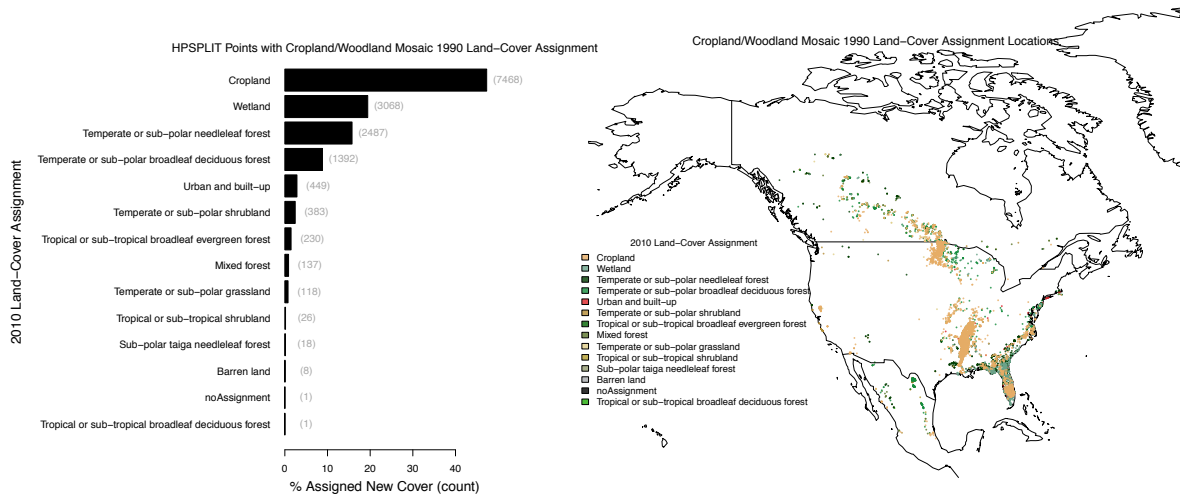


Figure S11

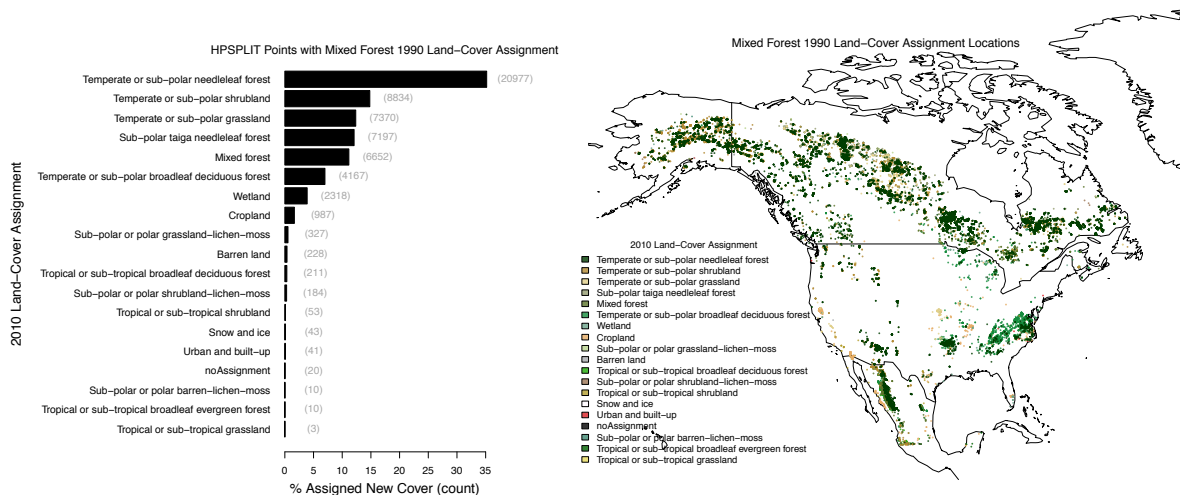
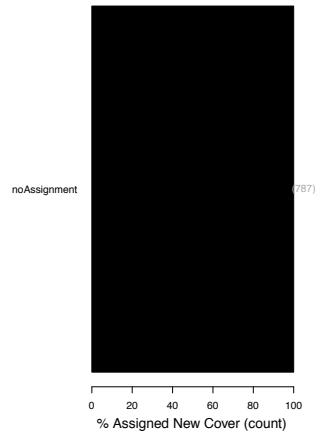


Figure S12

2010 Land-Cover Assignment

HPSPLIT Points with Unlabelled land area 1990 Land-Cover Assignment



Unlabelled land area 1990 Land-Cover Assignment Locations

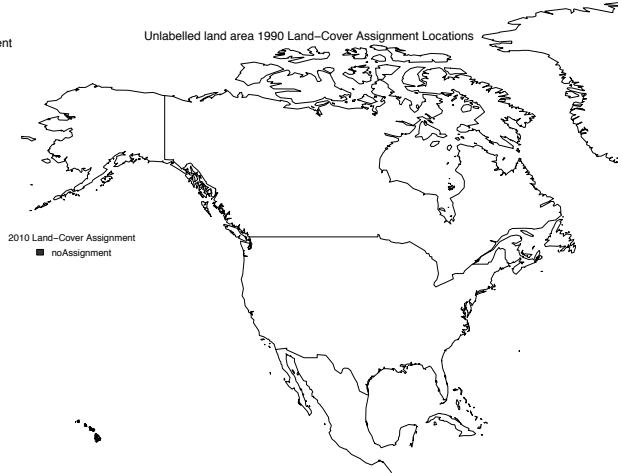
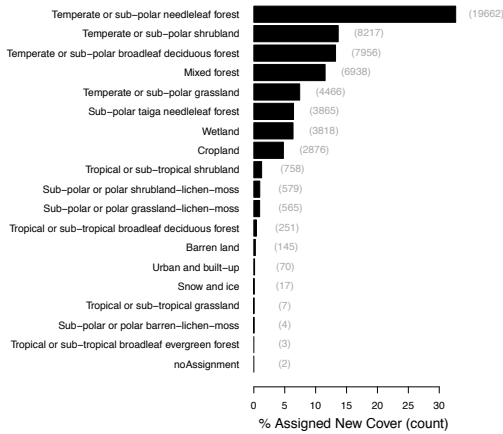


Figure S13

2010 Land-Cover Assignment

HPSPLIT Points with Deciduous Broadleaf Forest 1990 Land-Cover Assignment



Deciduous Broadleaf Forest 1990 Land-Cover Assignment Locations

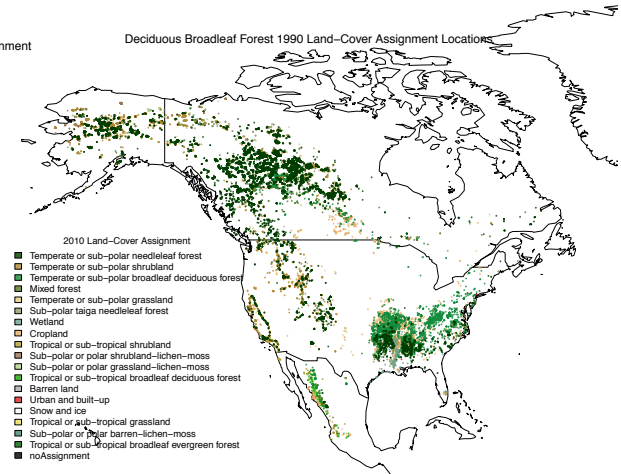
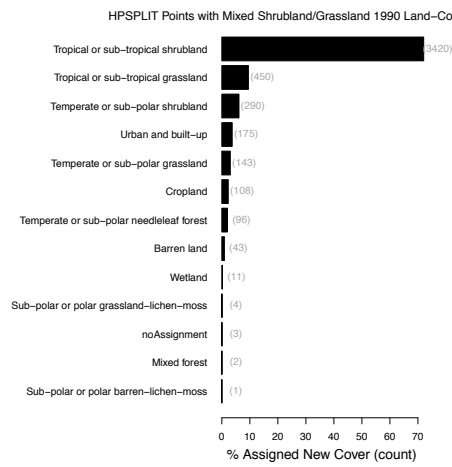


Figure S14

2010 Land-Cover Assignment



Mixed Shrubland/Grassland 1990 Land-Cover Assignment Locations

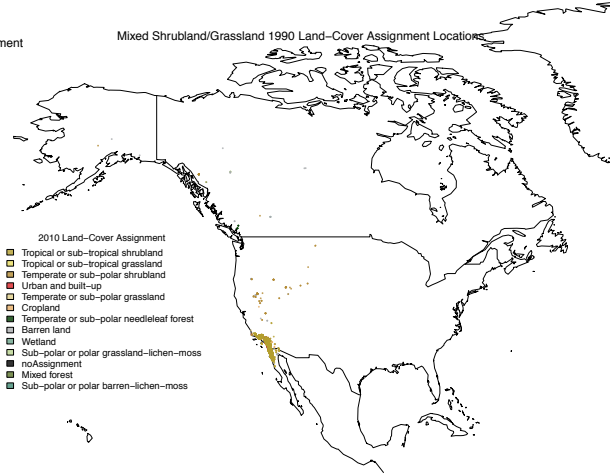
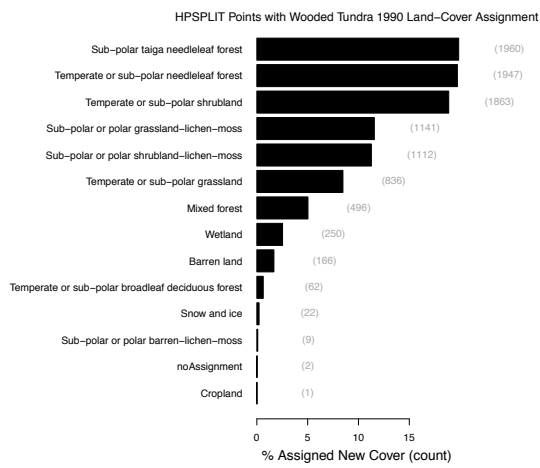


Figure S15

2010 Land-Cover Assignment



Wooded Tundra 1990 Land-Cover Assignment Locations

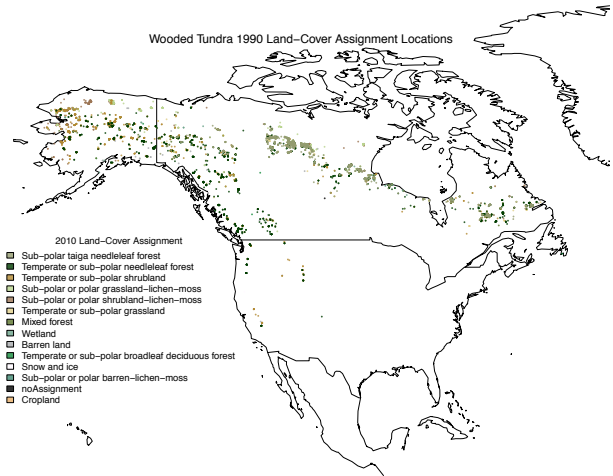


Figure S16

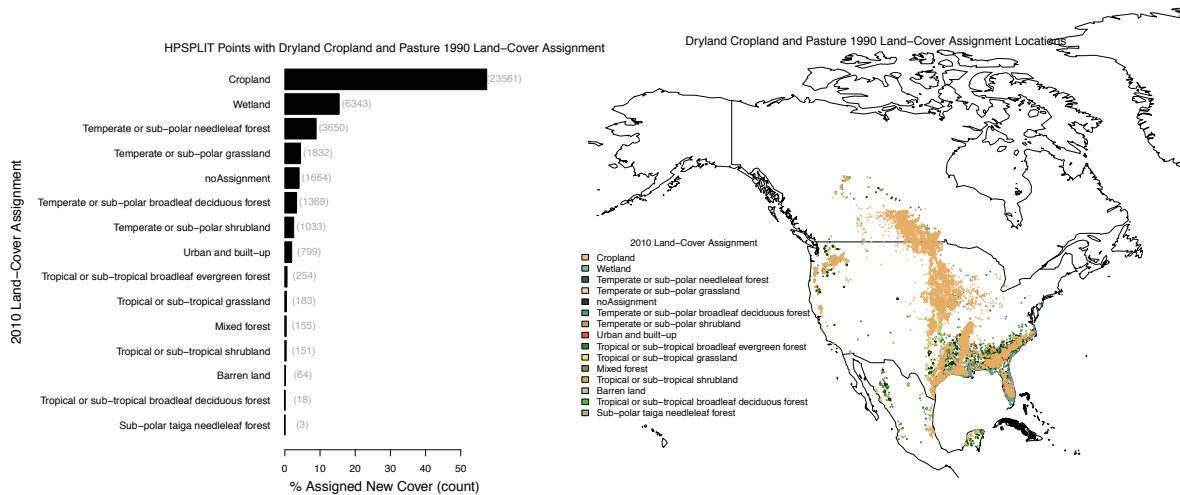


Figure S17

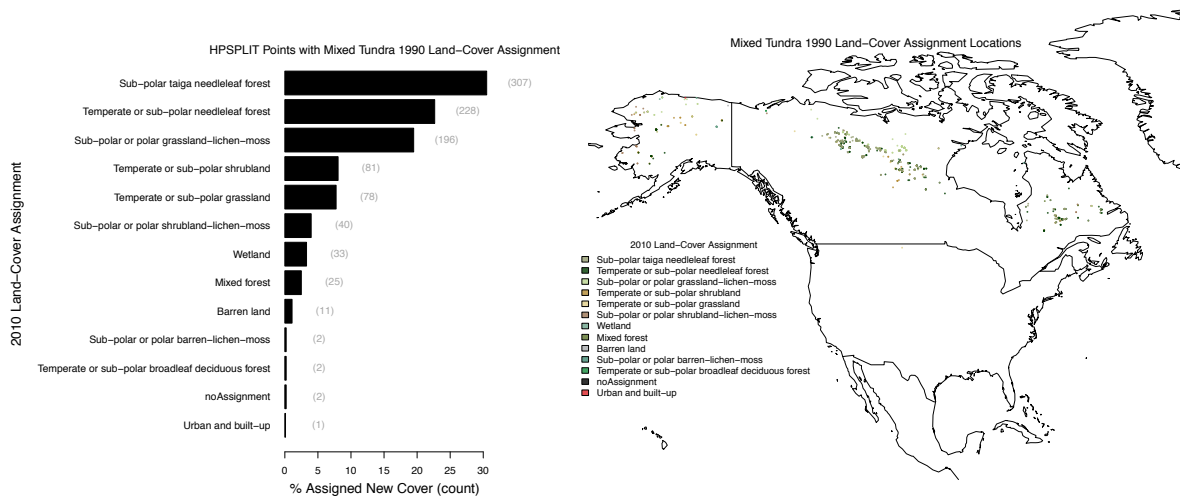


Figure S18

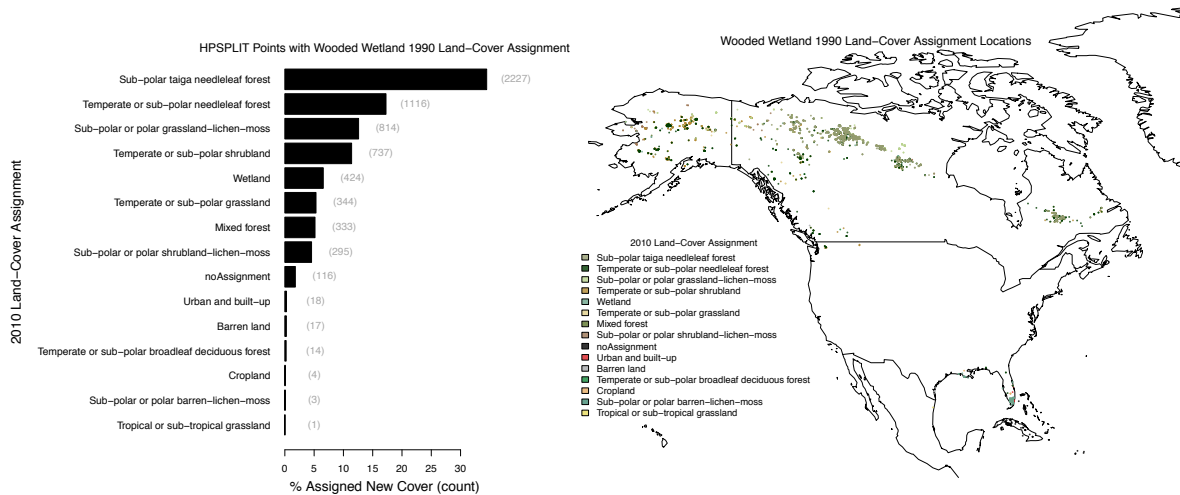


Figure S19

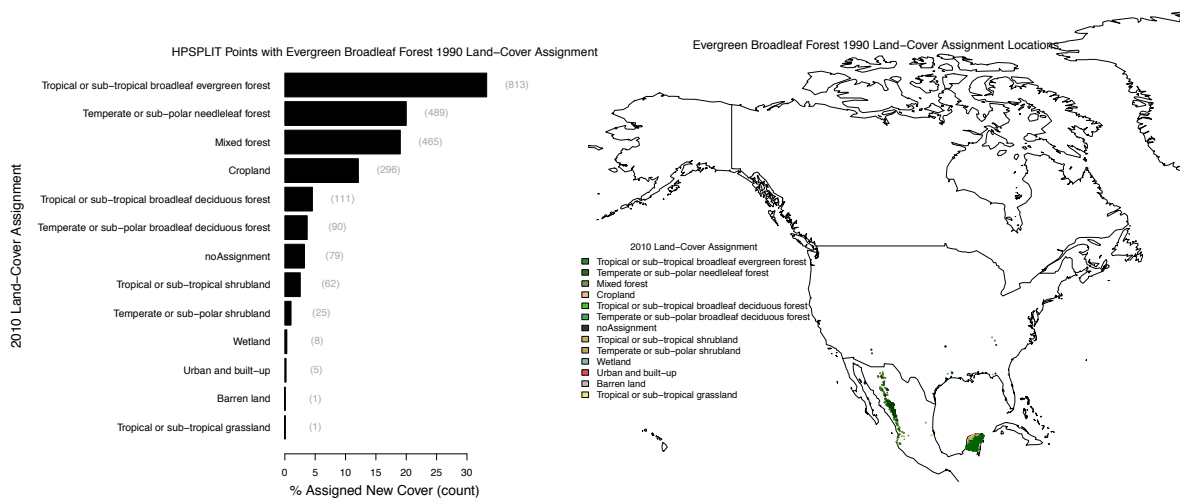


Figure S20

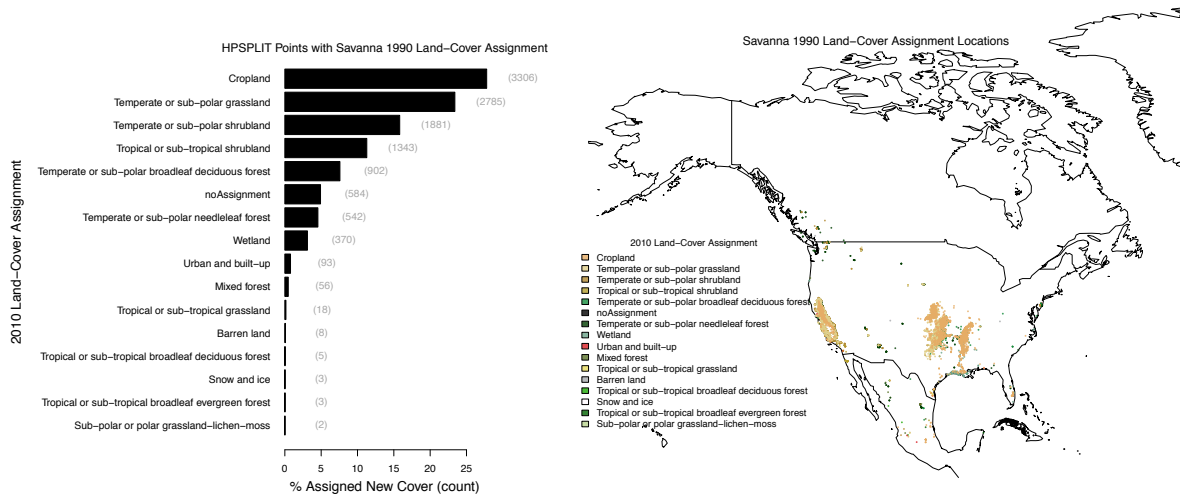


Figure S21

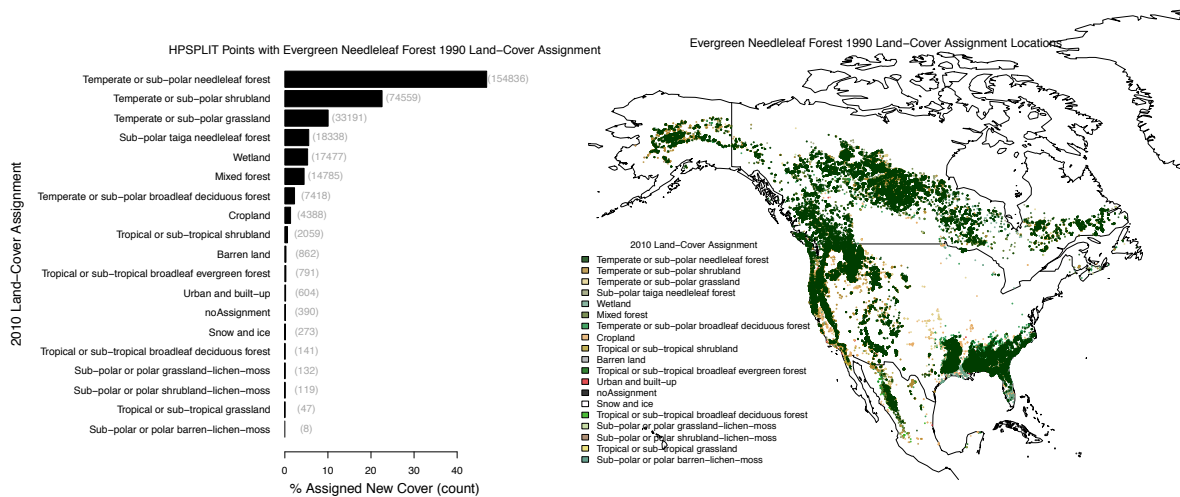


Figure S22

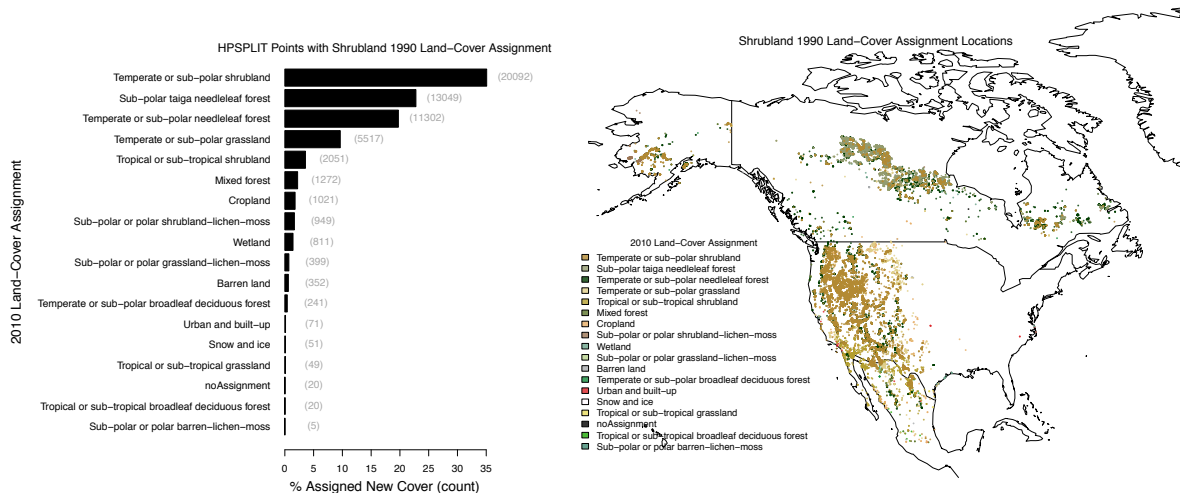


Figure S23

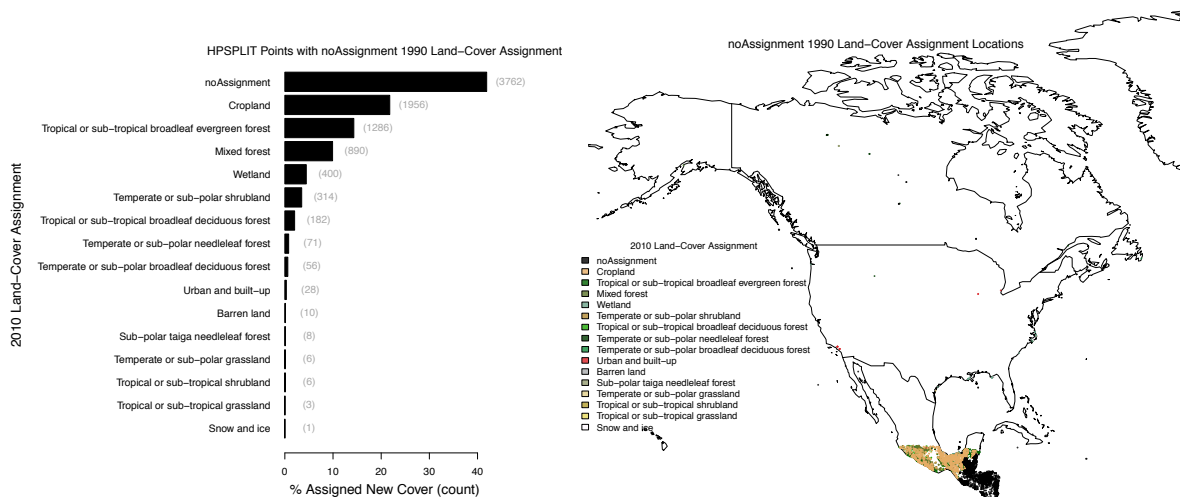


Figure S24

S9.2 Comparison of 1990 AVHRR land-cover data to Google Earth visible imagery

The following weaknesses were observed when comparing the land cover assignment made using the methods described in Sect 2.3 of the manuscript to visible imagery provided by Google Earth. Steven Brey extensively audited the quality of the automated land cover assignments by plotting HYSPLIT point locations in Google Earth and using the visual imagery to make my own human assessment of the land cover. Determining plant species is not possible using this method, but it is possible to differentiate crops, grass, forest, water, and urban land cover types.

- Cropland and grassland seem to get mixed up in dry places. Heavily irrigated (green in visible Google Earth imagery) farmland appears to more regularly be classified as cropland. I observed that croplands in Eastern Colorado are often classified as grassland.
- The summit of Mount Rainier and Mount Baker are mixed forest. That is nonsense as these are heavily glaciated peaks and this dataset does have glaciers and snow cover. It correctly assigned snow and ice to the summit of a mountain in the Alaskan Range.

- There is also a consistent issue with assigning forest land cover classifications to agriculture in Western Washington. Because of the age of this dataset it is possible that this was indeed forest in the early 90s and has since been converted to cropland.
- At the interface between grass, shrubs and forests it takes a considerable distance to transition assignments to forest. For example, the data assign Arthurs Rock in Lory State Park Colorado, a forested area, as grassland.
- There are around ~10,000 HYSPLIT points (~1.3%) that are not given a land type assignment because the land cover data is convinced they are in urban areas or water, which my current methods do not allow. One example of when my methods fail is the HYSPLIT point that occurred on 2005-09-29 at (34.195, -118.259), near the middle of the Verdugo Mountains in Southern California. These mountains are less than 5 km across and are surrounded by expansive heavily developed cities that include Pasadena, Glendale, and Burbank California.

Overall the land cover assignments seem to make sensible assignments. For the purpose of distinguishing crops from forest from shrubs this dataset and methods described in Sect 2.3 of the manuscript appear affective.

S10 Additional HMS smoke plume operational analysis details

Presently, there is no comprehensive validation of HMS smoke plume analysis. One of the reasons in that there is no spatially and temporally comprehensive ground truth to compare to. Other satellite data would need to be used and these would have their own uncertainties. In the manuscript we state that the largest uncertainty for the smoke plume analysis is likely to be the edges of the smoke plume. In aggregate this is true, but may not be the largest uncertainty for every individual smoke plume. Below is an example of how the edge of a smoke plume can be uncertain, as described by an HMS analyst.

Description of smoke plume analysis on 9/23/2017: We [HMS analyst] observed agricultural burning in the mid/lower Mississippi Valley the day before (Fri 9/22/2017). When I was drawing my smoke on the morning of the 23rd I could see a remnant plume from the previous evening that was clearly associated with one of the larger fires and it was somewhere over southwest MO and vicinity. This plume was attached to a larger area of lighter density smoke that extended to the east into the Ohio Valley. As is typical in the eastern half of the US in the summer there was also sulfate haze. Since there was no hard edge on the eastern extent of the smoke I had to make a best guess as to how far the smoke extended. The problem is most pronounced with larger smoke plumes as they become more detached from the source fire since they gradually disperse and lose their sharp edge.

Many of the archived smoke polygons have straight-line edges particularly during the summer and over the ocean. The straight edges signify a boundary in which smoke-plume-detection analysis is performed. The smoke-plume-detection analysis is performed in five sectors. Each sector displays satellite imagery in a Lambert conic conformal projection. After analysis in all five regions has been performed, they are pieced together to form a single analysis. Strait edges of individual smoke GIS polygons occur when smoke plumes from different regions are pieced together. Not all sectors are analyzed year round. There is no analysis for Alaska or Northern Canada between November 1st and May 1st.

There is not always a HYSPLIT point associated with every smoke plume and vice versa. Often (especially during the summer when there are many wildfires producing a large amount of smoke) analysts observe smoke that has drifted a long way and become detached from the fire that produced it. In this case the smoke plume is not associated with any HYSPLIT points on that day. For example, the wildfires in Alaska and Northern Canada in 2015 produced smoke that drifted southeast into the Great Lakes and Mid Atlantic region and eventually reached Europe. This transport occurred over several weeks. When HMS analysts drew the smoke plumes as they traveled over the eastern part of the U.S., they did not associate the smoke with HYSPLIT points from the current day. There are also instances of HYSPLIT points when no smoke plumes are analyzed. For example, this can occur when HYSPLIT points are analyzed where there are many small fires, but no smoke plume analysis is done due to cloud cover.

S11 Code repository:

In an effort to be as open, transparent, and reproducible as possible, all work associated with this project is stored in the following subversion repository: <http://salix.atmos.colostate.edu/svn/smokeSource/>. This repository includes every version of all code, figures, and writing associated with this project. Please direct questions about this repository to sjbrey@rams.colostate.edu.

S12 Interactive Version of Figure 13:

A R Shiny application allows for interactive exploration of manuscript Fig. 13, including the ability to add or remove regions, as well as change between EDAS and GDAS meteorology. <https://stevenjoelbrey.shinyapps.io/smokeWheel/>

The Code for the app is located here: <https://github.com/stevenjoelbrey/smokeWheel>

References

Draxler, Roland R., and G. D. Hess. An Overview of the HYSPLIT₄ Modeling System of Trajectories, Dispersion, and Deposition. *Australian Meteorological Magazine* 47, no. 4 (December 1, 1998): 295308.

Stein, A. F., R. R. Draxler, G. D. Rolph, B. J. B. Stunder, M. D. Cohen, and F. Ngan. NOAA's HYSPLIT Atmospheric Transport and Dispersion Modeling System. *Bulletin of the American Meteorological Society* 96, no. 12 (May 4, 2015): 205977. doi:10.1175/BAMS-D-14-00110.1.

Draxler, Roland. NOAA - Air Resources Laboratory - FAQ - How Do I Estimate the Absolute (in Km) and Relative (%) Errors When Using the HYSPLIT Trajectory Model?, September 23, 2008. http://www.arl.noaa.gov/faq_hg11.php.

Kanamitsu, Masao. Description of the NMC Global Data Assimilation and Forecast System. *Weather and Forecasting* 4, no. 3 (September 1, 1989): 33542. doi:10.1175/1520-0434(1989)004<0335:DOTNGD>2.0.CO;2.

Val Martin, M., J. A. Logan, R. A. Kahn, F.-Y. Leung, D. L. Nelson, and D. J. Diner. Smoke Injection Heights from Fires in North America: Analysis of 5 Years of Satellite Observations. *Atmos. Chem. Phys.* 10, no. 4 (February 15, 2010): 14911510. doi:10.5194/acp-10-1491-2010.

Paugam, R., M. Wooster, S. Freitas, and M. ValMartin. A Review of Approaches to Estimate Wildfire Plume Injection Height within Large-Scale Atmospheric Chemical Transport Models. *Atmos. Chem. Phys.* 16, no. 2 (January 26, 2016): 90725. doi:10.5194/acp-16-907-2016.